Université d'Ottawa • University of Ottawa

PERMISSION DE REPRODUIRE ET DE DISTRIBUER LA THÈSE

PERMISSION TO REPRODUCE AND DISTRIBUTE THE THESIS

NOM DE L'AUTEUR / NAME OF AUTHOR:	Shahram Bayani Keivani
ADRESSE POSTALE / MAILING ADDRESS:	407-219 Bell Street Ottawa, Ontario K1R 7E4
GRADE / DEGREE:	**ANNÉE D'OBTENTION / YEAR GRANTED**
Master of Applied Science- Civil Engineering	2003
TITRE DE LA THÈSE / TITLE OF THESIS:	
Seismic Evaluation of Existing Reinforced Concrete Bridges in Ottawa Region	

L'auteur permet, par la présente, la consultation et le prêt de cette thèse en conformité avec les règlements établis par le bibliothécaire en chef de l'Université d'Ottawa. L'auteur autorise aussi l'Université d'Ottawa, ses successeurs et cessionnaires, à reproduire cet exemplaire par photograhie ou photocopie pour fins de prêt ou de vente au prix coûtant aux bibliothèques ou aux chercheurs qui en feront la demande.

Les droits de publication par tout autre moyen et pour vente au public demeureront la propriété de l'auteur de la thèse sous réserve des règlements de l'Université d'Ottawa en matière de publication de thèses.

The author hereby permits the consultation and the lending of this thesis pursuant to the regulations established by the Chief Librarian of the University of Ottawa. The author also authorizes the University of Ottawa, its successors and assignees, to make reproductions of this copy by photographic means or by photocopying and to lend or sell such reproductions at cost to libraries and to scholars requesting them.

The right to publish the thesis by other means and to sell it to the public is reserved to the author, subject to the regulations of the University of Ottawa governing the publication of theses.

N.B. LE MASCULIN COMPREND ÉGALEMENT LE FÉMININ

Bayani 13.5.2003

DATE

Bayani

(AUTEUR) SIGNATURE (AUTHOR)

Université d'Ottawa · University of Ottawa

Université d'Ottawa · University of Ottawa

FACULTÉ DES ÉTUDES SUPÉRIEURES ET POSTDOCTORALES

FACULTY OF GRADUATE AND POSTDOCTORAL STUDIES

BAYANI KEIVANI, Shahram

AUTEUR DE LA THÈSE - AUTHOR OF THESIS

M.A.Sc. (Civil Engineering)

GRADE - DEGREE

Civil Engineering

FACULTÉ, ÉCOLE, DÉPARTEMENT - FACULTY, SCHOOL, DEPARTMENT

TITRE DE LA THÈSE - TITLE OF THE THESIS

Seismic Evaluation of Existing Reinforced Concrete Bridges in Ottawa Region

Nove Naumoski and Murat Saatcioglu

DIRECTEUR DE LA THÈSE - THESIS SUPERVISOR

EXAMINATEURS DE LA THÈSE - THESIS EXAMINERS

H. Tanaka

M. Cheung

S. Foo

J.-M. De Koninck, Ph.D.

LE DOYEN DE LA FACULTÉ DES ÉTUDES SUPÉRIEURES ET POSTDOCTORALES

SIGNATURE

DEAN OF THE FACULTY OF GRADUATE AND POSTDOCTORAL STUDIES

Seismic Evaluation of Existing Reinforced Concrete Bridges in Ottawa Region

By

Shahram Bayani Keivani

A thesis
Presented to the University of Ottawa on partial fulfillment of the requirements for
Master of Applied Science in Civil Engineering

Department of Civil Engineering
University of Ottawa
Ottawa, Canada
K1N 6N5

April 2003

The M.A.Sc. in Civil Engineering is a joint program
with Carleton University administered by the
Ottawa-Carleton Institute for Civil Engineering

THE UNIVERSITY OF OTTAWA-FACULTY OF GRADUATE STUDIES

CERTIFICATE OF EXAMINATION

Examining Board

_____ _____

_____ _____

Advisor

_____

The thesis by
Shahram Bayani Keivani
entitled
Seismic Evaluation of Existing Reinforced Concrete
Bridges in Ottawa Region

is accepted in partial fulfillment
of the requirements of the degree of
Master of Applied Science (Structural Engineering)
in the
Department of Civil Engineering

Date: _____

_____
Chairperson of Examining Board

Dedicated to all the Bahá'ís of Iran for their love and passion.

Acknowledgments

I wish to express my sincere gratitude to my supervisor, Dr. Nove Naumoski, for his guidance and support during the course of this study. I would also like to thank Dr's Murat Saatcioglu and Simon Foo for their assistance. Many thanks are extended to Mr. John Ecclef and Mr. Don Cullen of the Transportation and Public Works Department of the City of Ottawa for their assistance in the selection of the bridges considered in this study.

My great and sincere acknowledgement is extended to the National Spiritual Assembly of the Bahá'ís of Canada for their continuous support and understanding during my studies in Canada.

Abstract

Many existing bridges, especially those built before 1970, were designed with minimum or no seismic considerations. Past experience has shown that such bridges are very vulnerable when subjected to moderate and strong earthquake motions. This was illustrated during the 1989 Loma Prieta, the 1994 Northridge, and the 1995 Kobe earthquakes, when many existing bridge collapsed or were severely damaged. Such a poor performance of the bridges was attributed primarily to the fact that the seismic effects were underestimated in the pre-1970's design practice.

In Ottawa region, a great expansion of highway bridges occurred in the 1950's to 1970's, before modern bridge design codes were developed. Statistics show that the number of existing bridges designed according to substandard seismic codes is significantly larger than the number of new, well-designed bridges. Given this, it is essential to develop methods for evaluation and retrofit of existing bridges in order to reduce the risk from seismic actions.

In this study, seismic evaluation was conducted to eight bridges located in the Ottawa region and designed according to the pre-1970's bridge codes. In addition, one new bridge, built 1994, was analyzed and was used as a reference case for comparing the performance of older and new bridges. Inelastic models were developed for each bridge and nonlinear dynamic analyses were conducted by using excitation motions compatible with the design spectrum for Ottawa, prescribed by the latest Canadian national code for bridge design. The performance of the bridges was assessed by analyzing the responses represented by curvature ductilities, shear demands, and lateral drifts. The results indicated that the performance of most of the selected bridges is acceptable for the seismic excitations used in this study.

Table of Contents

Chapter 4

Chapter 5

Chapter 6

Chapter 7

Chapter 8

List of Tables

List of Figures

Notations

A	Zonal acceleration ratio
B	Width of a bridge
C_{sm}	Elastic seismic response coefficient
d_b	Diameter of longitudinal reinforcing steel
D	Dead load
EQ	Earthquake load
f_c'	Cylinder compressive strength of concrete
f_{cc}'	Compression strength of confined concrete
f_s	Stress in reinforcing steel
f_{sm}	Specified maximum strength of reinforcing steel
f_y	Yield stress of reinforcing steel
f_{yh}	Yield strength of transverse reinforcing steel
f_u	Ultimate stress of reinforcing steel
I	Importance factor
L	Span of a bridge
M_y	Yielding moment of member
S	Site coefficient
S_p	Center-to-center spacing of longitudinal girders
T_m	Period of vibration of the m^{th} mode
α	Skew parameter
ε_c	Compression strain of concrete
ε_{cc}	Strain at peak stress for confined concrete
ε_{cu}	Ultimate compression strain of concrete
$\varepsilon_{s,hrd}$	Hardening strain of reinforcing steel
ε_{sm}	Reinforcing steel strain at the maximum tensile stress
φ_m	Flexural maximum curvature of a section

φ_y	Flexural yielding curvature of a section
μ_c	Curvature ductility factor
ρ	Confinement steel ratio
ψ	Skew angle

CHAPTER 1

INTRODUCTION

1.1 General

Past earthquakes, including the 1989 Loma Prieta, the 1994 Northridge and the 1995 Kobe earthquakes revealed a number of deficiencies in the design of old bridges. Most of these deficiencies indicated that no sufficient attention was paid in the past on the seismic design of bridges. It seems that before 1970, the designers were primarily concerned with live loads (i.e. traffic loads) in the design of bridges, and little or no attention was paid on lateral loads from seismic excitations. As a result of this, the main focus in the design of bridges was the superstructure. The substructures were not properly designed to resist the expected seismic forces. An obvious proof for this was the poor performance of highway bridges especially during the 1989 Loma Prieta, California earthquake when many bridges collapsed because of inadequate seismic resistance of the substructures.

Bridges designed according to pre-1970 codes have many deficiencies in regard to their resistance when subjected to seismic actions. Low shear capacity, inadequate anchorage, and poor confinement are the common deficiencies in old bridges. Based on observations of the performance of bridges subjected to seismic motions, Lwin (1997), Xiao (1997) and Chai (1991), provided a list of deficiencies of bridges designed before 1980. A summary of these deficiencies is as follows:

- In-span hinges having narrow supports,
- Simple supported beams with narrow support width in piers,
- Poor strength and detail in members and connections,

- Inadequate flexural, shear and torsional capacities of members and connections,
- Inadequate confinement reinforcement in compression members,
- Short lap splice and anchorage length of reinforcement bars, which cause an undependable flexural capacity of members,
- Inadequate footing and foundation capacity, mainly due to the lack of top mat and shear reinforcements.

Given these deficiencies, the old bridges are considered to be very vulnerable for seismic actions. Some of the factors that affect the seismic vulnerability of highway bridges, as summarized by Kawashima (1997), are as follows:

- Design code and standard specifications (bridges designed in accordance with older codes are in greater risk),
- Type of superstructure (arch, rigid frame, and continuous girder bridges have lower vulnerability than simply supported girders),
- Shape of superstructure (skewed or curved bridges do not necessarily have higher vulnerability than straight bridges),
- Materials of superstructure (in general, reinforced concrete bridges or prestressed concrete bridges have lower vulnerability than steel bridges, although the difference is negligible),
- Slope in bridge axis causes higher vulnerability,
- Type of substructure (bridges supported by single columns have higher vulnerability, while multi-column substructures provide redundancy),
- Height of piers (higher piers have higher vulnerability),
- Ground condition (bridges constructed on soft soil are more vulnerable),
- Ground motion (bridges subjected to stronger ground motions have higher vulnerability; experience shows that for peak ground accelerations larger than 0.4g, the vulnerability increases significantly).

Many highway bridges in the Ottawa region were designed and built between 1950 and 1970, following the design requirements prescribed by the American Association of State Highway and Transportation Officials (AASHTO). It is well recognized that the design of bridges at that time underestimated the seismic effects. As an example, in 1958, AASHTO introduced design provisions following the 1943

California Department of Transportation (CALTRANS) provisions. The lateral seismic forces at that time were calculated as a percentage of the weight of the bridge and depended on the footing type. The percentages ranged from 2 percent for spread footings on firm soil, to 6 percent for piled footings (Sexsmith et al. 1997). The observations from past earthquakes showed that the actual forces are much larger than the foregoing percentages.

Based on the foregoing discussion, it is obvious that evaluation studies of the seismic performance of existing bridges are needed in order to determine their actual seismic resistance. Such studies should determine which bridges and which structural components of the bridges are seismically vulnerable. The results from the evaluation study can be used for both the development of prioritization scheme of the bridges for retrofit and the selection of appropriate retrofitting technique.

1.2 Objective and Scope of the Study

The objective of this study is to perform seismic evaluation of existing bridges in the Ottawa region. To achieve this objective, eight old bridges built between 1957 and 1973 were selected and analyzed into detail. In addition, one new bridge, built 1994, was analyzed and was used as a reference case for comparing the performance of older and new bridges. Inelastic models were developed for each bridge and nonlinear dynamic analyses were conducted by using excitation motions compatible with the design spectrum for Ottawa, prescribed by the latest Canadian national code for bridge design. The performance of the bridges was assessed by analyzing the responses represented by curvature ductilities, shear demands, and lateral drifts.

1.3 Outline of Thesis

Chapter 2 presents a review of the available literature related to seismic evaluation of reinforced concrete bridges. The main characteristics of the bridges analyzed in this study are presented in Chapter 3. In Chapter 4, the computer program used for the analyses, and the modelling of the bridges are described. Chapter 5 presents the stress-strain models of concrete and steel, together with the hysteretic model used for reinforced concrete members under cyclic loads. The development of seismic excitations

used in the analyses is described in Chapter 6. The results from the analyses are discussed in Chapter 7. Chapter 8 presents the main conclusions that resulted from the analyses of the selected bridges.

CHAPTER 2

LITERATURE REVIEW

2.1 General

Historically, the first seismic evaluations were conducted in early 1970's. The significant damage of highway bridges during the 1971 San Fernando, California earthquake triggered a series of seismic evaluations (Kawashima et al. 1997). Following this earthquake, lateral forces were significantly increased in the design of bridges. Later, following the substantial damage and collapse of many existing bridges during the 1989 Loma Prieta, California earthquake, CALTRANS and the Federal Highway Administration (FHWA) funded the Applied Technology Council (ATC) to review the bridge design criteria and to provide suggestions for improvements of the bridge design codes. Based on the findings of this project, an extensive retrofitting program of 2000 seismically deficient bridges was undertaken. This program was underway when the 1994 Northridge, California earthquake occurred. This earthquake also caused extensive damage of bridges. However, it was encouraging that no serious damage was observed on the retrofitted bridges (Yashinsky, 1998).

In Japan, evaluations were conducted on highway bridges with spans longer than 15 m. These evaluations were primarily based on visual inspections of deterioration, devices for preventing falling-off of superstructure, the strength of substructures, and the stability of foundations. Approximately 40,000 bridges were evaluated and 11,800 bridges were found to require strengthening (Kawashima et al. 1997).

In 1990, the Washington State Department of Transportation (WSDOT) initiated a 20-year bridge seismic retrofit program for highway bridges. With this program, the

seismic vulnerability of highway bridges built before 1983 was evaluated and about 1000 bridges were identified as "high risk bridges" in the event of a major earthquake (Lwin, 1997).

Saiidi et al. (1998) evaluated the performance of bridges in the Reno-Sparks area of Nevada. A total of 26 bridges were analyzed to determine their displacement response, column forces, and displacement ductility demands. Results of the nonlinear analyses indicated that bridges with one or two columns per pier were vulnerable for the expected peak acceleration of 0.3g.

Haroun et al. (1994) conducted comprehensive experimental and analytical studies for the assessment of seismic behavior of existing bridge pier walls. It was found that the length of the lap splice of the vertical reinforcement had a significant effect on the ductility of the walls.

Harik et al. (1997) investigated the seismic performance of the Brent-Spence Bridge (Ohio) under simulated earthquake loading. In this study, site-specific ground motion scenarios were developed representing probable earthquake motions that might occur at the bridge site.

Priestley and Seible (1997) conducted a series of full-scale tests to investigate the bent details of the Santa Monica Viaduct that was damaged during the 1989 Loma Prieta, California earthquake. The effect of lap-splice details of the columns was the focus of their study. It was found that joint shear failure occurred because of the lack of detailing of the joints.

Aschheim, Moehle and Mahin (1997) conducted extensive investigations related to the design and evaluation of reinforced concrete bridges. These investigations resulted in guidelines for evaluation methodologies, uncertainties in the evaluations, and demand and capacity estimations for reinforced concrete bridges.

Lehman and Moehle (2000) conducted experimental studies on the seismic performance of well-confined bridge columns. In this study, columns with different longitudinal reinforcement ratio and aspect ratio were tested in order to assess the response of bridge columns to lateral loads.

The British Columbia Ministry of Transportation and Highways conducted seismic evaluations of several bridges. It was found that most of the investigated bridges

required retrofitting. The Vancouver's 40-year-old Oak Street Bridge was one of these bridges, which was retrofitted in 1997 (Sexsmith et al. 1997).

Lowes and Moehle (1999) performed a series of experimental tests to evaluate the seismic behavior of beam-column T-joints of older reinforced concrete bridges. It was found that concrete bridges constructed in the 1950s and 1960s are vulnerable because of the insufficient joint strength due to lack of transverse reinforcement in joints, insufficient anchorage length of the reinforcing bars in columns, and discontinuity of longitudinal reinforcement in bridge members.

Casas (1999) investigated the performance of reinforced concrete bridges in Spain by using two quite different evaluation methods. It was concluded in this study that the reliability-based evaluation approach gives more realistic results than the deterministic evaluation approach.

In addition to the foregoing analytical and experimental investigations, a number of computer programs for nonlinear analyses of reinforced concrete structure have been developed. The most widely used of these programs are SAP Nonlinear, IDARC, DRAIN-2D, and RUAUMOKO. The analyses in this study were conducted using the program IDARC.

CHAPTER 3

DISCRIPTION OF BRIDGES

3.1 Introduction

The seismic assessment of existing bridges is usually conducted in two stages. In the first stage, a study is carried out in order to rank the bridges according to their risks. This study is normally called a prioritization study or screening, and is primarily based on a review of bridge drawings, site conditions, visual inspections of bridge conditions, and review of the seismic activity of the bridge locations. The result from this study is a prioritization scheme that ranks the bridges according to their risks. A typical procedure for screening of existing bridges is proposed by Filiatrault et al. (1994). Other procedures include those proposed by the Applied Technology Council (1983), the CALTRANS (Gates et al. 1991), and the Japan Ministry of Construction (Kawashima et al. 1991). As an example, the basic risk components and their contributions (in percentage) according to the CALTRANS procedure for bridge prioritization (i.e. ranking) are given in Table 3.1 (Priestley et al. 1996).

The second stage consists of a detailed structural analysis of those bridges for which the prioritization study (i.e. the first stage) showed that are more vulnerable to seismic effects. Using a proper methodology, the seismic demands are compared with the capacities of the structural members. This study would show which structural members would be critical during seismic excitations. Based on the results from this study, decisions can be made for strengthening of the bridges.

3.2 Selection of Bridges

Because of the large number of existing reinforced concrete bridges, an attempt was made to limit the number of analyses by selecting representative bridges. The main criterion was to select older reinforced concrete bridges, (approximately 30 to 50 years old) since it is a common belief that older bridges do not have sufficient seismic resistance. Other parameters that were considered in the selection process were: type of structural system, number of spans, number of columns per bent, column dimensions, and foundation soil conditions. By reviewing the bridge design drawings at the Transportation Department of the City of Ottawa, 8 old bridges, built between 1957 and 1973 were selected for this study. One relatively new bridge, built 1994, was also selected as a representative of well-designed bridges. The reason for including a new bridge in the study was to compare the results of the older bridges with those of the new bridge.

The selected bridges have different structural systems for carrying the gravity and lateral loads. Four of the bridges were constructed on soft soil having pile systems, while the other five were built on bedrock using shallow foundations. These two soil conditions cover a variety of foundation conditions of the existing bridges in the area. It is believed that the selected bridges are well representative of the existing older reinforced concrete bridges in the Ottawa region.

3.3 Description of Bridges

The bridges considered in this study are listed in Table 3.2. All the bridges are located in the City of Ottawa and are currently under the jurisdiction of the Transportation Department of the City of Ottawa. The characteristics of the bridges that are of interest for this study are described hereafter. Additional information can be found in the design drawings.

Bridge #1

Bridge #1 is shown in Fig.3.1. It was built in 1957 and is a three-span rigid frame bridge over the Rideau River. The total length of the bridge is 70.11 m, which includes two end spans of 21.34 m each and a middle span of 27.43 m. The bridge has a skew of 6 degrees, with a normal width of 13.67 m. Each span includes four tapered T-section

girders for supporting the 20 cm thick deck slab. The substructure consists of two reinforced concrete bents (four columns per bent), and two abutments. The foundations of both the bents and the abutments are strip footings on rock.

The four columns of each bent are 762 ×762 mm square columns. Each column is reinforced longitudinally with twelve No. 11 bars (diameter d_b=35.7 mm). This corresponds to a longitudinal reinforcement ratio of 2.08%. The transverse reinforcement of the columns consists of three sets of No. 3 stirrups (diameter d_b=11.3 mm) at 305 mm spacing, which provide a volumetric reinforcement ratio of 0.34%.

The compressive strength of the concrete used for the entire structure is 3300 psi (22.8 MPa). No information could be obtained from the original drawings regarding the yield stress of the reinforcing steel used in the structure. Therefore, the minimum yield strength of 275 MPa was used, as recommended by Clause 14.6.3.3 of the CHBDC (see Table 3.3) for the bridges constructed in between 1956-1978.

Bridge #2

Bridge #2 is located in the eastern part of the city of Ottawa (see Fig. 3.2). It was built in 1957, and provides an overpass route on the Queensway. The bridge has no skew. It is composed of two equal spans of 24.16 m long. Each span consists of six steel girders, which are simply supported on sliding-rocking bearings at the abutments and the bent. The fixed bearings are at the two abutments, while the moveable bearings are at the bent. The steel girders carry an 18 cm thick composite deck, 12.5 m wide. The superstructure is divided into two parts by an expansion joint at the bent. The substructure includes two seat-type abutments and one pile-supported bent. The bent consists of three circular columns with a diameter of 914 mm each, and a cap beam of 914× 1280 mm.

The reinforcement of each of the columns consists of twelve No. 11 bars (diameter d_b=35.7 mm), which provide a longitudinal reinforcement ratio of 1.84%. Spirals with ½ inch (12.7 mm) diameter at 3 inches (50.8 mm) spacing were used for the transverse reinforcement with an equivalent spiral ratio of 0.83%. The material strengths obtained from the original drawings are 3000 psi (20.7 MPa) for the compressive strength of the concrete, and yield strength of f_y =375 MPa for hard grade bars.

Bridge #3

Bridge #3 was constructed in 1965. It is a three-span, continuous, prestressed multi-cell box girder structure. The AASHO standard specifications (1961) were used in the design of this bridge. The total length of the bridge is 67.40 m. The bridge has three spans with lengths of 19.41 m, 31.55 m, and 16.44 m, as shown in Fig. 3.3. The bridge has a skew of 22.81 degrees. The deck is a continuous prestressed box girder over two triple-column bents. The prestress force is provided by 24 cables (8 per each box) type S-A-37 composed of 37-0.276 inch (7 mm) diameter wires, only in the longitudinal direction. The jacking force of each cable at the final stage is 350 kips (1550 kN). There are horizontal diaphragms in the deck (in the transverse direction) at the abutments, bents, and at the middle of each span.

The columns have circular cross sections with a diameter of 1067 mm. At the bottom (i.e. at the surface of the foundation), the cross sections of the columns are reduced over a height of 12.7 mm; the diameter of the reduced cross sections is 610 mm. There is a rigid connection between the columns and the superstructure. Both abutments are seat-type abutments, with moveable bearings. The foundations of both the abutments and the bents consist of pile footings.

The longitudinal reinforcement of the column consists of thirteen No. 11 (diameter d_b=35.7 mm) bars i.e. a reinforcement ratio of 1.46%. The transverse reinforcement consists of a No. 5 (diameter d_b=16 mm) spiral with a spacing of 64 mm, i.e. 1.30% confinement steel ratio. The longitudinal reinforcement at the reduced sections consists of the anchor bars from the foundation. The number and the diameter of the anchor bars are the same as those of the longitudinal bars of the columns above the reduced sections. The length of the anchor bars is 1500 mm. The transverse reinforcement along the anchor bars consists of a spiral No. 4 (diameter d_b=12.7 mm), with a spacing of 305 mm, which provides a confinement steel ratio of 0.34% at the reduced sections.

The strength of the concrete used in the deck and in the bent columns is 5000 psi (34.5 MPa). According to the original drawings, reinforcing steel of hard or intermediate grade was permitted to be used. In this study, $f_y = 345$ MPa was used based on the CHBDC-Clause 14.6.3.3, Table 3.3.

Bridge #4

Bridge #4 was built in 1965. It is 38.68 m long, with two spans with a length of 19.34 m each (see Fig. 3.4). The bridge was designed following the AASHO (1961) specifications. The bridge has a skew of 24.78 degrees. The superstructure consists of a continuous, voided prestressed concrete slab. The width of the deck is 15.80 m. The thickness of the slab is 84 cm. The substructure consists of abutments and a bent. The abutment is a wall-type abutment with a mat foundation. The bent has two circular columns. Each column has a separate foundation on rock. The diameter of the columns is 762 mm. The connection between the columns and the concrete deck slab consists of fixed bearing anchors.

The strength of the concrete of the prestressed deck and the columns is f_c'=5000 psi (34.5 MPa). The reinforcing steel conforms to the C.S.A. specification G30 (1954), and various grade bars (i.e. standard, intermediate, and hard grade) were used. The yield strength of $f_y = 345$ MPa was assumed in this study according to the CHBDC-Clause 14.6.3.3 (see Table 3.3).

The longitudinal reinforcement in the columns consists of twenty No. 11 bars (diameter d_b=35.7 mm) with a reinforcement ratio of 4.41%. The transverse reinforcement consists of spiral No. 5 (diameter d_b=16 mm) with a spacing of 64 mm. The transverse reinforcement ratio is 1.88%. The prestressing of the deck slab was conducted using 34 longitudinal tendons which were stressed to 279 kips (1241 kN) from both ends simultaneously. In addition to the longitudinal tendons, six transverse tendons were used in the cap beam over the bent, which were stressed to 347 kips (1543 kN) from one end only.

Bridge #5

The bridge structure consists of two parallel bridges. In this study, only the newer bridge was analyzed. It was constructed in 1968 to carry the extra traffic of the old bridge. The bridge was designed following the specifications of the CSA-S6. It has four spans with lengths of 13.72 m, 18.90 m, 18.90 m, and 13.72 m (see Fig. 3.5). The total length of the bridge is 65.24 m. This bridge has no skew. From a structural point of view, the bridge is similar to the bridge #1.

The superstructure consists of a concrete slab supported by four continuous reinforced concrete girders. The girders are connected to each other by eleven diaphragms (above the bents and intermediate diaphragms) over the length of the bridge. The deck slab is 20 cm thick. The width of the deck is 10.97 m. The width of the girder is 500 mm, and its depth varies from 685 mm to 1600 mm.

The substructure consists of three bents. Each bent has four rectangular columns connected by a crash strut. The dimensions of each column are 610×549 mm. Each column is reinforced with ten No. 11 bars (diameter d_b=35.7 mm). The longitudinal reinforcement ratio is 3.25%. Ties No. 4 (diameter d_b=12.7 mm) at a distance of 305 mm were used as transverse reinforcement. The transverse reinforcement ratio for the columns is 0.77%.

All concrete members, except the footings, have compressive strength of f_c'=3000 psi (27.6 MPa). The reinforcing steel is deformed hard or intermediate grade, in accordance with C.S.A. G30. Given the year of the construction of the bridge, yield strength of f_y=275 MPa was used in this study, as suggested by CHBDC-Clause 14.6.3.3 (see Table 3.3).

Bridge #6

Bridge #6 was constructed in 1968. It was designed following the CSA S-6 (1966) design provisions. The bridge represents a railway overhead structure. It consists of 3 spans with lengths of 16.20 m, 23.28 m and 17.70 m (see Fig. 3.6). The total length of the bridge is 57.18 m. The bridge has a skew of 28.62 degrees and a transverse slope of 5.4%.

The superstructure consists of a cast in place reinforced concrete slab, with expansion joints at the abutments. The slab is 19.66 m wide and 0.762 m thick. It is prestressed longitudinally using 32 tendons. The total prestressing force (of all tendons) is 16694 kips (74255 kN).

The substructure consists of two bents and wall-type abutments. Each bent consists of three columns, a collision strut, and a cap beam. The columns have circular cross sections with a diameter of 914 mm. Each column has rigid connections at both ends. The longitudinal reinforcement of the columns consists of twelve No. 11 bars

(diameter d_b=35.7 mm), which provides reinforcement ratio of 1.84%. The transverse reinforcement consists of a spiral No. 5 (diameter d_b=16 mm). The transverse reinforcement ratio is 1.31%.

The concrete of the deck slab, bents, cap beams, and the collision strut, has a compressive strength of 5000 psi (34.5 MPa). Hard and intermediate grade, high bond deformed bars were used for reinforcement. The yield strength of the reinforcement was assumed 345 MPa, according to CHBDC, Clause 14.6.3.3 (see Table 3.3).

The two abutments transfer the loads by twenty steel-bearing piles driven to rock. Each column is supported by a single caisson on rock.

Bridge #7

Bridge #7 was designed in 1970 to improve the local access of near-by areas. The AASHO specifications were used in the design. As shown in Fig.3.7, the bridge has three spans. The two end spans are 21.33 m and the middle span is 38.10 m long. The total length of the bridge is 80.76 m. The superstructure consists of three steel box girders. These girders support the 18 cm thick concrete deck and are sitting on rubber type bearings. The width of the deck is 13.12 m. The bridge has no skewness.

The substructure consists of two reinforced concrete bents (two columns per each bent) and two seat-type abutments. The foundation consists of very long, tube pile footings for both the bents and abutments. The dimensions of the bottom sections of the columns are 1067×635 mm, and those of the top sections are 1372×965 mm. The longitudinal reinforcement of the columns consists of eighteen No. 18 bars (diameter d_b=56.4 mm) providing longitudinal reinforcement ratios of 6.86% and 3.51% at the bottom and the top sections respectively. Stirrups No. 3 (diameter d_b=11.3 mm) at a distance of 406 mm were used as transverse reinforcement. The confinement ratio is 0.24% at the bottom section, and 0.16% at the top section of each column.

The concrete in the columns of the bents and the cap beams has a compressive strength of 5000 psi (34.5 MPa). The yield strength of the reinforcement is f_y=345 MPa.

Bridge #8

Bridge #8 is shown in Fig. 3.8. It was constructed in 1973, and has three spans with lengths of 16.92 m, 28.04 m, and 27.74 m. The total length of the bridge is 72.70 m. Each span has five precast girders (C.P.C.I type IV prestressed girders), which sit on natural rubber bearing pads, on the abutments and the bents. The deck consists of 19 cm thick reinforced concrete slab that sits on the precast girders. The width of the deck is 12.80 m. The bridge has a skew of 30 degrees. The design live load for this bridge is based on the AASHO HS-20-44 requirements. The ACI 515-57 provisions were used for design of the reinforced concrete components.

The substructure consists of two reinforced concrete bents (three columns per bent), and two seat-type abutments. Each column has circular cross section with diameter of 914 mm. The bents have strip footings on rock. Sixteen No. 11 bars (diameter d_b=35.7 mm) were used as longitudinal reinforcement in the columns, which provide longitudinal reinforcement ratio of 2.45%. The transverse reinforcement in the columns consists of 5/8 inch diameter spirals (diameter d_b=16 mm) with a spacing of 89 mm. This provides confinement ratio of 1.13%.

The compressive strength of the concrete in the abutments is 3000 psi (20.7 MPa). High-grade steel bars with yield strength of 345 MPa were used for reinforcement.

Bridge #9

Bridge #9 is shown in Fig. 3.9. It was built in 1994. This bridge was selected as a representative of new bridges, and was used as a reference for comparing the performance of the eight older bridges. The bridge was designed in accordance with the Ontario Highway Bridge Design Code (OHBDC-1983). It has three spans with lengths of 14.0 m, 19.0 m, and 14.0 m. The total length is 47.0 m. The bridge has a skew of 4.5 degrees.

The superstructure consists of cast-in-place post-tensioned, continuous concrete slab. The thickness of the slab is 80 cm. The width of the deck is 25.91 m.

The substructure consists of two seat-type abutments and two bents with different heights. As shown in Fig. 3.9, the east bent is 7.30 m high, and the west bent is 9.21 m high. Each bent has four columns. The columns have circular cross sections with

diameter of 1200 mm. The columns of the west bent are reinforced by twenty eight 30M bars (diameter d_b=29.9 mm), which provide reinforcement ratio of 1.73%. The columns of the east bent are reinforced by twenty eight 25M bars providing reinforcement ratio of 1.24%. The transverse reinforcement for both bents is the same and consists of 15M spirals spaced at 80 mm. This corresponds to confinement ratio of 0.95%.

The concrete of the superstructure has compressive strength of 35 MPa. The compressive strength of the concrete of the substructure is 30 MPa. The reinforcing steel has yield strength of 400 MPa.

The foundation consists of a steel pipe pile system. The ends of the piles reach a shale bedrock foundation.

Table 3.1 Risk components and their contributions (in percentage) according to the CALTRANS prioritization scheme.

Risk Components	**Contribution (%)**
Year of construction	13
Expected ground acceleration	12
Soil condition	12
Hinges	11
Single-column	10
Traffic volume	8
Height of columns	7
Skew	7
Facilities crossed	6
Route type	5
Detour	5
Abutment	4

Table 3.2 Characteristics of the bridges used in this study.

Bridge No.	Year of design	Superstructure type	Total length (m)	Deck width (m)	No. of spans	Skewness (degree)	f_c' (MPa)	f_y (MPa)	Site conditions
1	1957	Rigid frame	70	13.67	3	6	22.8	275	Soil profile I
2	1957	Steel girder	48	12.5	2	----------	20.7	350	Soil profile IV
3	1965	Prestressed concrete box girder	68.3	18.4	3	22.81	34.5	345	Soil profile IV
4	1965	Prestressed slab	39.01	15.54	2	24.78	34.5	345	Soil profile I
5	1968	Rigid frame	63.4	11	4	----------	27.6	275	Soil profile I
6	1968	Prestressed slab	57.2	19.6	3	28.62	34.5	345	Soil profile I
7	1970	Steel box girder	80.1	13.1	3	----------	34.5	415	Soil profile IV
8	1973	Precast AASHTO girder	72.5	11.6	3	30	20.7	345	Soil profile I
9	1994	Post-tension slab	47	25.9	3	4.5	35 for deck 30 for pier	400	Soil profile IV

Note: Soil profile type I designates bedrock, and soil profile type IV designates soft soil.

Table 3.3 Recommended yield strength of steel, according to the Canadian Highway Bridge Design Code, Clause 14.6.3.3.

Date of Bridge Construction	Grade (MPa)			
	Struc.	Med.	Hard.	Unknown
Before 1914	-----	-----	-----	210
1914-1955	230	275	345	230
1956-1978	275	345	415	275
After 1978 -stirrups and ties	300	350	400	300
-remainder	300	350	400	350

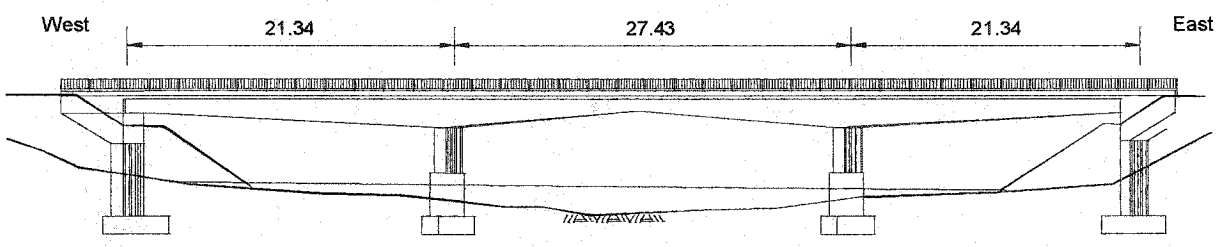

ELEVATION

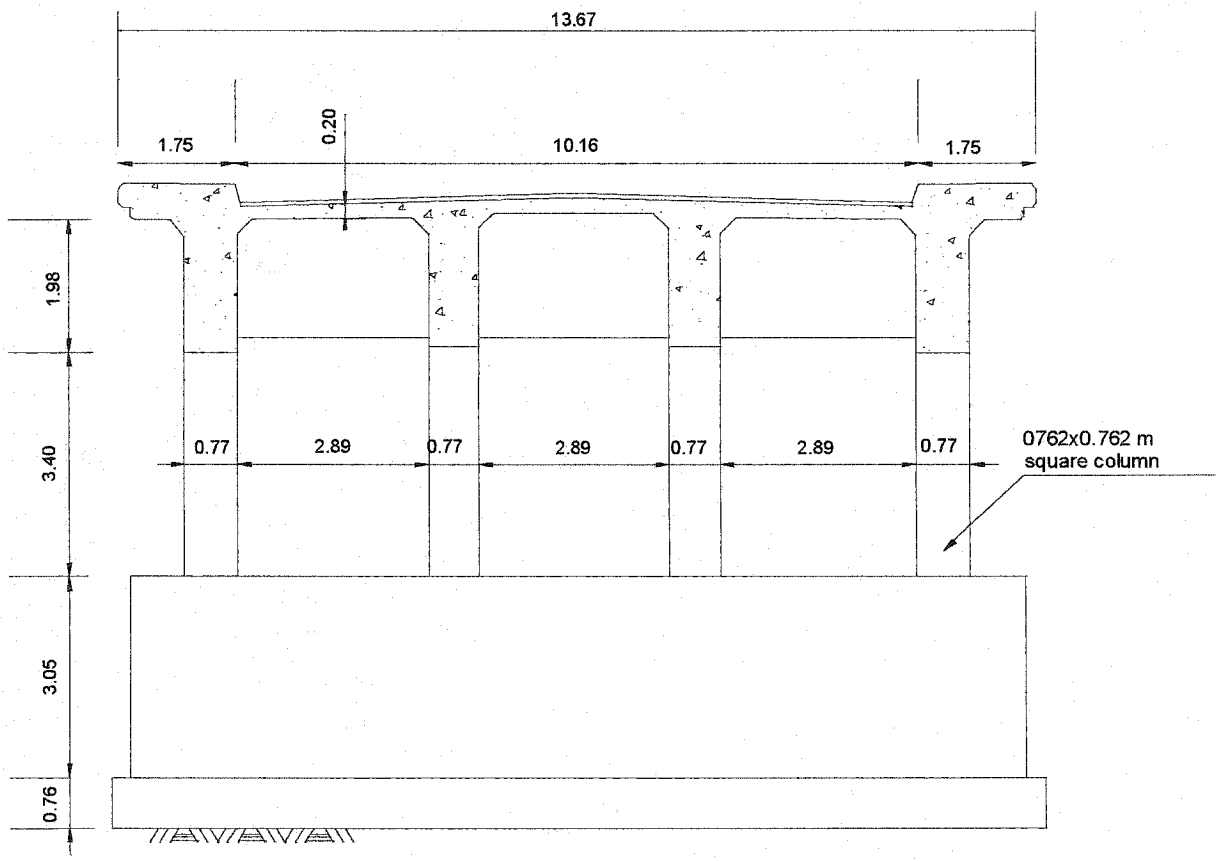

CROSS SECTION

Note: All dimensions are in meter

Fig. 3.1 Elevation and cross section of Bridge #1.

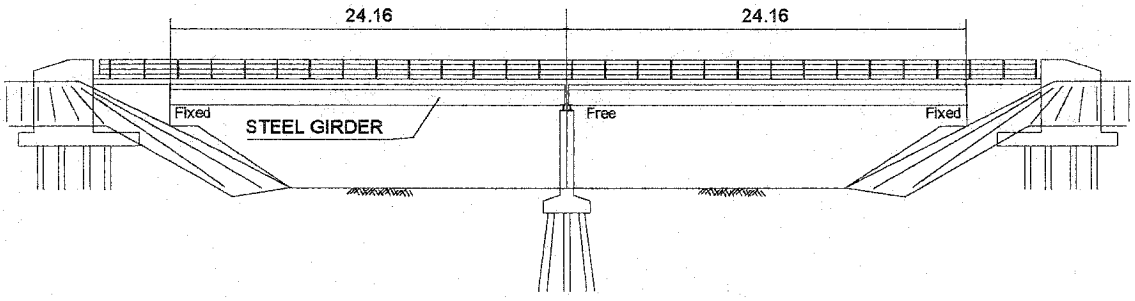

ELEVATION

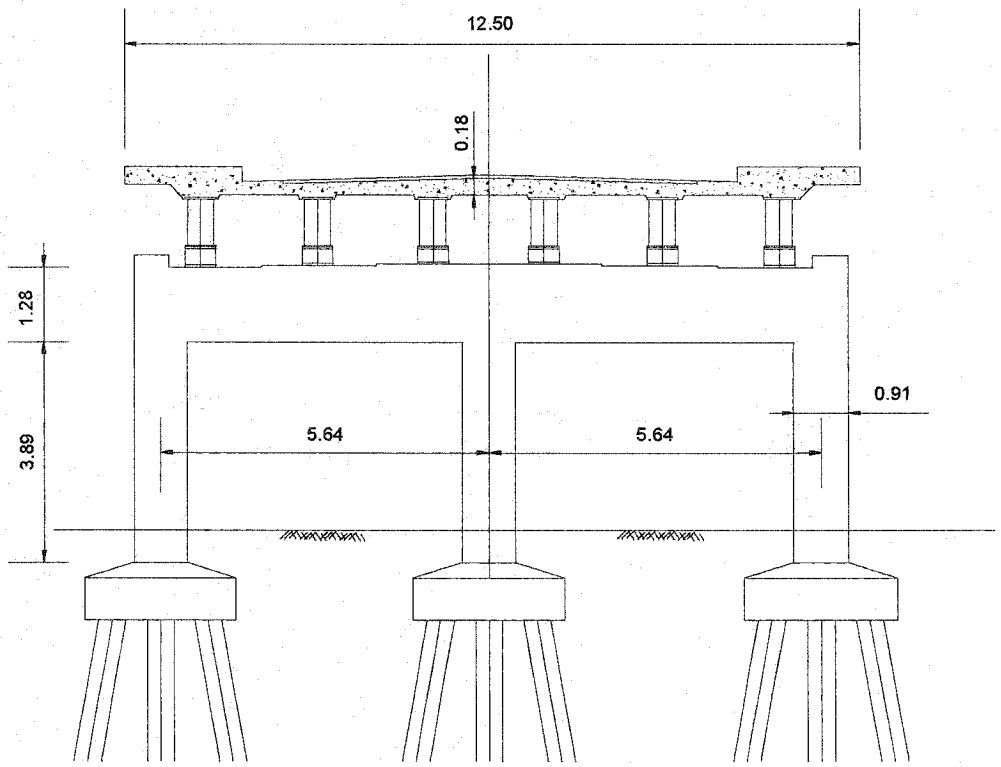

CROSS SECTION

Note: All dimensions are in meter

Fig. 3.2 Elevation and cross section of Bridge #2.

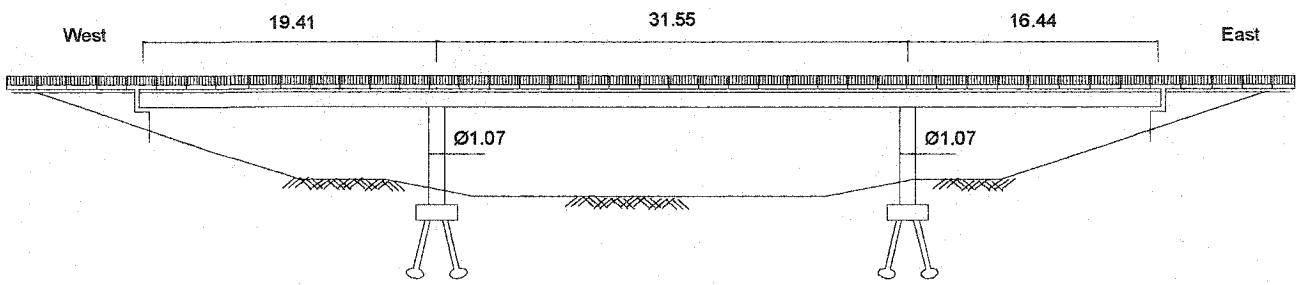

ELEVATION

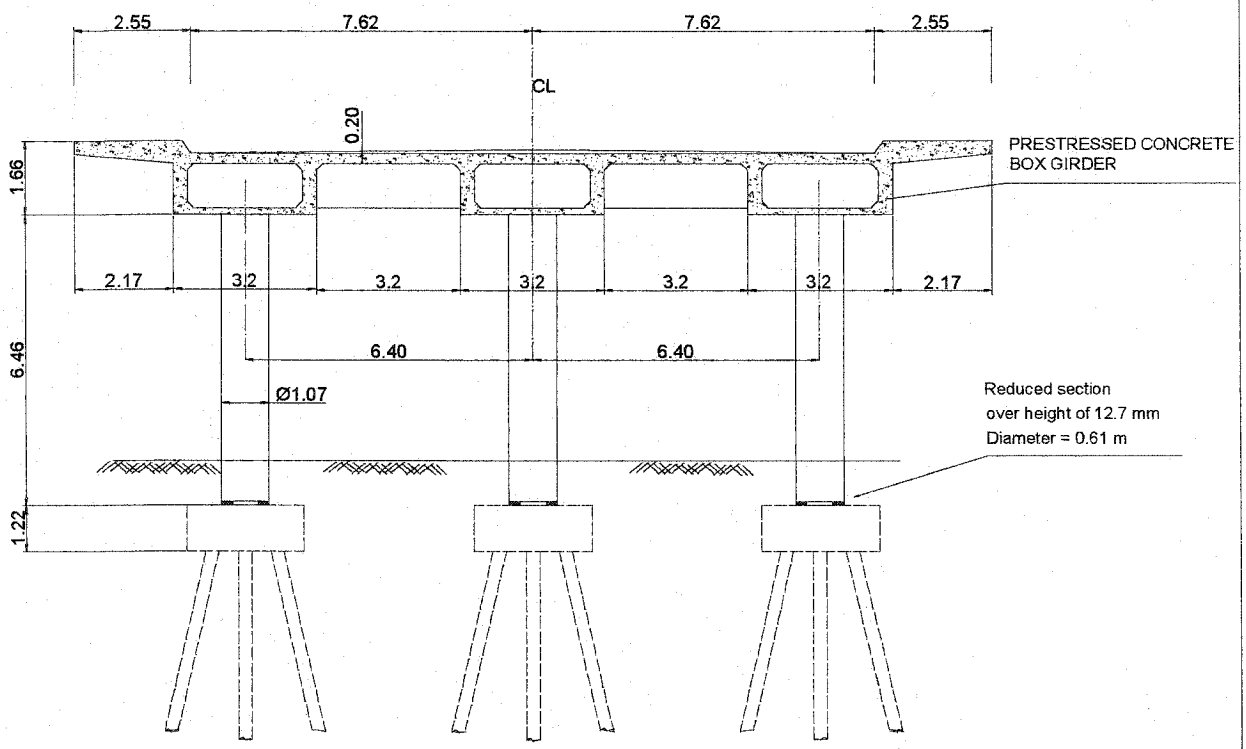

CROSS SECTION

Note: All dimensions are in meter

Fig. 3.3 Elevation and cross section of Bridge #3.

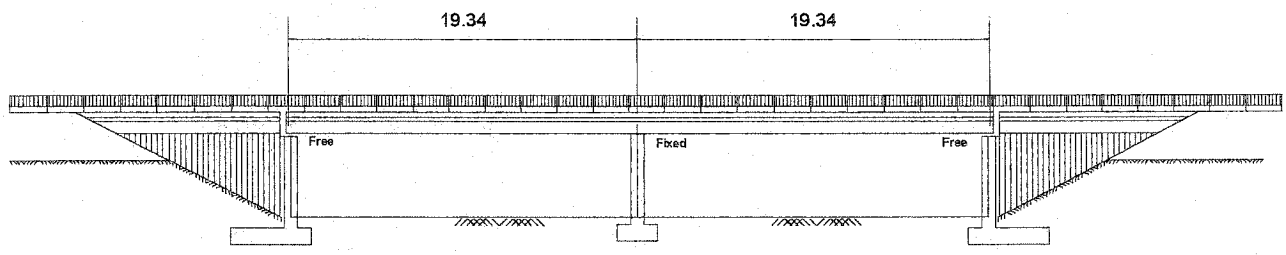

ELEVATION

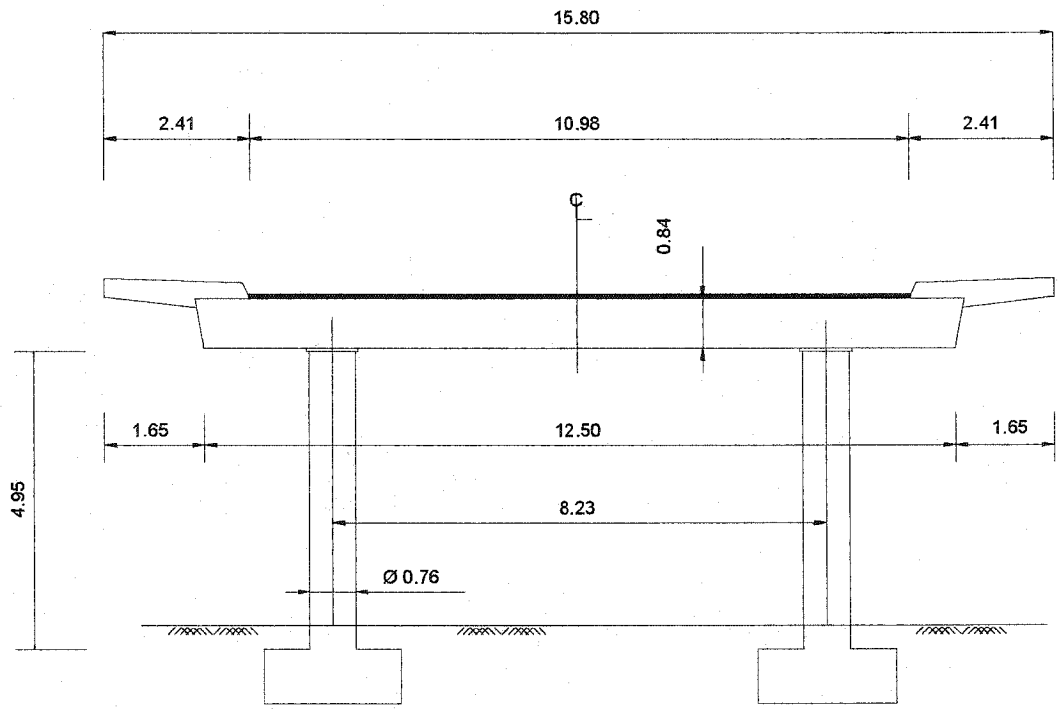

CROSS SECTION

Note: All dimensions are in meter

Fig. 3.4 Elevation and cross section of Bridge #4.

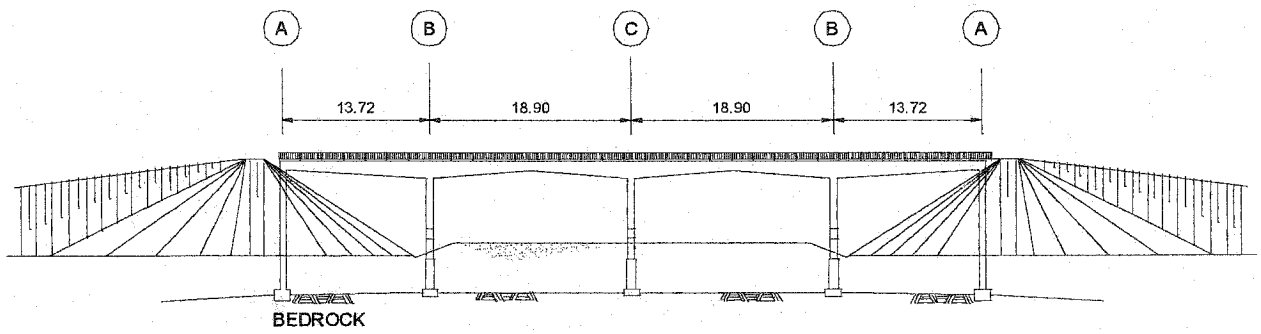

ELEVATION

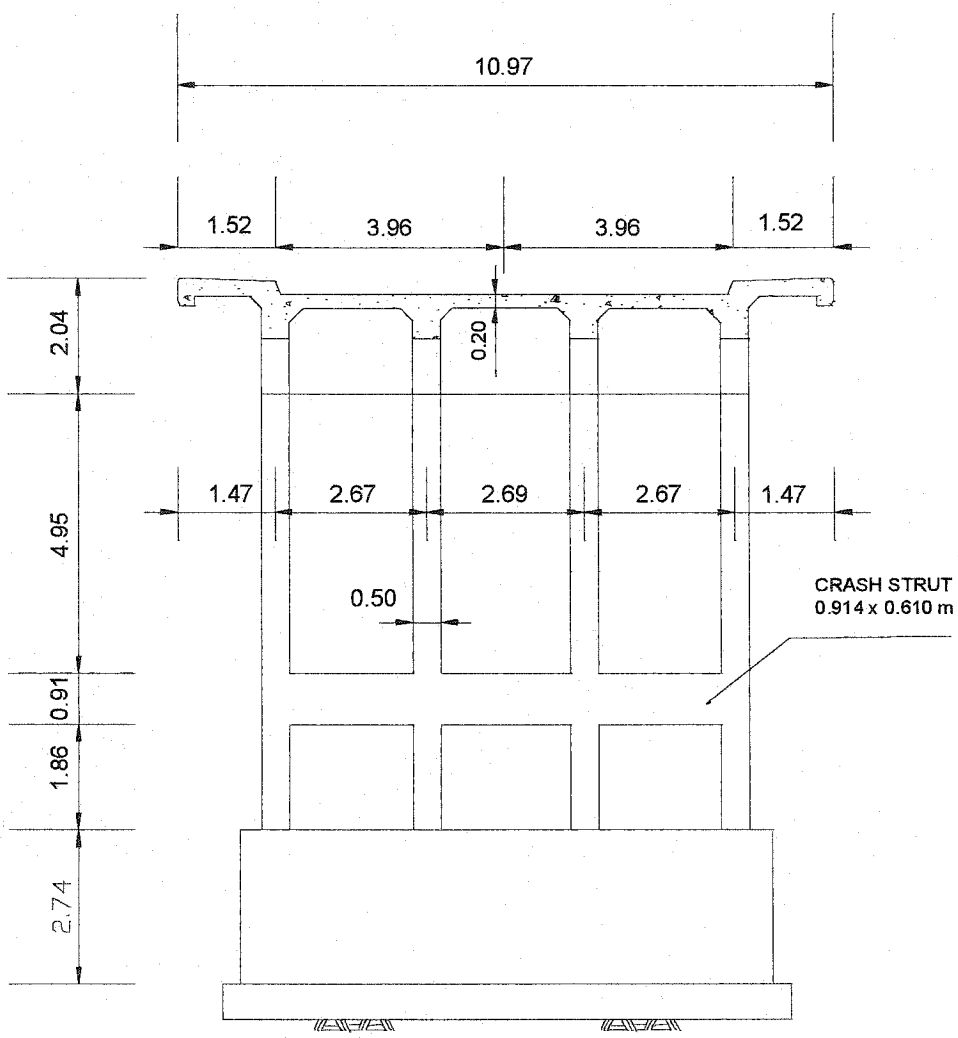

CROSS SECTION

Note: All dimensions are in meter

Fig. 3.5 Elevation and cross section of Bridge #5.

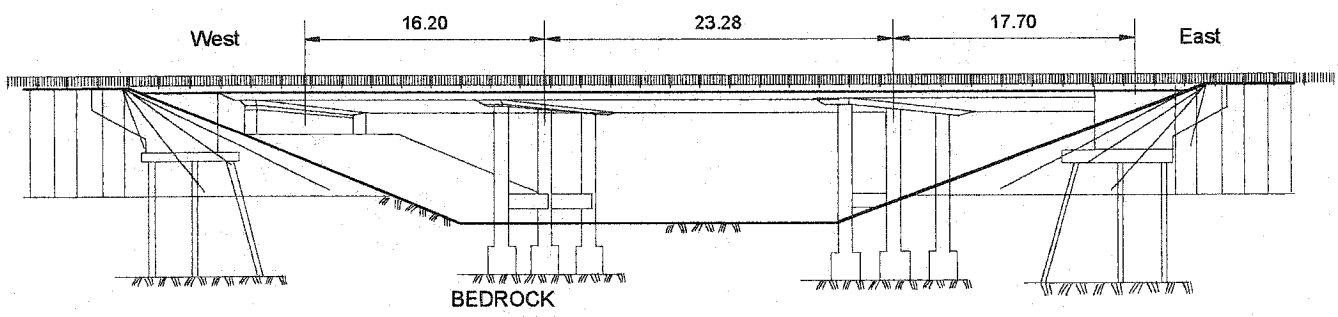

ELEVATION

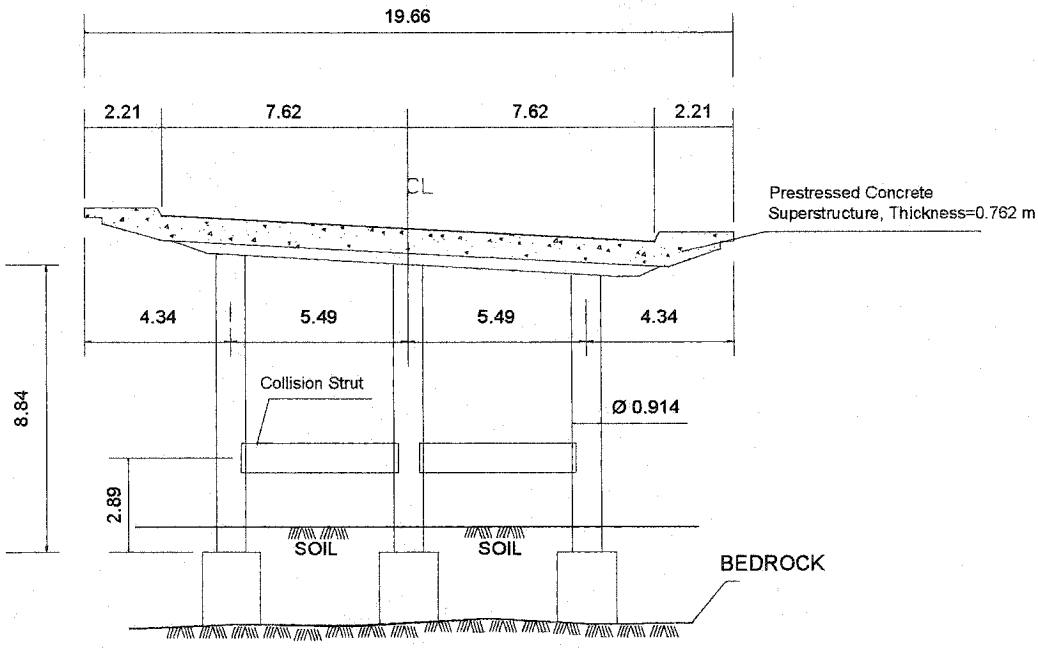

CROSS SECTION

Note: All dimensions are in meter

Fig. 3.6 Elevation and cross section of Bridge #6.

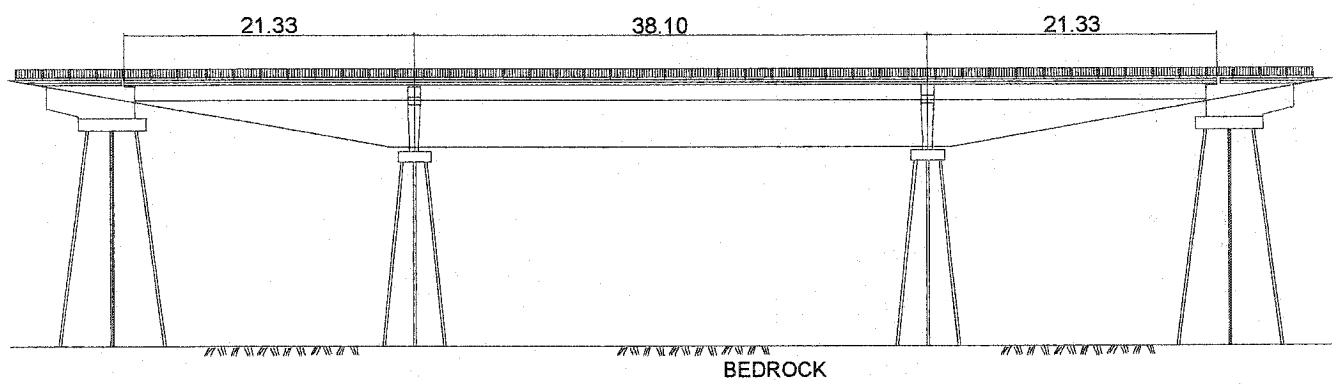

ELEVATION

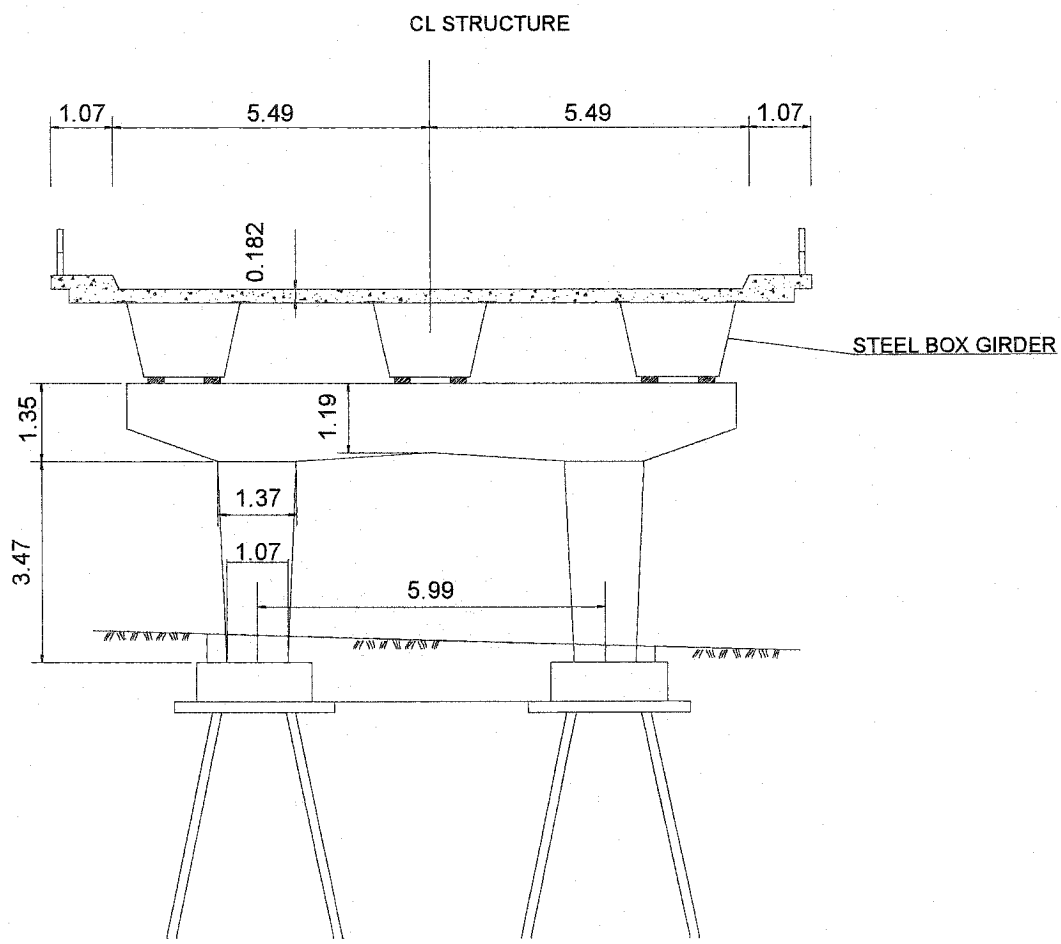

CROSS SECTION

Note: All dimensions are in meter

Fig. 3.7 Elevation and cross section of Bridge #7.

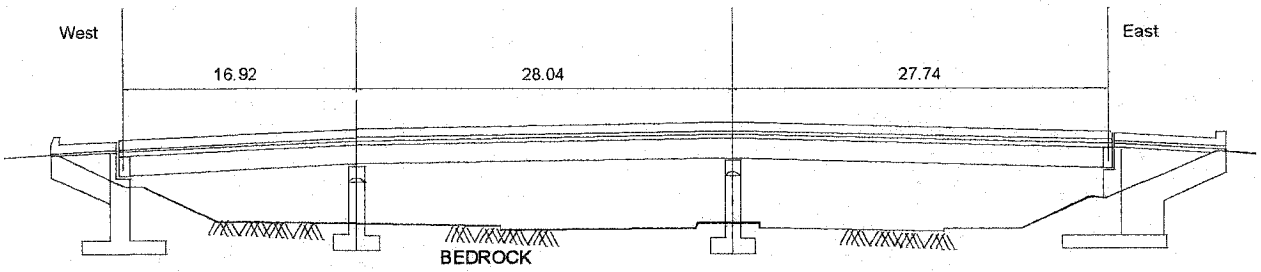

ELEVETAION

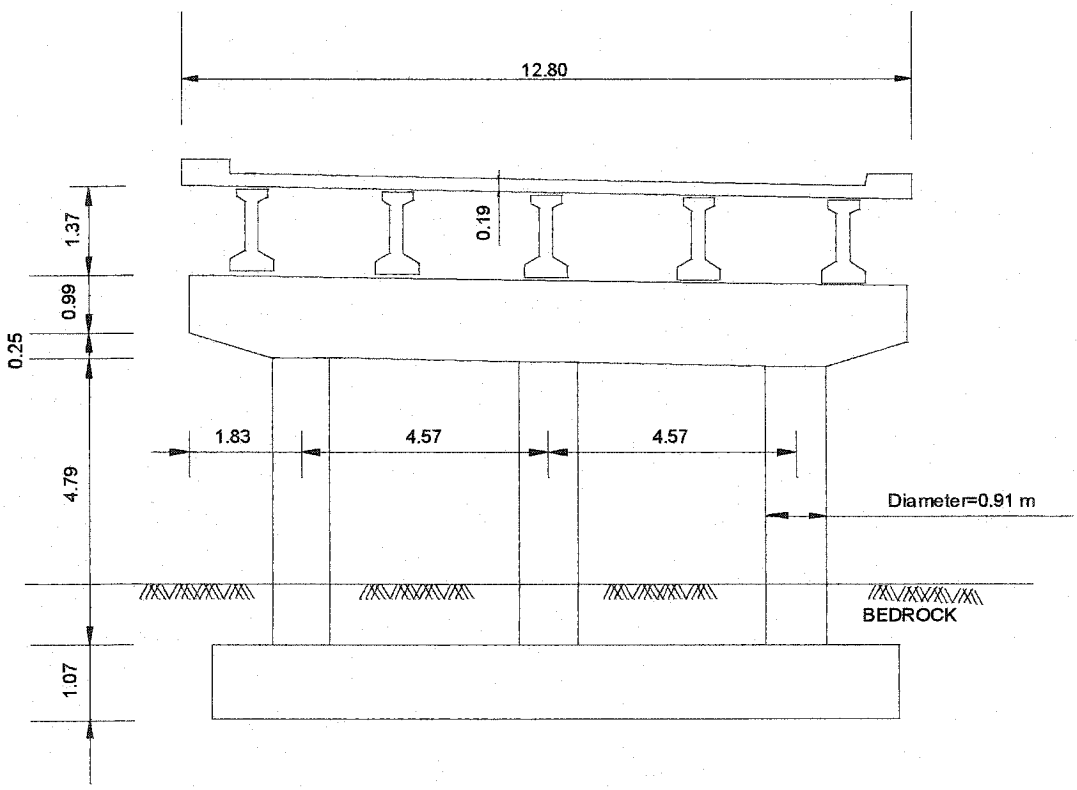

CROSS SECTION

Note: All dimension are in meter

Fig. 3.8 Elevation and cross section of Bridge #8.

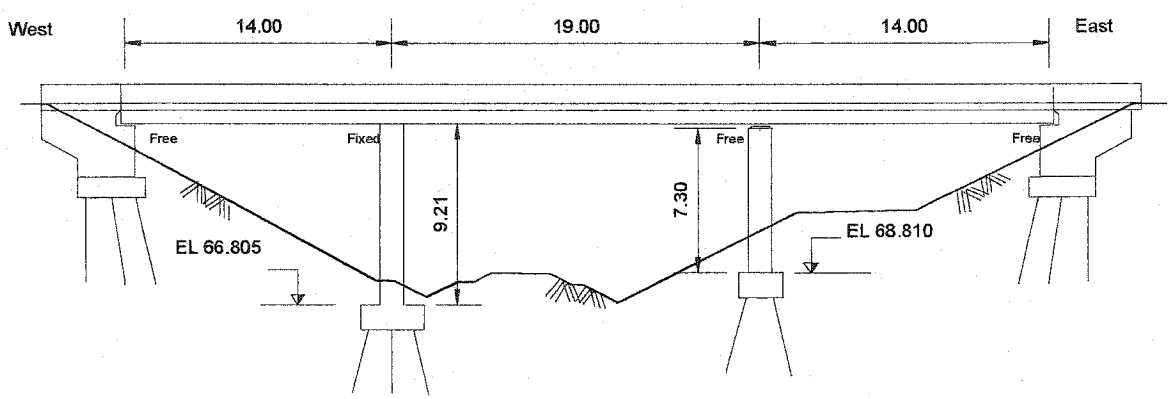

ELEVATION

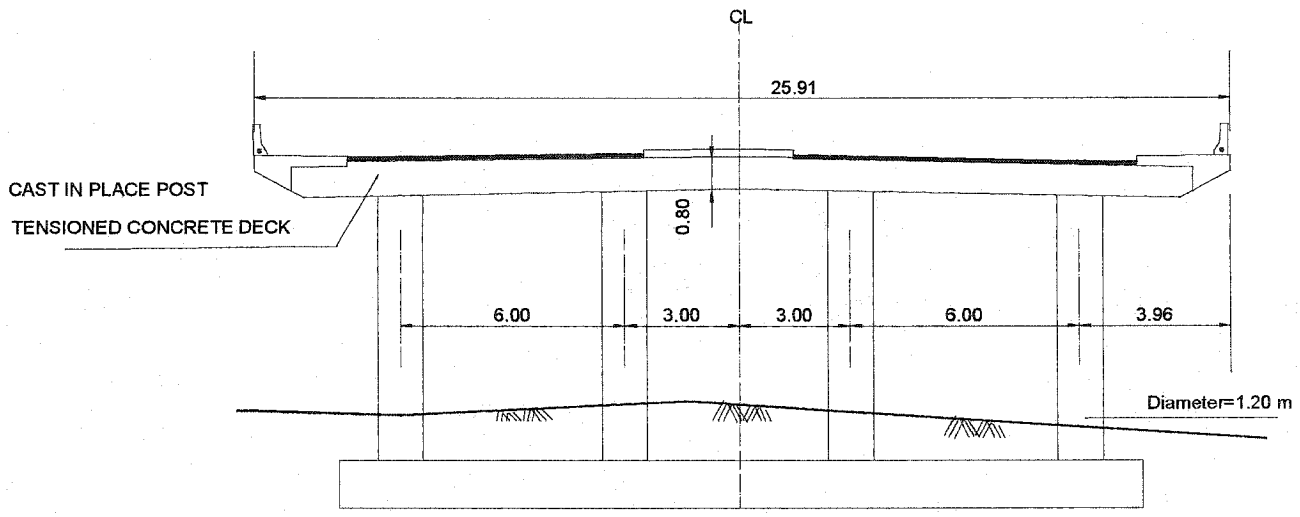

CROSS SECTION

Note: All dimensions are in meter

Fig. 3.9 Elevation and cross section of Bridge #9.

CHAPTER 4

MODELLING OF BRIDGES

4.1 Introduction

The behavior of a reinforced concrete structure when subjected to seismic excitation is normally investigated using computer programs for nonlinear dynamic analysis. In this study, the program IDARC (Inelastic Damage Analysis of Reinforced Concrete) (Kunnath et al. 1994) was used for analyses of the selected bridges. The program is developed for two-dimensional analyses. It requires analytical model of the structure, and a seismic excitation. This section describes the models of the bridges. The modelling parameters (constitutive models for concrete and steel, moment-curvature relationships, and hysteretic model parameters) are discussed in Chapter 5, and the seismic motions are described in Chapter 6.

4.2 Characteristics of the IDARC Model

The program IDARC (Kunnath et al. 1994) is developed for two-dimensional analysis of reinforced concrete structures. Therefore, the structural model is represented by a 2-D model. Among the different types of elements incorporated in IDARC, the beam-column element was used for the development of the analytical models of the bridges. This element is represented by a simple flexural spring in which shear deformation effects are included. Axial deformation effects, in addition to flexural and shear deformations are included in column elements, but no interaction between bending moment and axial load is taken into account. The effect of axial deformation is ignored in

beams. Given these assumptions, each beam has four degrees of freedom (rotation and vertical displacement at each end) and each column has six degrees of freedom. The flexural model takes into account a combination of concentrated plasticity at the member ends and distributed flexibility along the member. The modelling for shear deformations is accomplished by means of an equivalent spring that acts in series with the flexural spring. The stiffness of a given member is represented by the equivalent stiffness of the shear and flexural springs. The program takes into account P-Δ effects.

4.3 Modelling of the Selected Bridges

For each bridge, separate models were developed for the longitudinal and transverse direction. The geometrical properties and the masses were calculated from the original drawings. The beams and columns were assumed as line elements, connected at their ends to form frames.

The bearings (both the fixed and moveable) were simplified in the modelling of the bridges. In the longitudinal direction, the bearings were modelled using column elements with a very high axial stiffness, and negligible flexural stiffness. High shear stiffness was used for these elements to ensure that the shear forces are transferred properly between the superstructure and substructure. In the transverse direction, no movement of the superstructure at the bearings was assumed.

Bridge #1

The model of the bridge is shown in Fig. 4.1. For the modelling in the longitudinal direction, one of the interior girders with effective flange width was selected as a representative of the whole bridge. Each span was divided into four segments and each segment was modelled as a beam. The nodal weights and dead loads were obtained from the geometry of the bridge. The total mass of the superstructure was then divided into discrete concentrated masses according to the length of the superstructure, spans, and distance between the girders.

For the transverse direction, two models were considered. The first model was that of the abutment, with nodal weights corresponding to a half of the end span of the

bridge. The second model was for one of the bents. The nodal weights for this model represent the weights of a half of the end span and a half of the middle span of the bridge.

Bridge #2

The models of bridge #2 are shown in Fig. 4.2. In the longitudinal direction, the central bent was modelled as a single-degree-of-freedom (SDOF) system. The mass of the SDOF system represents the total mass of the superstructure and a half of the mass of the bent. The system has equivalent axial stiffness and flexural stiffness of all the columns of the bent.

In the transverse direction, the bent was modelled as a frame, with nodal masses concentrated at the top of each column. The nodal masses represent a half mass of the superstructure.

Bridge #3

The models of bridge #3 are shown in Fig. 4.3. Since this bridge has concrete box girders, the model used for the longitudinal direction is quite similar to that of bridge #1. The only difference is that the abutments of this bridge were modelled as columns with an infinite axial stiffness but no flexural stiffness. These assumptions provide both: free movements of the superstructure in the longitudinal direction, and proper transfer of the vertical loads from the superstructure to the abutment.

In the transverse direction, the west bent was modelled only. This was because the west end span is longer than that the east end span, and consequently the masses that act on the west bent are larger than those on the east bent. The masses of the model correspond to those of a half of the west end span and a half of the middle span. As shown in Fig. 4.3, additional nodal points were included in the middle of each span. This was primarily because the reinforcement of the beam is different in the mid span compared with that above the columns.

Bridge #4

The models of bridge #4 are shown in Fig. 4.4. In the longitudinal direction, the deck slab is treated as a two-span beam, supported at the abutments and in the mid-span,

i.e. at the bent. Each span was divided into four segments and nodal masses were concentrated at the nodes between the segments. Since the connection between the deck slab and the columns (of the bent) is not rigid (see Fig. 3.4), artificial elements were used to model the beam-column connections. Similar artificial elements were also used to model the support conditions at the abutments. With these (artificial) elements, the model consisted of a two-storey frame; note that the artificial second storey was just several centimeters high. At the bent, a column element with properties representing those of the two actual columns was used for the first storey. The second storey column at the bent had very large axial and shear stiffness, and negligible flexural stiffness. Similarly, the support conditions at the abutments were modelled using artificial column element at the second storey, which had very large axial stiffness, but negligible shear and flexural stiffness. It should be noted that the effect of the prestressing forces was taken into account in the development of the moment-curvature relationships of the beam sections.

In the transverse direction, the bridge was modelled as a two-storey frame with over hang beams in the second storey. As for the longitudinal direction, the second storey was several centimeters high artificial storey, and was used only to model the support conditions. The mass concentrated at the nodal points of the beam elements represent the mass of a half of the superstructure. An effective width of the slab was used in the model.

Bridge #5

Bridge #5 was modelled as shown in Fig. 4.5. The modelling of this bridge was very similar to that of Bridge #1. The only difference is in the model of the transverse direction, in which the crash struts are included. Both the models of the central bent and the abutment were considered in the transverse direction to determine which of these two models is more critical.

Bridge #6

The models of this bridge are shown in Fig. 4.6. In the longitudinal direction, the prestressed superstructure with rigid connections between the columns and the concrete slab was modelled as a three-span frame. The stiffness of the each column element in the

model represents the overall stiffness of the three columns of the corresponding bent. The superstructure was treated as a beam with a width equal to that of the slab.

For the transverse direction, the model of the east bent was used. This bent is more critical since the masses associated with this bent are larger than those of the west bent. The effective width of the cap beam was calculated according to the code. The gravity loads carried by the east bent were applied to the cap beam. The nodal masses for this model were computed using the mass of the half of the east end span and the mass of the half of the middle span of the bridge (see Fig. 3.6).

Bridge #7

The models of this bridge are shown in Fig. 4.7. In these models, the steel box girders were not modelled as structural members, and only the weight of these girders were taken into account. In the longitudinal direction, each bent was modelled as a single cantilever column (i.e. SDOF system) with a proper nodal mass and lateral stiffness. The mass of each of SDOF system corresponds to that of a half of the superstructure.

In the transverse direction, each bent was modelled as a portal frame with overhanging beams at both sides. The nodal masses of each model represent the mass of a half of the end span and half of the middle span. An additional node in the middle of the span was used to include the effect of the tapered cap beam.

Bridge #8

Figure 4.8 shows the longitudinal and transverse models of bridge #8. Both the longitudinal and the transverse models are associated with the east bent, since this bent caries larger weight than the west bent. Given the simplicity of the system, no special consideration was needed for the modelling. The corresponding nodal masses and lateral stiffness were calculated for both the longitudinal and the transverse directions.

Bridge #9

In comparison to the other bridges, this bridge has a more complex system due to its special geometry and bearing conditions. The models of this bridge are shown in Fig. 4.9. As shown in Fig.3.9 the east bent is about 2 meters shorter than the west bent, which

can attract higher shear forces. On the other hand, the top connection of the columns of the east bent is such that only shear forces can be transferred between the columns and the deck. Given this, the global model of the bridge in the longitudinal direction, which could produce moment and shear forces in the east bent, was not possible by IDARC. Therefore, a separate model was developed to distinguish the longitudinal response of the east bent from the other part of the bridge.

In the first model, which was developed to investigate the effect of seismic forces for the whole bridge except the east bent, an element with large axial stiffness and no flexural stiffness was used for the east bent. With this assumption, the free sliding condition was provided for that location, while the vertical support was still kept. In the second model, the east bent was considered as a single cantilever column with the whole longitudinal seismic mass of the bridge. Although this assumption leads to a conservative shear demand on the east bent, there is no reason for a concern since all the results were within the acceptable range.

For the transverse direction, both the east and west bents were modelled separately and was found that the west bent was more critical than the east bent. The masses for the model of the west bent consisted of a half of the mass of the west end span and a half of the mass of the middle span. Similarly, the masses for the model of the east bent consisted of a half of the mass of the east end span and a half of the mass of the middle span.

4.4 Assumptions in the Modelling and Analyses of the Bridges

The following assumptions were made in the modelling and the analyses of the selected bridges:

- Seismic excitations were not applied in the longitudinal and transverse directions simultaneously,
- The effect of skewness was not taken into account,
- Possible deficiencies related to the reinforcement in joint connections and reinforcement lap splices were not considered,
- Foundation flexibility and soil bridge interaction were ignored,
- Torsion effects were not considered.

CHBDC allows ignoring some of these deficiencies under certain circumstances. For example, in the case of shallow superstructures (i.e. solid and voided slab bridges), if the skew parameter $\alpha = \frac{B \tan\psi}{L}$ does not exceed 1/6, and for slab-on-girder bridges, if the skew parameter $\alpha = \frac{S_p \tan\psi}{L}$ does not exceed 1/18, the analysis can be carried out by ignoring the effect of skewness. The parameters B, S_p, L, and ψ are defined as the width of a bridge, the center-to-center spacing of longitudinal girders, the span of the bridge, and the skew angle, respectively. These two conditions are satisfied in most cases of the bridges used in this study.

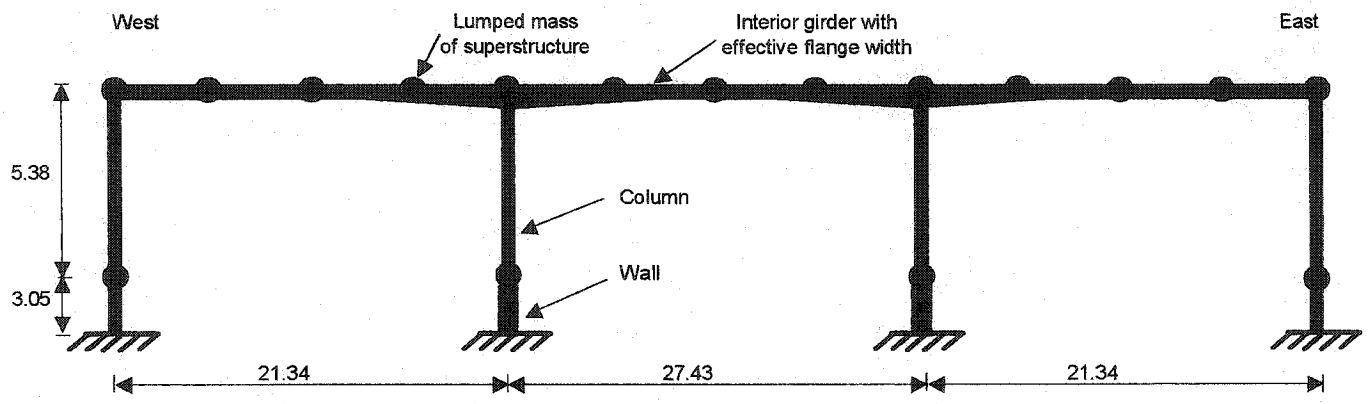

Bridge #1
Longitudinal Direction

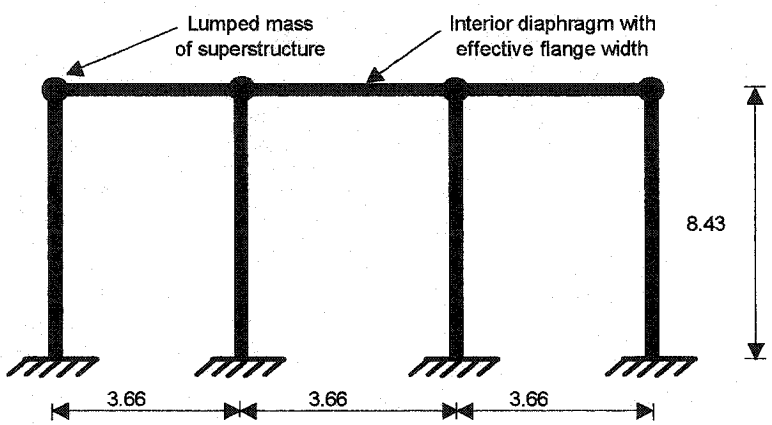

Bridge #1
East Abutment-Transverse Direction
(model #1)

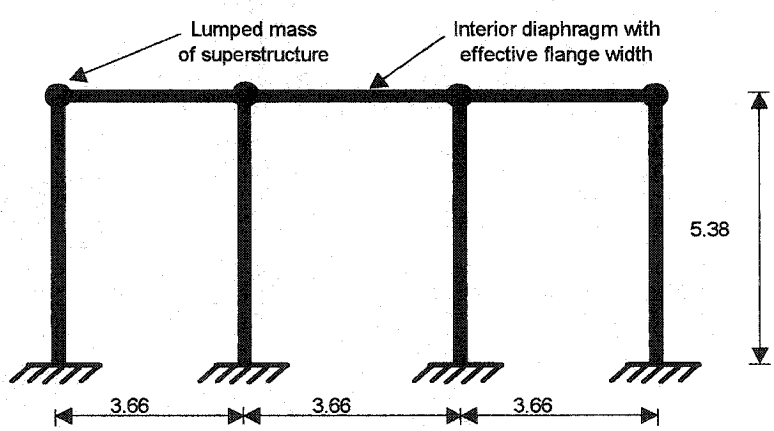

Bridge #1
East Pier-Transverse Direction
(model #2)

Note: All dimensions are in meter

Fig. 4.1 Longitudinal and transverse models of Bridge #1.

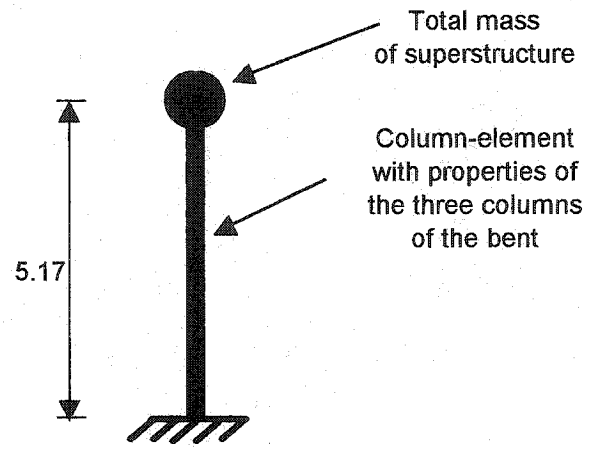

Bridge #2
Longitudinal Direction

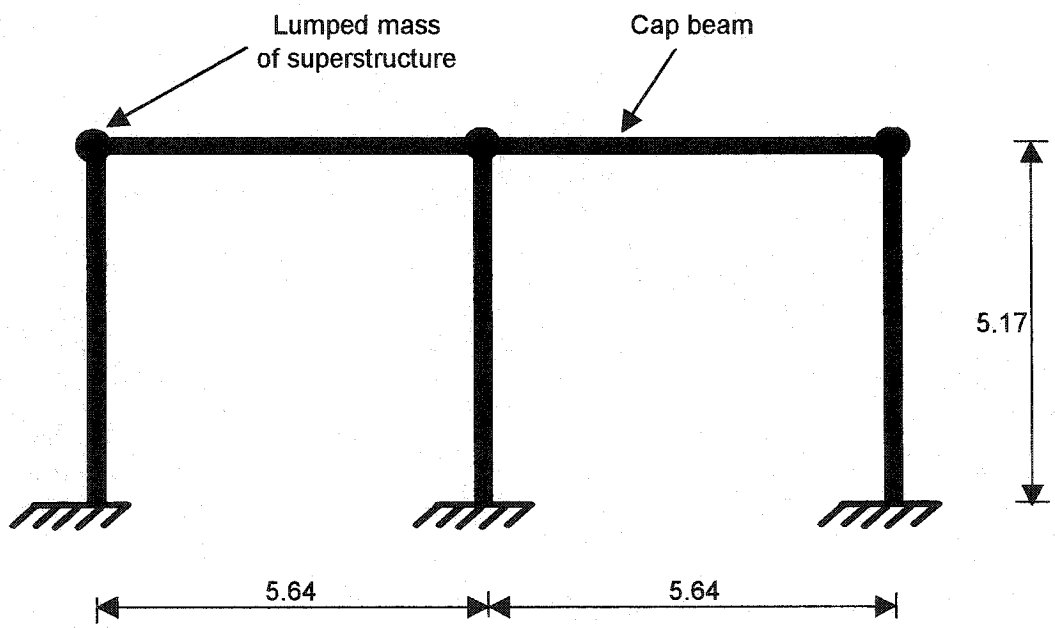

Bridge # 2
Transverse Direction

Note: All dimensions are in meter

Fig. 4.2 Longitudinal and transverse models of Bridge #2

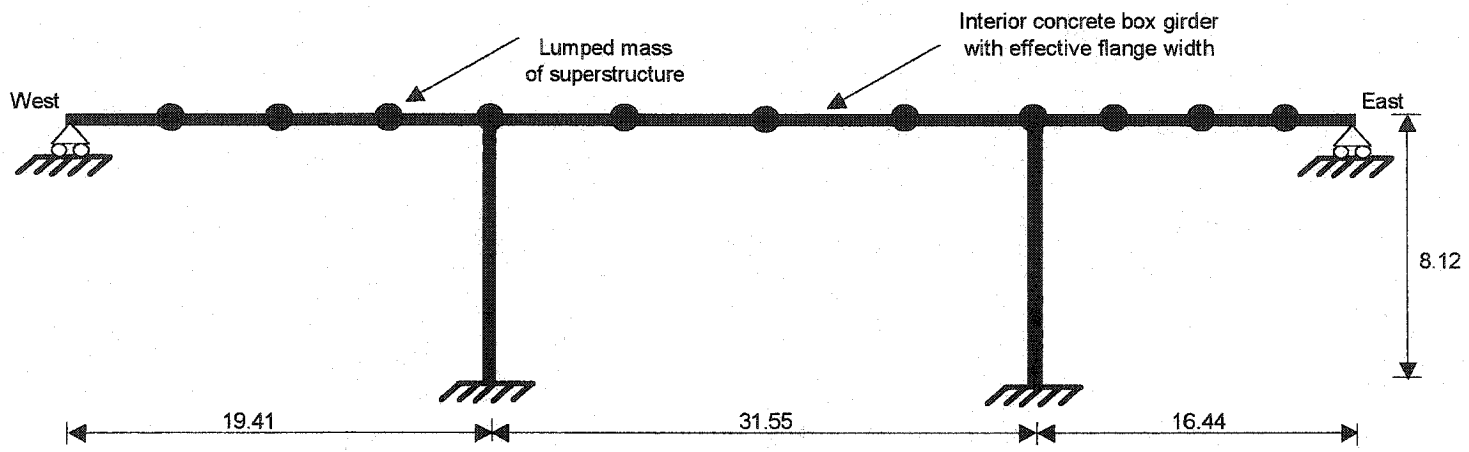

Bridge #3
Longitudinal Direction

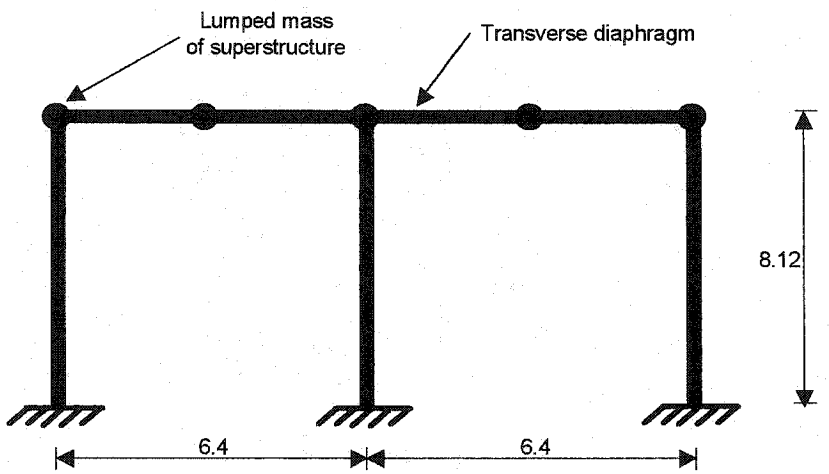

Bridge #3
East Bent-Transverse Direction

Note: All dimensions are in meter

Fig. 4.3 Longitudinal and transverse models of Bridge #3.

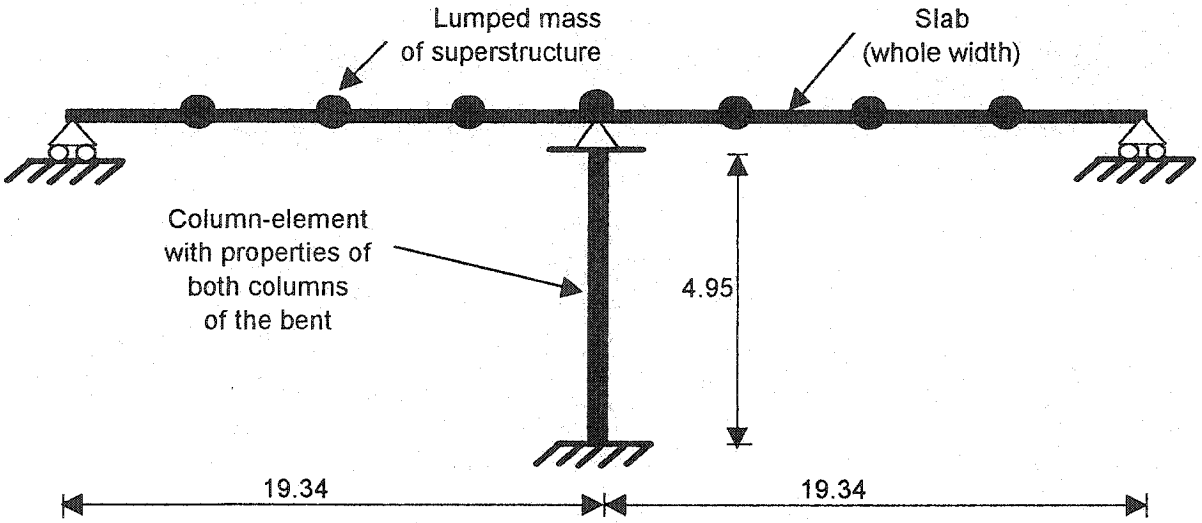

Bridge #4
Longitudinal Direction

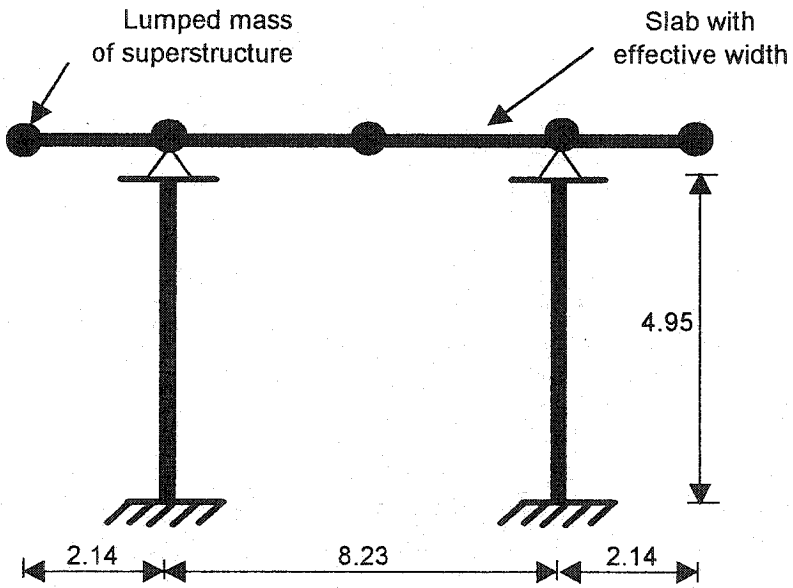

Bridge #4
Transverse Direction

Note: All dimensions are in meter

Fig. 4.4 Longitudinal and transverse models of Bridge #4.

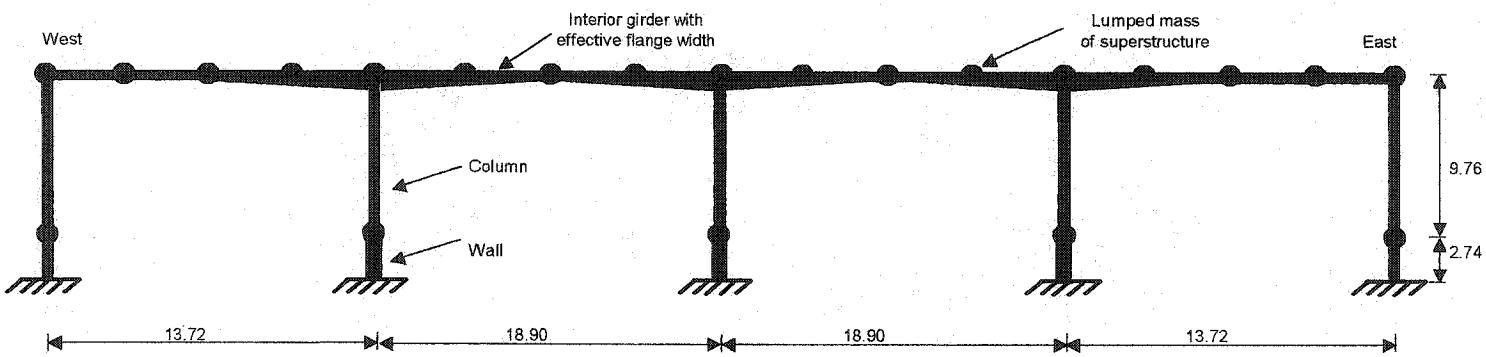

Bridge #5
Longitudinal Direction

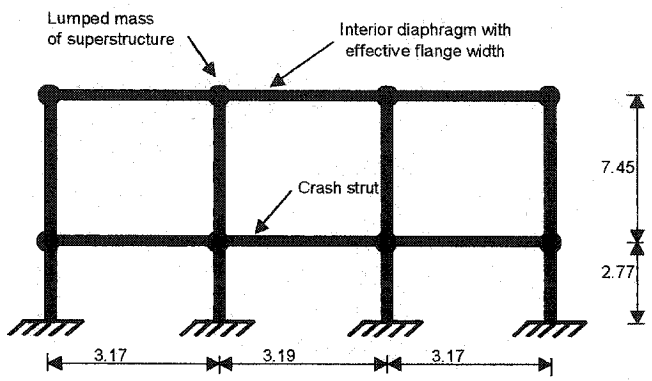

Bridge #5
Middle Bent-Transverse Direction

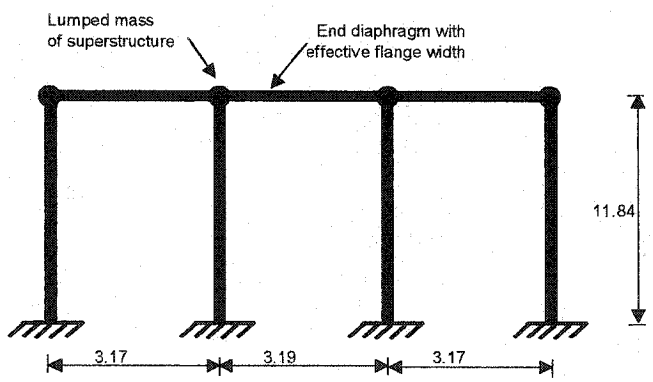

Bridge #5
Abutment-Transverse Direction

Note: All dimensions are in meter

Fig. 4.5 Longitudinal and transverse models of Bridge #5.

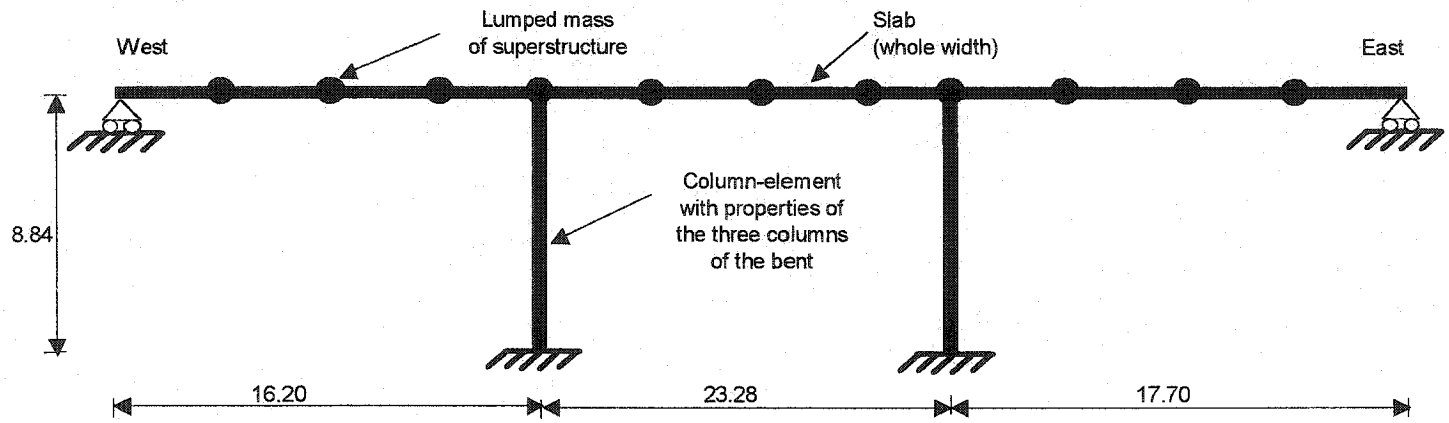

Bridge #6
Longitudinal Direction

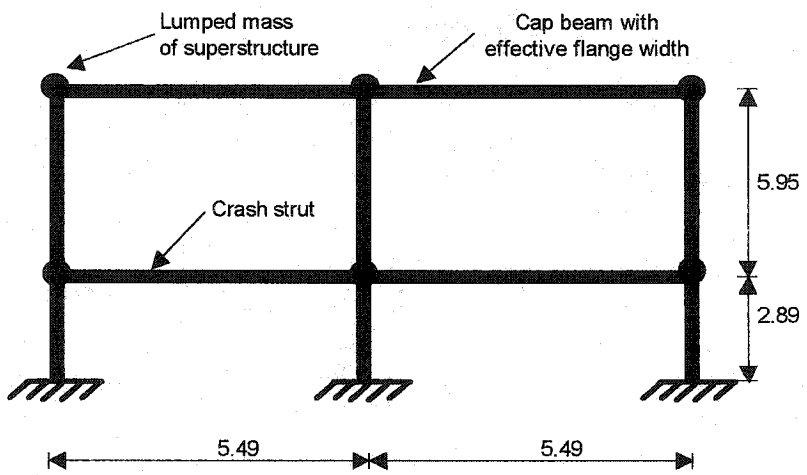

Bridge #6
East Bent-Transverse Direction

Note: All dimensions are in meter

Fig. 4.6 Longitudinal and transverse models of Bridge #6.

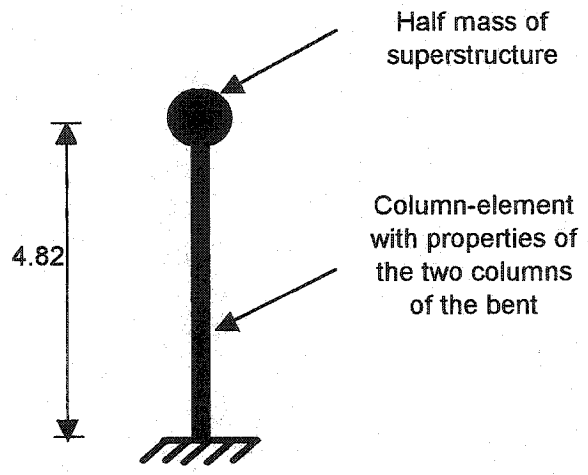

Bridge #7
Longitudinal Direction

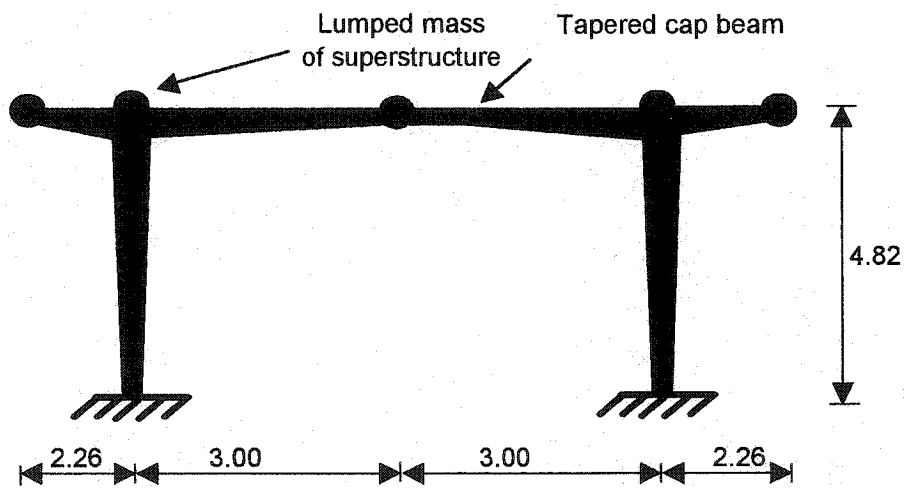

Bridge #7
Transvers Direction

Note: All dimensions are in meter

Fig. 4.7 Longitudinal and transverse models of Bridge #7.

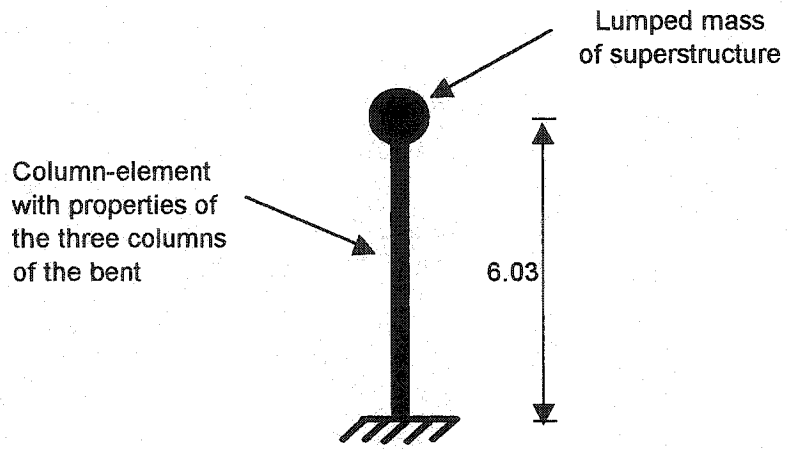

Bridge #8
East Bent-Longitudinal Direction

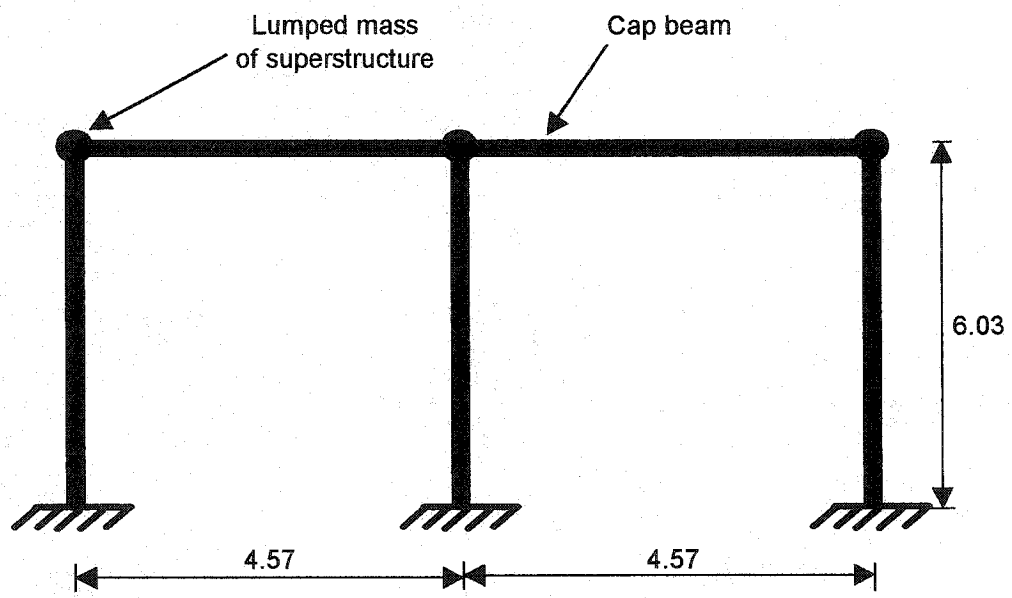

Bridge #8
East Bent-Transverse Direction

Note: All dimensions are in meter

Fig. 4.8 Longitudinal and transverse models of Bridge #8.

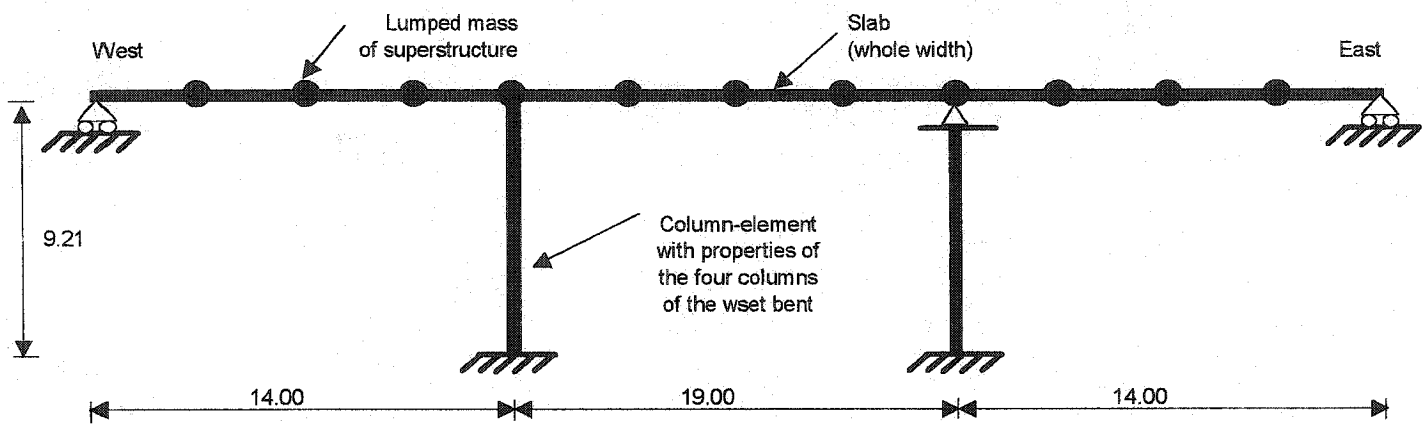

Bridge #9
Longitudinal Direction
(Model #1)

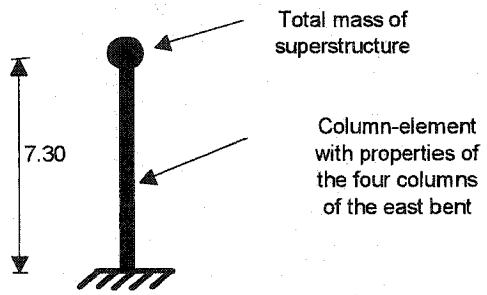

Bridge #9
East Bent-Longitudinal Direction
(Model #2)

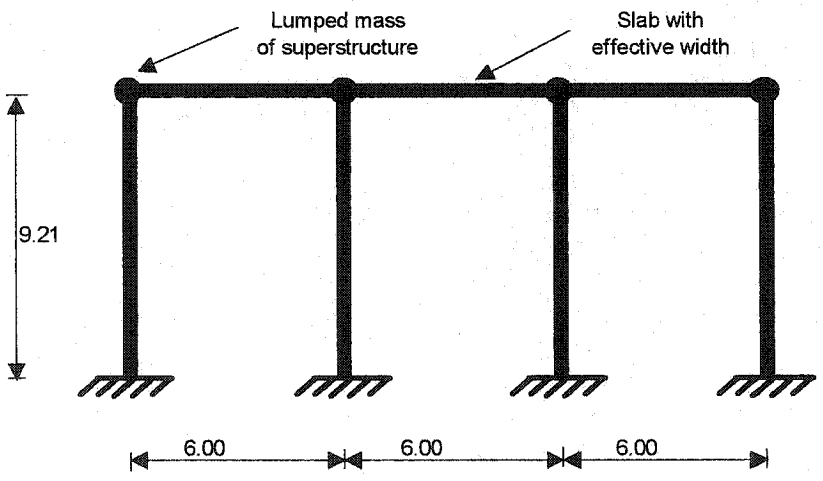

Bridge #9
West Bent-Transverse Direction

Note: All dimensions are in meter

Fig. 4.9 Longitudinal and transverse models of Bridge #9.

CHAPTER 5

MODELLING PARAMETERS

5.1 Introduction

For the purpose of the nonlinear dynamic analyses of the bridges, tri-linear moment-curvature relationships are required for the end sections of each element of the models. These relationships depend on the geometrical properties of the members, and the constitutive models of the concrete and reinforcing steel. In addition, the program requires parameters for the hysteretic model that defines the nonlinear deformations at the end sections of each member. This Chapter describes the constitutive models of the concrete and reinforcing steel, the development of the moment curvature relationships, and the control parameters of the hysteretic model used in this study.

5.2 Constitutive Model for Confined Concrete

Past earthquakes have shown that the performance of reinforced concrete bridges depends very much on the confinement of the structural members. Therefore, for the purpose of the evaluation studies, it is essential that the constitutive model of the concrete include the effect of the confinement. There are a number of strain-stress models of confined concrete. The model used in this study was that proposed by Mander et al. (1988). This model is recommended by ATC-32, CALTRANS, and FHWA (Dodd et al. 2000; Harmon et al. 2002). This model was developed for concrete sections subjected to uniaxial compressive loading, which are confined by transverse reinforcement. The model is shown in Fig. 5.1. Detailed explanations for this model can be found in Mander

et al. (1988), and Paulay and Priestley (1992), and therefore these will not be repeated here. However, it is useful to comment briefly on the main characteristics of this model. As shown in Fig. 5.1, the Mander model for confined concrete is represented by the curve that encloses the shaded area. This curve is defined by the confined concrete compressive strength, f'_{cc}, the confined concrete compressive stress, ε_{cc}, and the ultimate compressive strain, ε_{cu}, that corresponds to the first hoop fracture. As described in Mander (1988), and Paulay and Priestley (1992), these parameters can be determined using the compression stress of the concrete, f'_c, the compressive strain of the concrete, ε_c, the confinement steel ratio, ρ, the yield strength of the transverse (i.e. horizontal) reinforcement, f_{yh}, and the strain of the transverse reinforcement, ε_{sm}, at the maximum tensile stress. The values for f'_c and ρ were based on the information from the drawings. The values for f_{yh} were taken from the drawings where available, or were assumed following the CHBDC recommendations given in clause 14.6.3.3 (see Table 3.3). The remaining two parameters, i.e. ε_c and ε_{sm}, were taken as $\varepsilon_c = 0.002$, and $\varepsilon_{sm} = 0.1$.

5.3 Constitutive Model for Reinforcing Steel

Figure 5.2 shows a typical stress-strain curve for reinforcing steel. The curve consists of four segments, i.e. an initial linear elastic segment with modulus of 200 GPa, followed by a yield plateau, a strain-hardening, and finally a range in which stress drops off until fracture happens. In this study, the yield strength f_y was taken from the drawings where available, or was assumed in accordance with CHBDC recommendations given in clause 14.6.3.3 (see Table 3.3). The strain at which the hardening begins was taken as $\varepsilon_{s,hrd} = 0.01$, and the strain at the maximum stress was taken as $\varepsilon_{sm} = 0.1$. The ultimate stress was taken f_u=1.5 f_y, as suggested by Priestley (1996) for typical North American reinforcement.

5.4 Computation of Moment-Curvature Relationship

The program RCSection 1.3 (Goudreault, 2000) was used for the calculation of the moment-curvature relationships for the beams and columns. This program has the ability to model stress-strain curves for the reinforcing steel by taking into account the

effect of strain-hardening. Different compression stress-strain models for concrete are incorporated in the program. A sensitivity analysis was conducted to investigate the effects of different stress-strain models on the moment-curvature relationships. It was found that the final results, especially the yield curvatures, were relatively close.

The ultimate curvature, which is representative of the maximum deformation capacity of a section, corresponds to one of the following two cases, which is reached first:

- The specified ultimate compression strain, ε_{cu}, in the extreme fiber of the section, or
- The specified maximum strength, f_{sm}, of the longitudinal reinforcement bars.

A typical moment-curvature relationship is shown in Fig. 5.3. The computed moment-curvature relationship was simplified into a tri-linear envelope for using in IDARC. The first segment corresponds to the uncracked stiffness, the second segment corresponds to the region between cracking and yielding, and the third segment corresponds to the post-yielding range.

The calculation of the moment-curvature relationships for all the column sections was based on the gravity load on the columns. However, the axial load during earthquake motions varies with time. To investigate the effect of the axial loads on the moment-curvature relationship, sensitivity analyses were conducted for a typical section of the columns used in this study. First, a number of dynamic analyses were conducted for one of the selected bridges. From each of these analyses, the ratio of the peak axial loads (during the strong motion part of the earthquake motion) to the gravity loads was calculated. It was found that the maximum axial loads during the dynamic analyses were approximately 50% above or below the gravity loads. While this percentage depends on the geometry of the bridge, the weight of the bridge, etc., it is believed that 50% is a reasonable level of variations of the axial loads during strong earthquake motions. The next stage was the investigation of this fluctuation with regard to the moment-curvature relationships. For the decrease of the axial load down to 50% of the gravity load, a decrease of 10% to 15% was observed for the yielding strength. Naumoski et al. (1998) investigated the effects of such decrease in the yielding strength on the response

parameters (curvature ductilities and drifts), and found that these effects are not significant and can be neglected.

5.5 Hysteretic Modelling

During an earthquake event, different structural components may experience numerous deformation excursions beyond the cracking points. The inelastic response of the structural members depends significantly on the hysteretic model. IDARC uses tri-linear moment-curvature envelope with the ability to model the hysteretic characteristics such as stiffness degradation, strength deterioration, and pinching behavior. The hysteretic behavior under repeated loading is controlled by four user-defined parameters called hysteretic parameters. A brief description of these parameters is given hereafter.

5.5.1 Stiffness Degrading Parameter

This parameter defines the stiffness decay during seismic response. As shown in Fig 5.4, all unloading paths on the primary curve target a common point. This point is defined by the initial stiffness of the section prescribed by the moment-curvature envelope of the member, and HC (the indicator of stiffness decay) as the multiple of yielding moment. Based on experimental tests, the typical range for HC, is between 1.5 and 3.0 (Kunnath et al. 1994). Two extreme bonds of 0.10 and 10.0 are associated with severe degradation and negligible degradation respectively. In general, a larger value of HC means smaller stiffness degradation and vice versa. The nominal value for HC is 2.0 (Kunnath et al. 1994) and this value was used in this study.

5.5.2 Strength Deterioration Parameter

The strength deterioration is represented by two related parameters, ductility-based strength decay parameter, HBD, and energy-based strength decay parameter, HBE. The values of both the HBD and HBE parameters range between of 0.0 for negligible deterioration and 0.40 for severe deterioration. In this study, the value of 0.10 was used for both parameters to simulate the nominal degradation effects (Kunnath et al. 1994).

5.5.3 Pinching Control Parameter

Pinching behavior is either due to bond slip or crack closing (see Fig. 5.4). This effect is introduced in IDARC by the HS parameter, which ranges from 0.1 for extremely pinched loops to 1.0 for no pinching condition. The pinching effects are modelled by the program through the change of the unloading and reloading paths, when these paths are within the range between $HS \times M_y$ and $HS \times (-M_y)$, where M_y is the yielding moment of the section. The nominal value of HS=0.5 was used in this study as suggested by Kunnath et al. (1994).

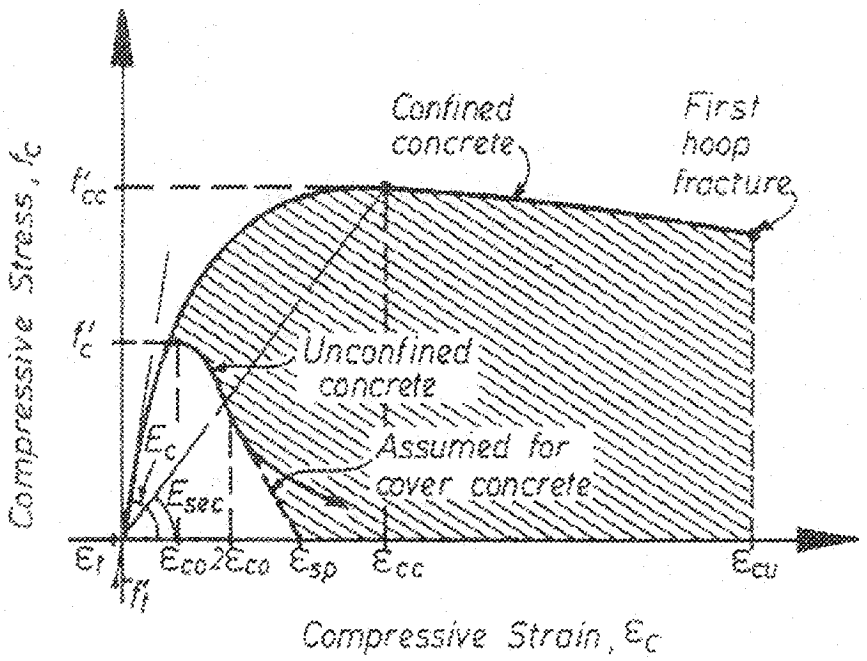

Fig. 5.1 Stress-strain model for concrete in compression (Adopted from Priestley et al. 1996).

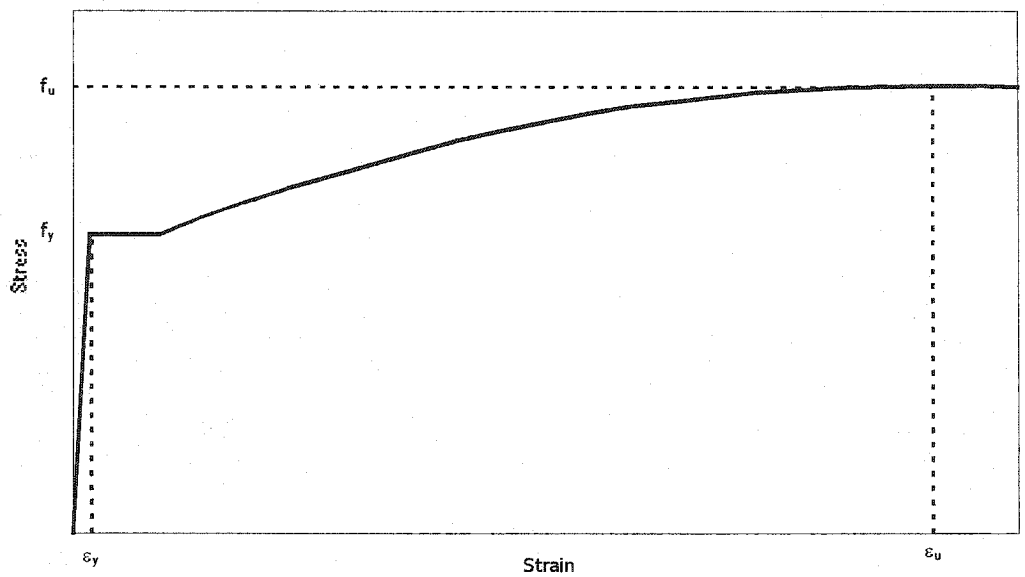

Fig. 5.2 Stress-strain model for reinforcing steel.

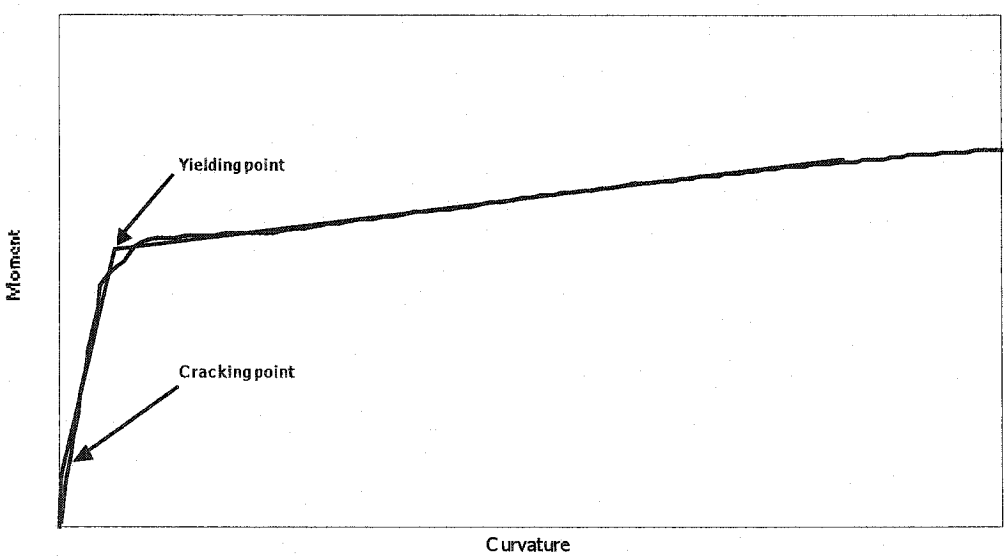

Fig. 5.3 Simplified tri-linear envelope for moment-curvature relationship.

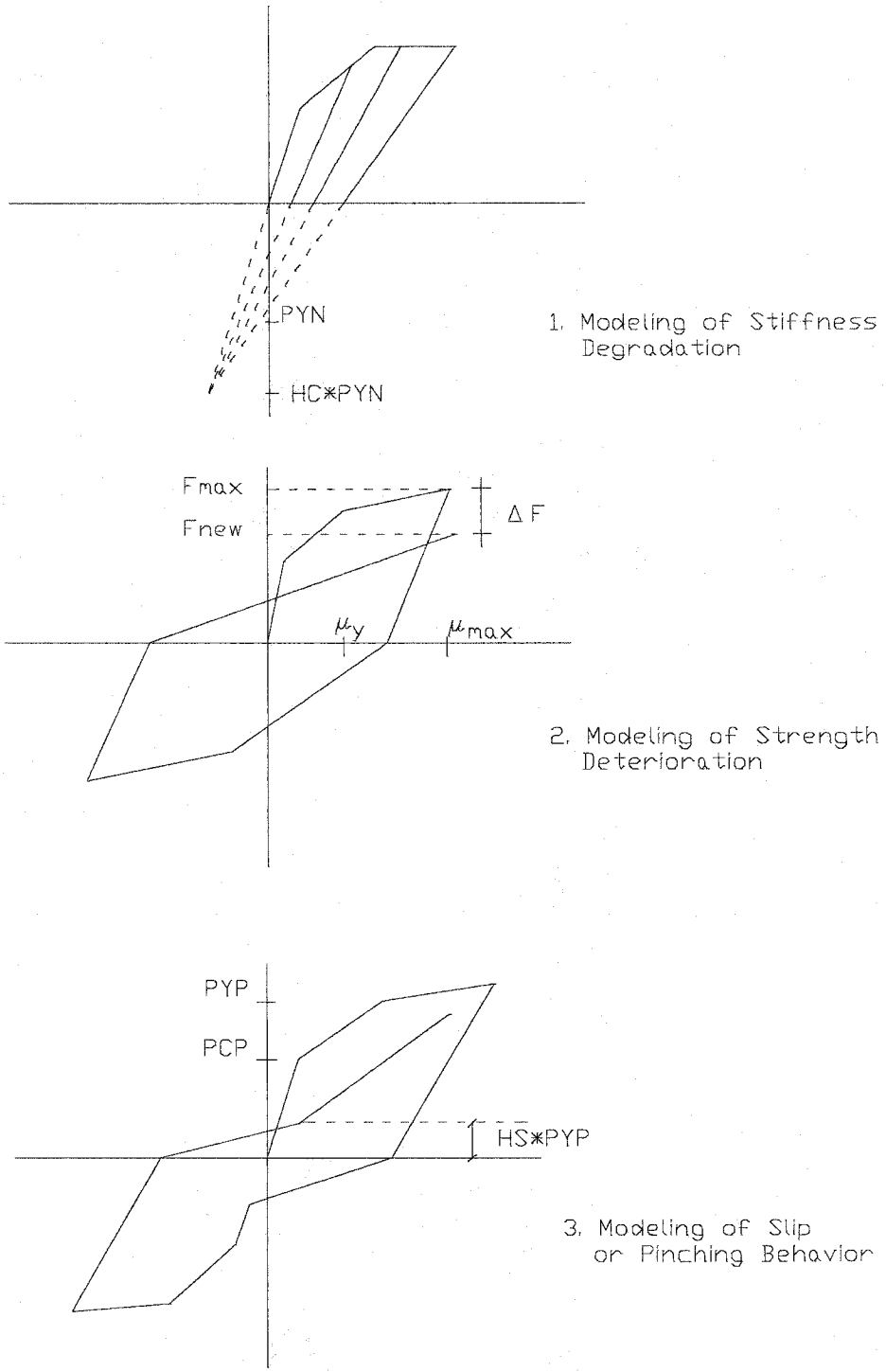

Fig. 5.4 Hysteretic model control parameters.

CHAPTER 6

INPUT GROUND MOTIONS

6.1 Earthquake Effects

According to the Canadian Highway Bridge Design Code (CHBDC), time history analysis method can be used for the seismic evaluation of existing bridges. The load factors and load combinations are as follows:

$$1.0D + 1.0EQ \tag{6.1}$$

where D = dead load

EQ = earthquake load

To do seismic analysis, input ground motions are required. These motions are represented by earthquake accelerograms. In general, it is preferable to use recorded accelerograms during strong earthquakes. However, because no recorded motions were available for the Ottawa region, artificial accelerograms were used in this study. These accelerograms were compatible with the seismic response coefficient prescribed by CHBDC. This coefficient represents the shape of the design spectrum, and is given as follows:

$$C_{sm} = \frac{1.2AIS}{T_m^{2/3}} \leq 2.5AI \tag{6.2}$$

where T_m = period of vibration of the m^{th} mode in seconds,

A = zonal acceleration ratio,

S = site coefficient,

I = importance factor, taken as I=1 for the bridges of this study.

The zonal acceleration ratio for Ottawa is A=0.2. This ratio represents the zonal acceleration ratio for probability of exceedance of 10% in 50 years. In regard to the site coefficient, two values were used in this study, i.e.

- S=1.0 (soil profile type I) for all the bridges on rock or firm soil, and,
- S=2.0 (soil profile type IV) for all the bridges on soft soil (see Table 3.2)

Figure 6.1 shows the seismic response coefficients (i.e. acceleration design spectra) for rock (S=1) and for soil (S=2), for the city of Ottawa. While CHBDC specifies a plateau in the short period range (shown with dashed line in Fig. 6.1), this was modified for the purpose of generation of artificial accelerograms, as shown in the figure.

6.2 Generation of Artificial Accelerograms

Different methods are available for the generation of artificial accelerograms. Most of these methods are based on random vibration theory, white noise, etc. In this study, the program SYNTH (Naumoski, 2001) was used for the generation of artificial accelerograms compatible with the design spectra for soft soil and for rock.

To generate an artificial accelerogram, the program requires: (i) the target spectrum, and (ii) an initial accelerogram. The program iteratively modifies the initial accelerogram until its spectrum matches the target spectrum. It is useful to mention that the program modifies only the Fourier amplitudes and not the Fourier phases of the initial accelerogram. In other words, the Fourier phases of the initial and the generated accelerograms are the same. Another important feature is that the initial and the generated accelerograms have very similar strong motion durations. In general, the initial accelerogram can be any accelerogram; it is needed just to start the generation process. However, it is recommended to use actual recorded accelerograms (i.e. accelerograms recorded during earthquakes) as initial accelerograms (Naumoski 2001).

For the purpose of this study, two ensembles of artificial accelerograms were generated, one ensemble compatible with the design spectrum for rock, and another

ensemble compatible with the design spectrum for soft soil conditions. Each ensemble consists of 15 accelerograms. To generate these accelerograms, a set of 15 accelerograms recorded during strong earthquakes around the world was used as initial accelerograms. These (initial) accelerograms were selected by Naumoski (1993) for use in Canada, and are shown in Table 6.1.

Figure 6.2 shows results from the SYNTH program, for the target spectrum representing the design spectrum for rock. It can be seen from Fig. 6.2 (a) that the generated accelerogram has a spectrum that well matches the target spectrum. Similarly, Fig. 6.3 shows results from the SYNTH program for the target spectrum representing the design spectrum for soft soil conditions. The good matching of the generated and the target spectra are evident from Fig. 6.3(a).

Table 6.1 Characteristics of the initial accelerograms used for the generation of artificial accelerograms compatible with the CHBDC design spectrum.

Record No.	Earthquake	Date	Magn.	Site	Comp.	Max. Acc. A (g)	Soil Condition
1	Imperial Valley California	May 18 1940	6.6	EL Centro	S00E	0.348	Stiff Soil
2	Kern County California	July 21 1952	7.6	Taft Lincoln School Tunnel	S69E	0.179	Rock
3	Kern County California	July 21 1952	7.6	Taft Lincoln School Tunnel	N21E	0.156	Rock
4	Borrego Mtn. California	April 8 1968	6.5	San Onofre SCE Power Plant	N57W	0.046	Stiff Soil
5	Borrego Mtn. California	April 8 1968	6.5	San Onofre SCE Power Plant	N33E	0.041	Stiff Soil
6	San Fernando California	Feb. 9 1971	6.4	3838 Lankershim Blvd., L.A.	S90W	0.15	Rock
7	San Fernando California	Feb. 9 1971	6.4	Hollywood Storage P.E. Lot, L.A.	N90E	0.211	Stiff Soil
8	San Fernando California	Feb. 9 1971	6.4	3407 6th Street, L.A.	N90E	0.165	Stiff Soil
9	San Fernando California	Feb. 9 1971	6.4	Griffith Park Observatory, L.A.	S00W	0.18	Rock
10	San Fernando California	Feb. 9 1971	6.4	234 Figueroa St., L.A.	N37E	0.199	Stiff Soil
11	Near E. Coast of Honshu. Japan	Nov. 16 1974	6.1	Kashima Harbor Works	N00E	0.07	Stiff Soil
12	Near s. Coast of Honshu. Japan	Aug. 2 1971	7	Kushiro Central Wharf	N90E	0.078	Stiff Soil
13	Monte Negro Yugoslavia	Apr. 15 1979	7	Albatros Hotel, Ulcinj	N00E	0.171	Rock
14	Mexio Earthquake	Sept. 19 1985	8.1	El Suchil, Guerrero Array	S00E	0.105	Rock
15	Mexio Earthquake	Sept. 19 1985	8.1	La Villita, Guerrero Array	N90E	0.123	Rock

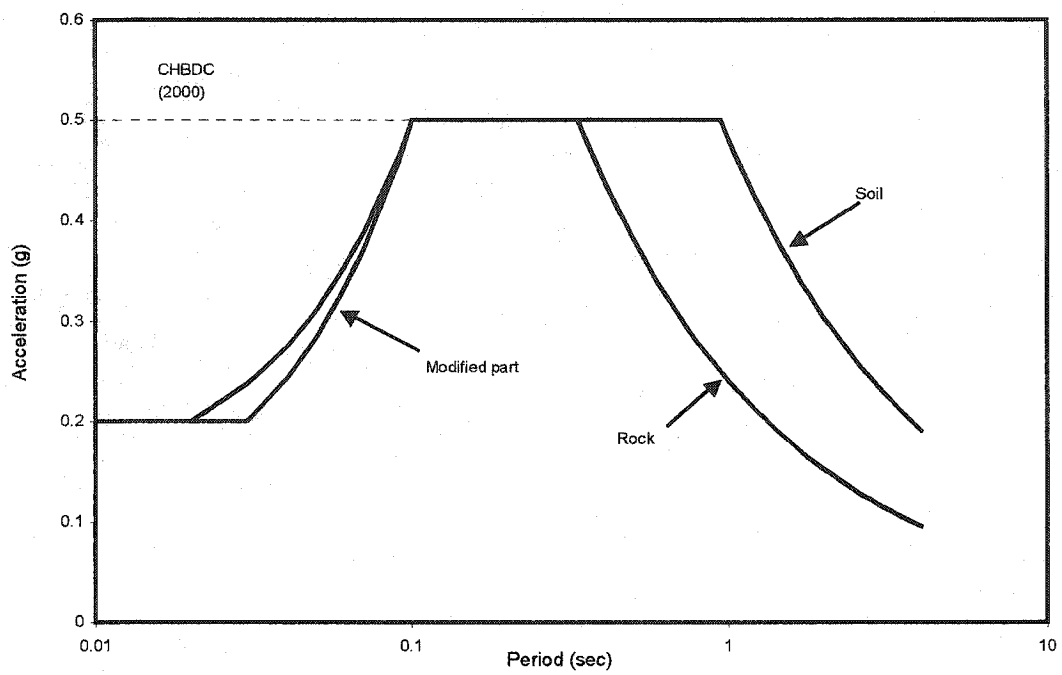

Fig. 6.1 Elastic seismic response coefficients for rock and soft soil for the City of Ottawa.

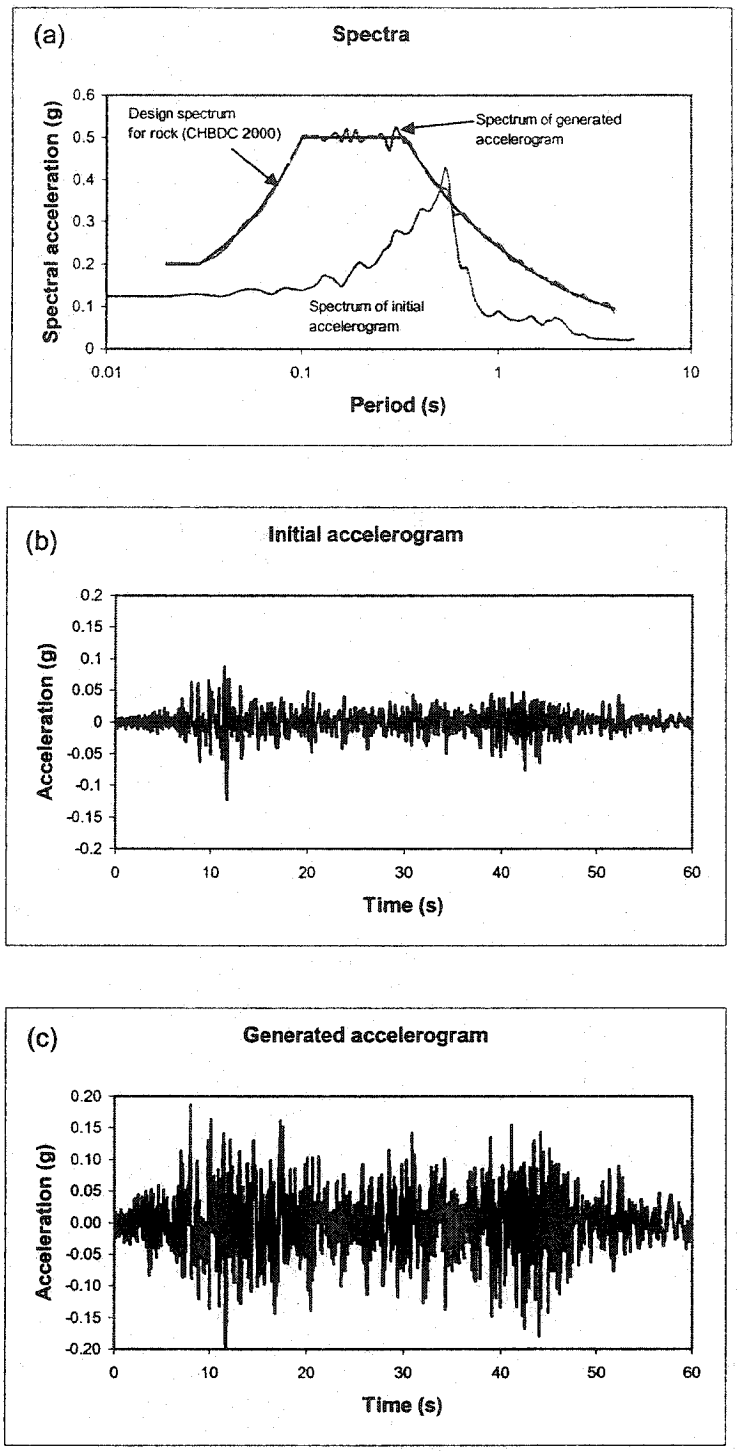

Fig. 6.2 Results from the generation of artificial accelerogram compatible with the CHBDC design spectrum for rock: (a) Spectrum of the initial accelerogram, design spectrum, and spectrum of the generated accelerogram, (b) Initial accelerogram, and (c) Generated accelerogram for rock.

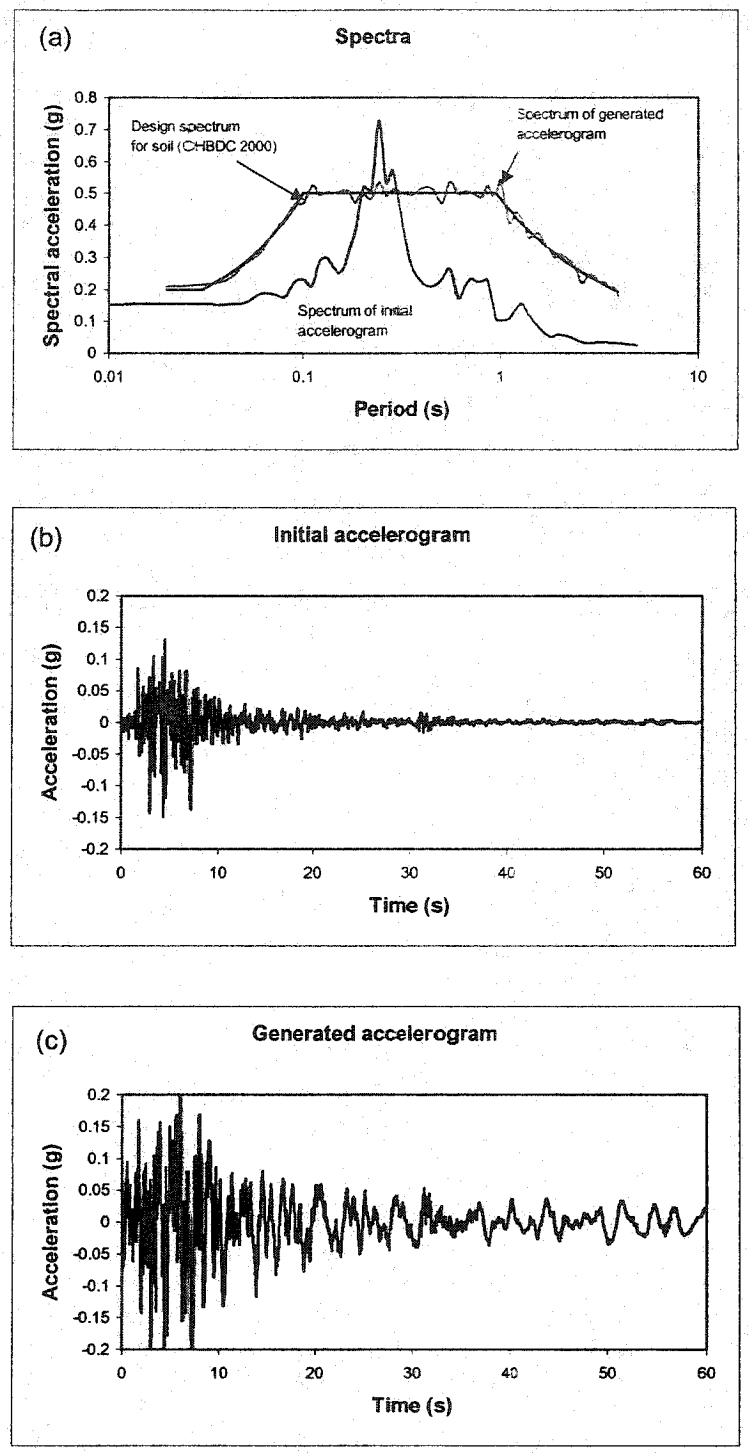

Fig. 6.3 Results from the generation of artificial accelerogram compatible with the CHBDC design spectrum for soft soil: (a) Spectrum of the initial accelerogram, design spectrum, and spectrum of the generated accelerogram, (b) Initial accelerogram, and (c) Generated accelerogram for soft soil.

CHAPTER 7

ANALYSIS AND RESULTS

7.1 Analysis of bridges

Each bridge was analyzed using the corresponding ensembles of records (i.e. for rock or soil condition). For each bridge, and each direction (longitudinal and transverse), 15 nonlinear dynamic analyses were conducted by subjecting the model simultaneously by horizontal and vertical excitations. The horizontal excitations were represented by the generated accelerograms. The vertical excitations were taken randomly from the generated horizontal accelerograms; the intensities of the vertical excitations were taken 2/3 of the actual intensity. The value of 2/3 is well accepted by engineers when expressing the intensity of vertical motions in terms of the intensity of horizontal motions at a given location.

For each model and for each of the 15 analyses, the maximum values of the lateral drift, curvature ductility, and shear demand/capacity ratios were calculated for each structural member. These values were further processed to calculate the mean (M) and the mean plus one standard deviation (M+SD) values. The evaluation of the bridge performance was based on the maximum M+SD values.

The lateral drift, curvature ductility, and shear demand are commonly used parameters in evaluation studies. The lateral drift is considered as representative of the global performance of a given structure. On the other hand, the curvature ductility and the shear demand are normally calculated for a given member or a section of a member and are considered as local deformation parameters.

In addition to the input motion, the response of highway bridges depends also on the dynamic characteristics of the bridges, i.e. natural periods (or frequencies) of vibrations. For highway bridges, the dynamic effects are primarily related to the fundamental periods. The fundamental periods for the longitudinal and transverse directions of the bridges considered in this study are listed in Table 7.1. It can be seen from this table that the periods range between 0.12 s for the transverse direction of bridge #7, to 1.36 s for the longitudinal direction of bridge #4.

The fundamental periods of the bridges constructed on rock are also shown in Fig. 7.1 together with the seismic design spectrum for rock. Similarly, Fig. 7.2 shows the fundamental periods of the bridges constructed on soft soil together with the corresponding design spectrum. These figures provide some qualitative indications of the elastic lateral forces as prescribed by the design spectra. However, these were not considered in this study. The main focus in this study were the forces and deformation parameters obtained from the nonlinear dynamic analyses.

7.2 Acceptable Levels of Response Parameters

7.2.1 Curvature Ductility Demand

The ductility can be defined as rotational, displacement, or curvature ductility. In this study, the curvature ductility was used primarily because the output from IDARC provides curvatures for each end section of each element. The curvature ductility is defined with the ratio of the maximum curvature at a section of a column or beam, φ_m, and the curvature corresponding to the flexural yielding of the column or beam, φ_y, i.e. φ_m / φ_y at the same location. The maximum curvatures, φ_m, of the columns and beams were extracted from the output files from IDARC. The yield curvatures were taken from the tri-linear envelopes of columns and beams, which are used as input in IDARC.

For the purpose of this evaluation, reference or acceptable curvature ductilities need to be known. Series of experimental studies conducted by Filiatrault (2000), Mes (1999), and Saadatmanesh (1996), showed that curvature ductility demands ranging from 2 to 5 can be considered acceptable for older reinforced concrete bridges designed according to pre-1970's codes (Heidebrecht et al. 2002; Saadatmanesh et al. 1996).

Similar findings were reported by Priestley and Seible (1994). Following Priestley et al. (1996), it was found that for a typical height and dimensions of the columns of the bridges used in this study, the range of curvature ductilities of 2 to 5 corresponds to displacement ductilities of 1.3 to 2.1. Based on this, curvature ductilities of less than 5 were considered acceptable in terms of the flexural deformations of the older bridges (i.e. bridges #1 to #8).

For new and well designed bridges, test results showed that curvature ductilities of 10 to 20 can be achieved (Watson and Park 1994; Al-Haddad 1995), which correspond to displacement ductilities of 3.5 to 6.1 for typical height and dimensions of the columns of the bridges used in this study. For the purpose of this study, the value of 20 was considered as the largest allowed curvature ductility for the new bridge (bridge #9).

7.2.2 Shear Demand/Capacity Ratio

The shear demand for each section of each member was obtained from the output files from IDARC. The calculation of shear capacity of the members was conducted following the ACI-318M-99 Building Code. The reason for using this code rather than other codes, in particular CSA standard or CHBDC, was the simplicity of the approach presented in ACI and its ability to computerize the calculations.

Shear demand/capacity ratios were calculated for both end sections of each member. A shear demand/capacity ratio of less than 1.0 indicates that the section can resist the shear force resulting from a given excitation, and the opposite is true for a value larger than 1.0.

7.2.3 Lateral Drift Demand

The drift of a column is defined as the ratio of the maximum relative displacement (of the top section relative to the bottom section) to its height in percentage. There are significant differences in the specifications of acceptable lateral drift. According to NBCC 1995, the maximum allowed drift for buildings is 2%. The Structural Engineers Association of California (SEAOC) has specified a relationship between the maximum drift and the performance level for buildings. According to SEAOC, the drift of 2.5% corresponds to a "near collapse performance". In addition, Wong et al. (1993) reported

that damage corresponding to drifts beyond 3% is difficult to be repaired. Given this, the drift of 2% was considered as acceptable value for the bridges considered in this study.

7.3 Discussion of Results

The results for the curvature ductilities are given in Table 7.2 and in Figures 7.3 to 7.11. Similarly, the shear demand/capacity ratios are presented in Table 7.3 and in Figures 7.12 to 7.20. The lateral drifts are listed in Table 7.4. It should be noted that all the results are at the M+SD level.

7.3.1 Curvature Ductility Demands

As shown in Table 7.2, the maximum curvature ductilities of the old bridges (i.e. bridges #1 to #8) range between 0.2 and 5.01. The largest value of 5.01 is at the bottom of the column of bridge #3. Large curvature ductilities were expected for this bridge because of the reduced sections at the bottom of the columns. Since the acceptable curvature ductility for old bridges is of the order of 5 (as discussed above), the flexural performance of the bridges #1 to #8 can be considered satisfactory.

The new bridge (bridge #9) has maximum ductility of 5.73. This value is well below the accepted maximum curvature ductility of 20 for new and well-designed bridges.

7.3.2 Shear Demand/Capacity Ratios

The shear demand/capacity (D/C) ratios are shown in Table 7.3. It can be seen from this table that most of D/C ratios are below 1, and only few members have D/C values larger than 1.0. As discussed earlier, D/C ratios of less than 1.0 indicates that the transverse reinforcement is sufficient to resist the shear forces during earthquake motions. Therefore, the discussion here will be primarily for the bridges with D/C values larger than 1.0, i.e. for bridge #3, bridge #6, and bridge #7 (see Table 7.3).

The maximum D/C values for the columns of bridge #3 are 1.27 for the longitudinal direction and 1.19 for the transverse direction. These values correspond to the reduced sections at the bottom of the columns. Such values were not surprising because of both, the reduced concrete section, and the insufficient transverse

reinforcement over the column portion with reduced section (i.e. spiral No. 4 with a spacing of 305 mm).

The maximum D/C value of 1.11 for bridge #6 is for the cap beam (i.e. for the transverse diaphragm) of the east bent. While the exceeding of 10% is not significant, it was also expected since no sufficient shear reinforcement is provided in the cap beam.

The maximum D/C values for the columns of bridge #7 are 1.35 for the longitudinal direction and 1.13 for the transverse direction. Such D/C values were also not surprising since these columns have very little transverse reinforcement (i.e. bars No. 3 at distance of 406 mm).

Based on this discussion, it can be concluded that the bridges #3 and #7 have inadequate shear resistance for the seismic motions used in this study.

7.3.3 Lateral Drift Demands

The lateral drift demands are shown in Table 7.4. It can be seen from this table that only bridges #3 and #4 have lateral drifts larger than the acceptable level of 2%. The drift demand for bridge #3 is 2.21% and that for bridge #4 is 2.79%. Both drift demands are for the longitudinal directions.

The drift of 2.21% for bridge #3 is due to the reduced sections at the bottom of the columns. This drift is slightly larger than the acceptable level 2%, and is not considered as critical for the seismic safety of bridge #3.

The drift of 2.79% for bridge #4 is of more concern. This drift is due to the fact that all the seismic forces in the longitudinal direction are resisted by the two columns of the bent. In the transverse direction, the drift is 1.27%, and is much smaller than that in the longitudinal direction. This is because the bent is stiffer in the transverse direction, and also because only a half of the seismic forces of the bridge are resisted by the bent, and the other half by the abutments.

In a summary, only bridge #4 is considered to be not satisfactory in terms of the lateral drift demand.

Table 7.1 Fundamental periods for the selected bridges.

Bridge No.	Fundamental period (sec)	
	Longitudinal direction	Transverse direction
1	0.27	0.2 East bent 0.15 East abutment (see Fig. 3.1)
2	0.45	0.14
3	0.75	0.75
4	1.36	0.96
5	0.69	0.79 Bent "A" 0.41 Bent "C" (see Fig. 3.5)
6	1.08	0.55
7	0.59	0.12
8	0.8 East bent 0.6 West bent	0.30 East bent 0.22 West bent (see Fig. 3.8)
9	0.55	0.54

Table 7.2 Maximum M+SD curvature ductility demands for the selected bridges.

Bridge No.	Substructure				Superstructure	
	Column		Crash beam	Cap beam	Longitudinal direction	Transverse direction
	Longitudinal direction	Transverse direction				
1	1.05	0.66	---	---	0.2	4.10
2	1.50	0.23	---	0.22	Steel beam	---
3	5.01	4.12	---	---	0.70	0.47
4	2.71	1.13	---	---	0.40	0.0
5	1.00	0.71	0.81	---	0.30	0.40
6	1.36	0.88	3.21	---	0.60	0.64
7	1.37	0.23	---	0.24	Steel girder	---
8	1.12	0.53	---	0.78	Concrete precast girder	---
9	5.73	1.05	---	---	0.80	0.66

Table 7.3 Maximum M+SD shear demand/capacity ratios for the selected bridges.

Bridge No.	Substructure				Superstructure	
	Column		Crash beam	Cap beam	Longitudinal direction	Transverse direction
	Longitudinal direction	Transverse direction				
1	0.53	1.09	---	---	0.30	0.63
2	0.29	0.18	---	0.46	Steel beam	---
3	1.27	1.19	---	---	0.60	0.16
4	0.26	0.25	---	---	0.30	0.07
5	0.17	0.47	0.47	---	0.20	0.27
6	0.25	0.29	0.34	---	0.30	1.11
7	1.35	1.13	---	0.18	Steel girder	---
8	0.27	0.35	---	0.79	Concrete precast girder	---
9	0.33	0.32	---	---	0.20	0.34

Table 7.4 Maximum M+SD drift demands (in %).

Bridge No.	Maximum drift ratio (%)	
	Longitudinal direction	Transverse direction
1	0.19	0.19
2	1.01	0.06
3	2.21	1.97
4	2.79	1.27
5	0.49	0.45
6	0.99	0.52
7	1.14	0.05
8	0.99	0.22
9	1.99	0.66

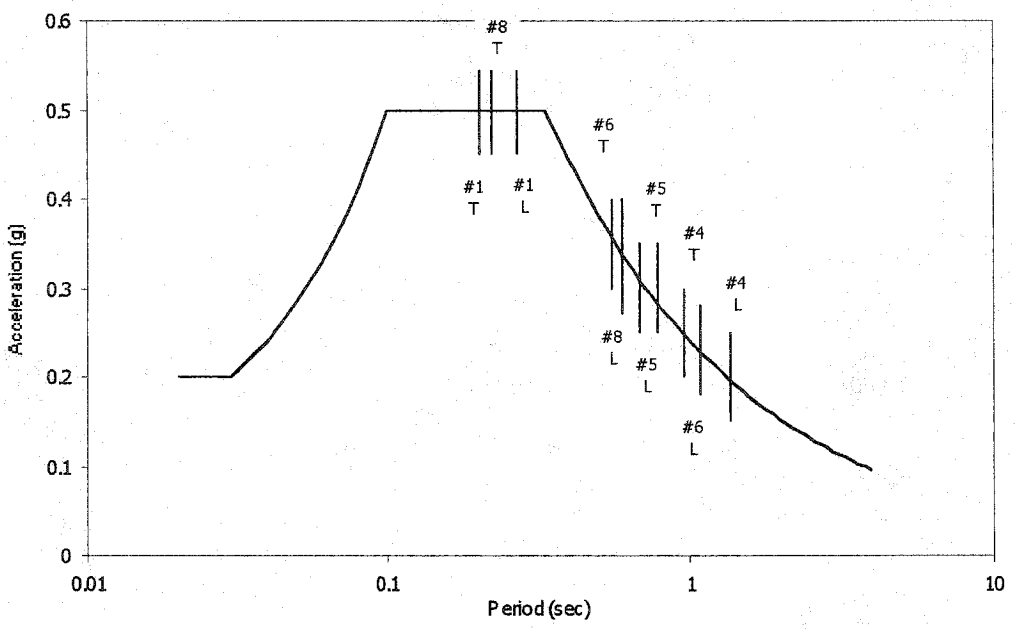

Fig. 7.1 Longitudinal and transverse fundamental periods of the selected bridges constructed on rock.

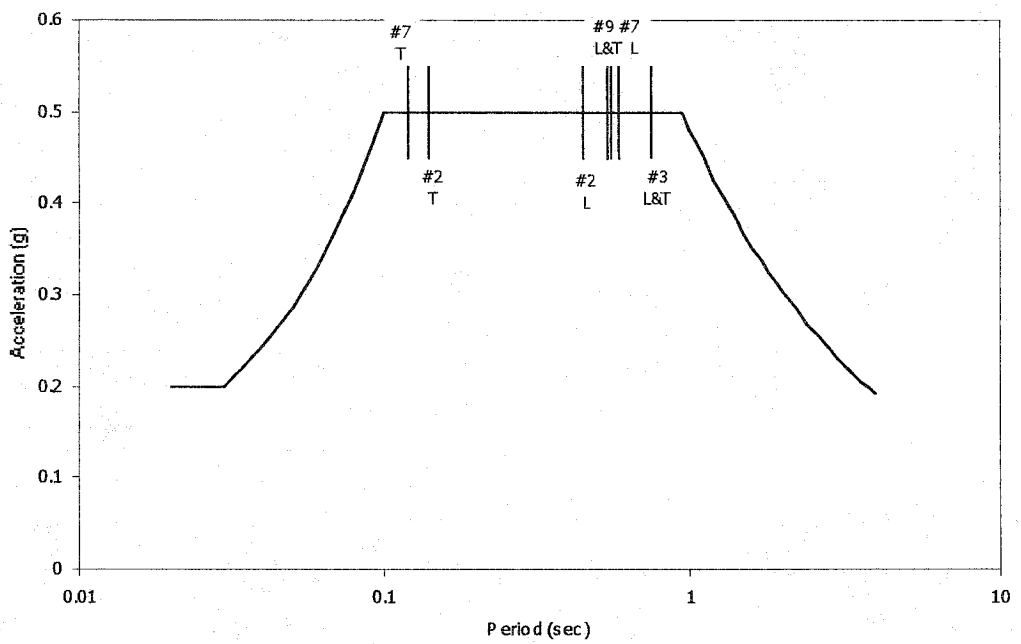

Fig. 7.2 Longitudinal and transverse fundamental periods of the selected bridges constructed on soft soil.

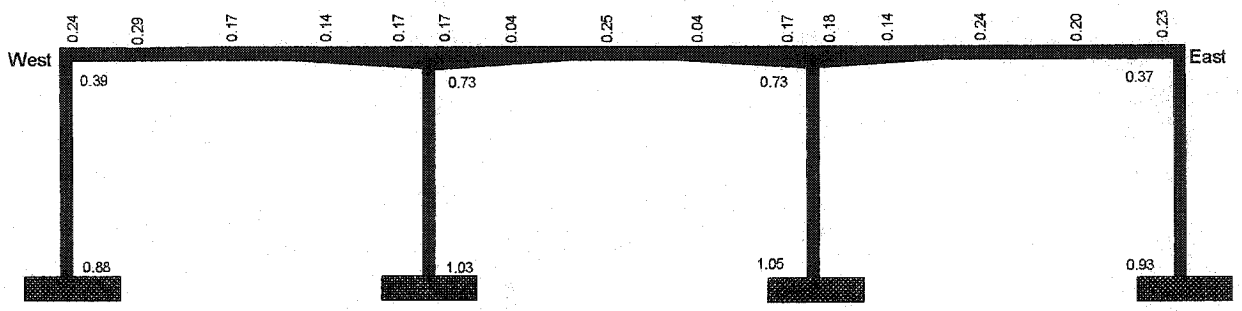

Bridge # 1
Longitudinal Direction

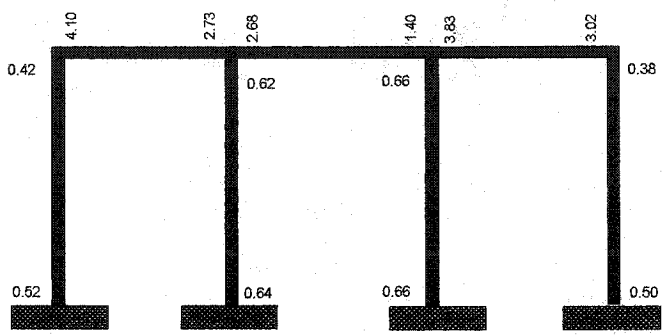

Bridge # 1
East Bent-Transverse Direction

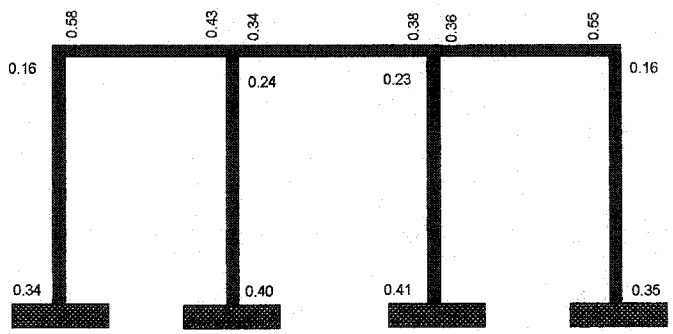

Bridge # 1
East Abutment-Transverse Direction

Fig. 7.3 Maximum M+SD curvature ductility demands for Bridge #1.

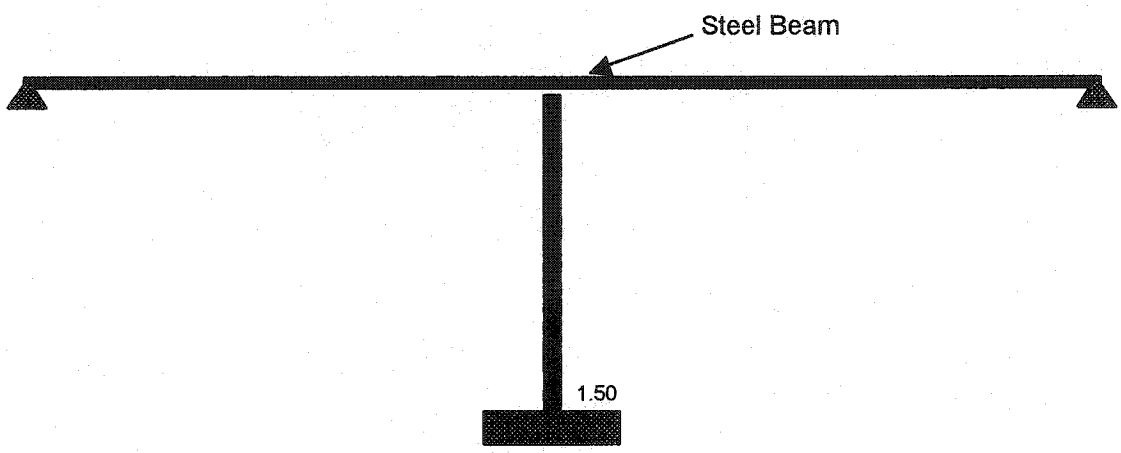

Bridge # 2
Longitudinal Direction

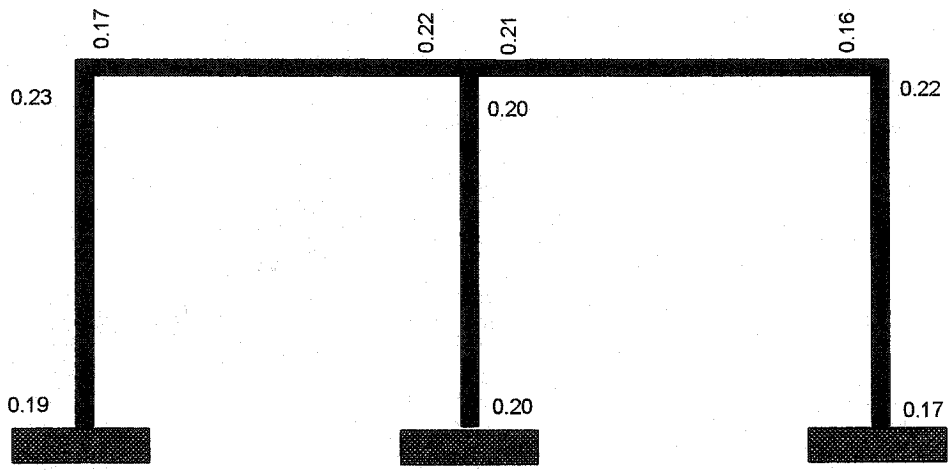

Bridge # 2
Transverse Direction

Fig. 7.4 Maximum M+SD curvature ductility demands for Bridge #2.

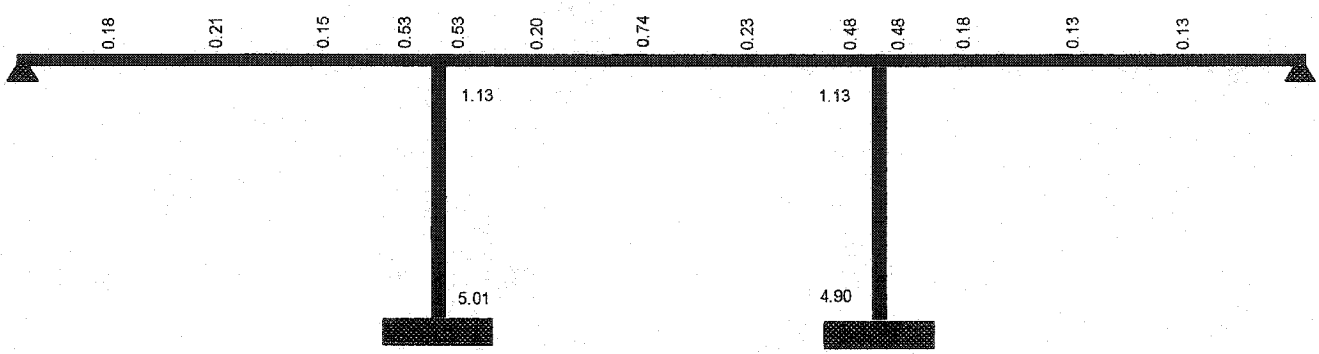

Bridge # 3
Longitudinal Direction

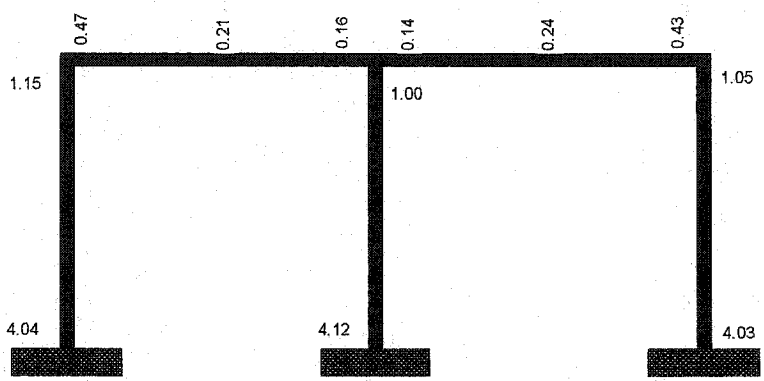

Bridge # 3
West bent-Transverse Direction

Fig. 7.5 Maximum M+SD curvature ductility demands for Bridge #3.

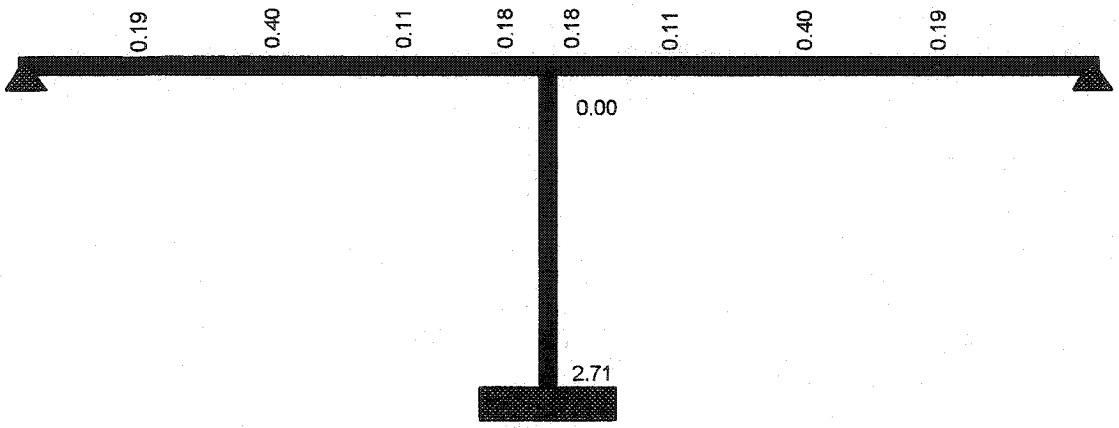

Bridge # 4
Longitudinal Direction

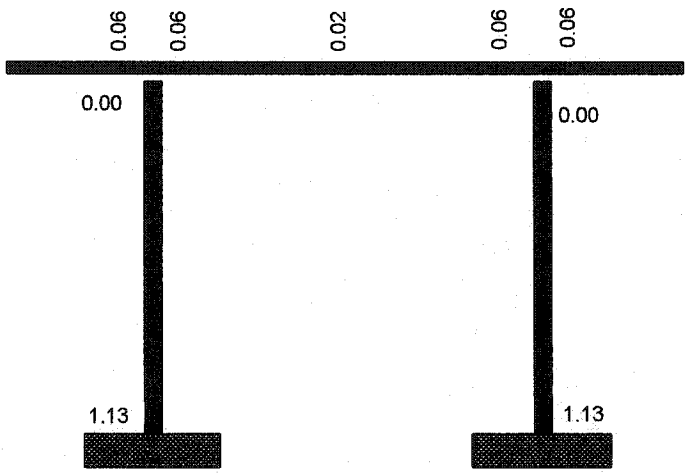

Bridge # 4
Transverse Direction

Fig. 7.6 Maximum M+SD curvature ductility demands for Bridge #4.

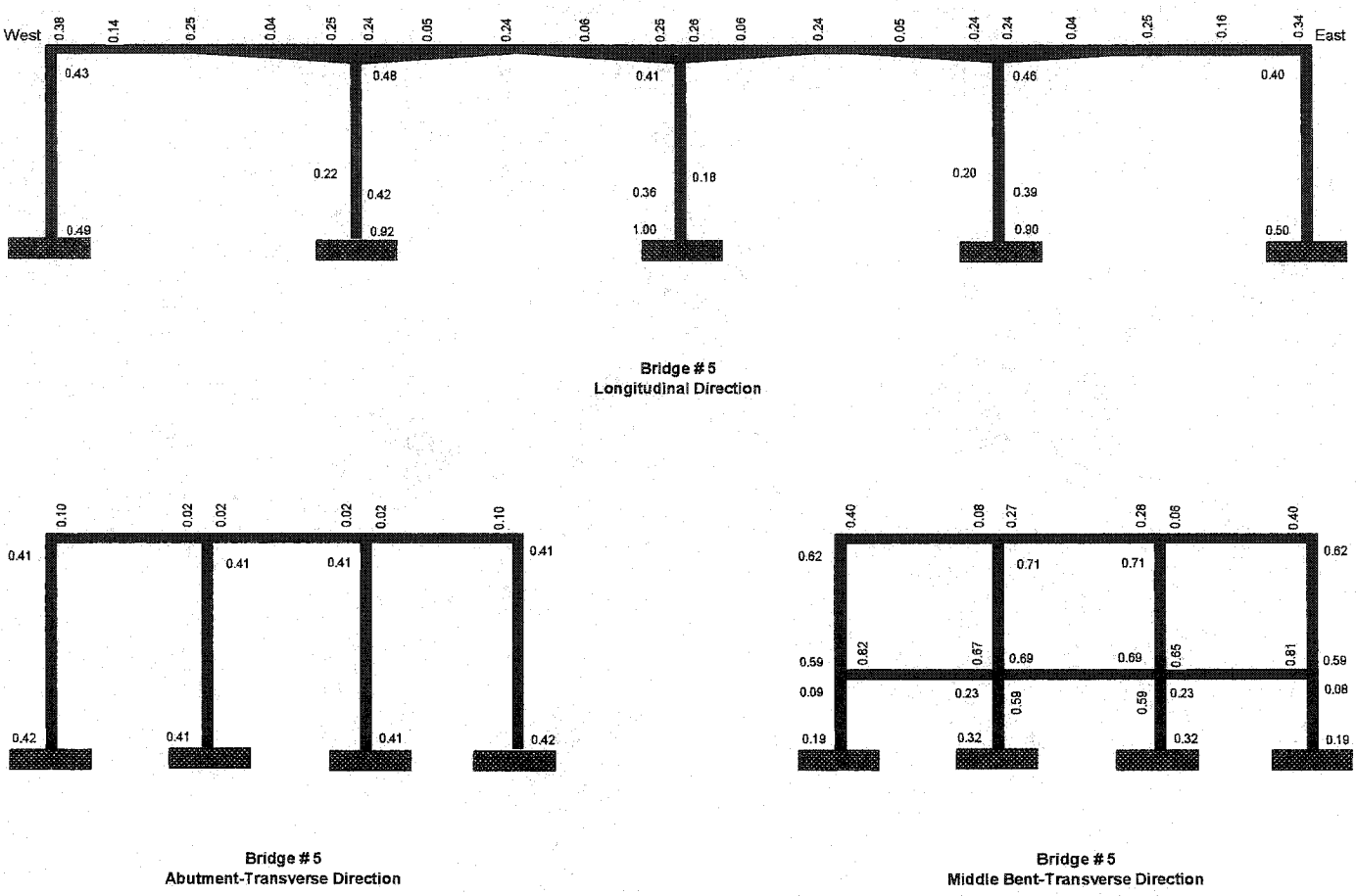

Fig. 7.7 Maximum M+SD curvature ductility demands for Bridge #5.

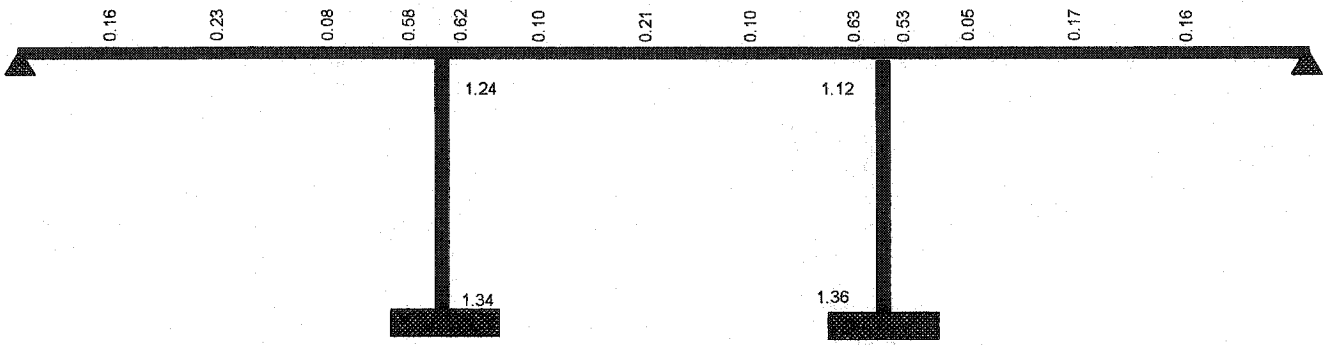

Bridge # 6
Longitudinal Direction

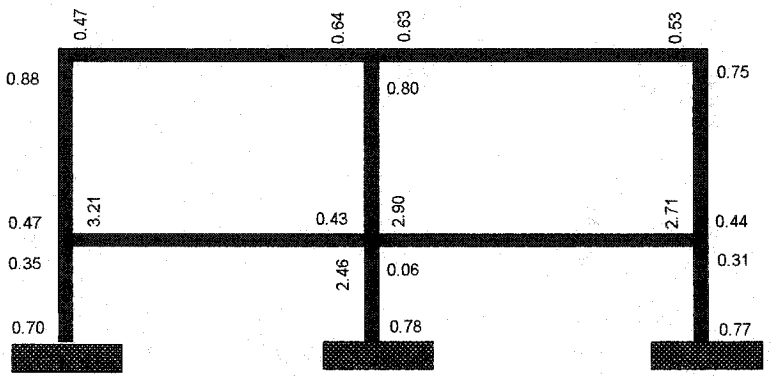

Bridge # 6
Transverse Direction

Fig. 7.8 Maximum M+SD curvature ductility demands for Bridge #6.

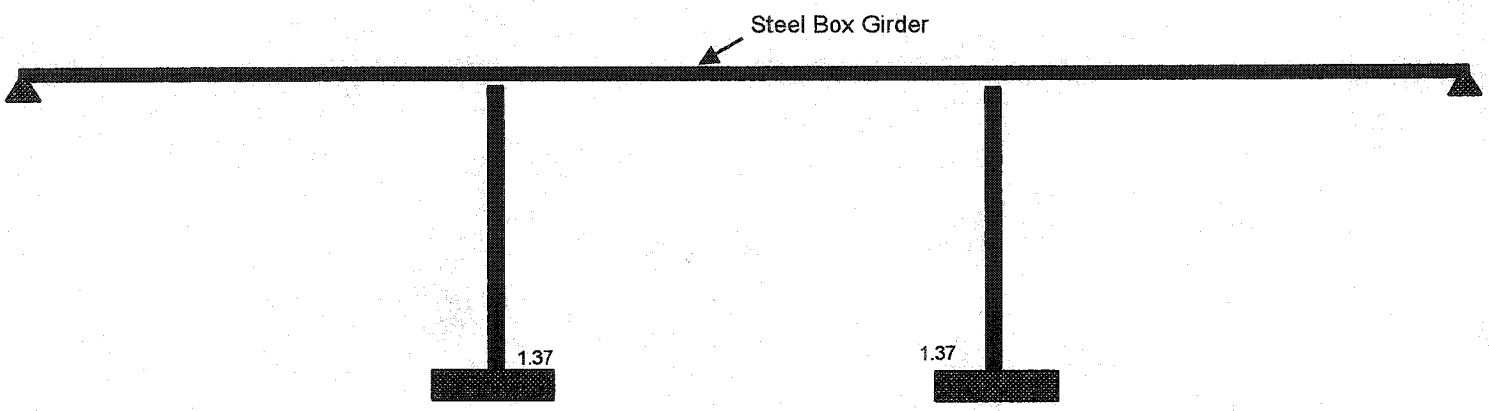

Bridge # 7
Longitudinal Direction

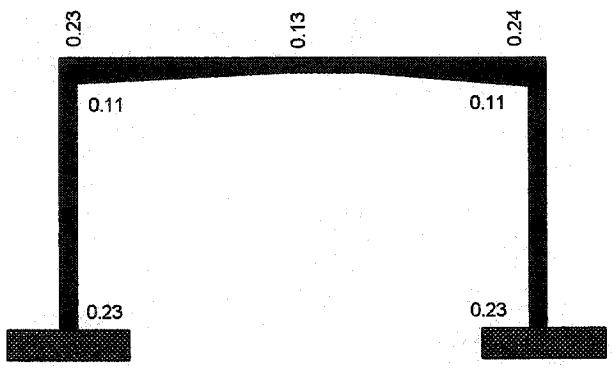

Bridge # 7
Transvers Direction

Fig. 7.9 Maximum M+SD curvature ductility demands for Bridge #7.

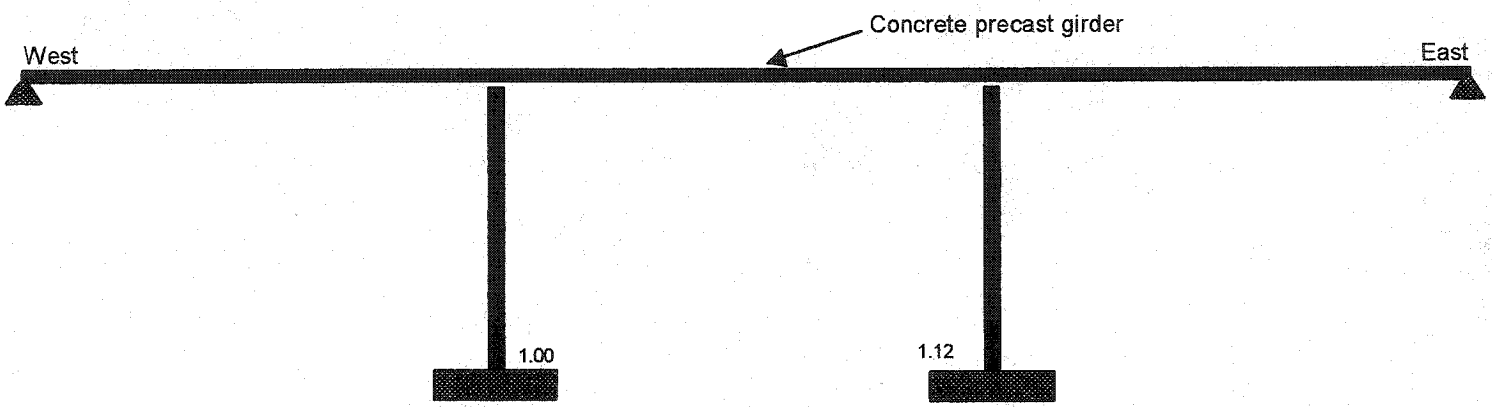

Bridge # 8
Longitudinal Direction

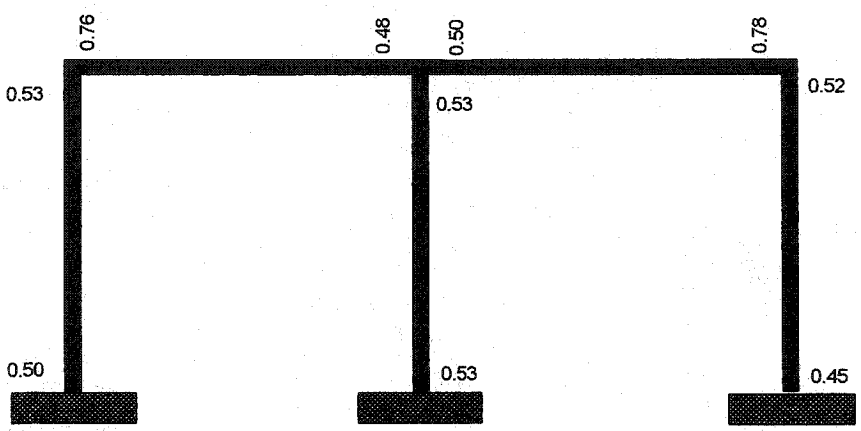

Bridge # 8
East Bent-Transverse Direction

Fig. 7.10 Maximum M+SD curvature ductility demands for Bridge #8.

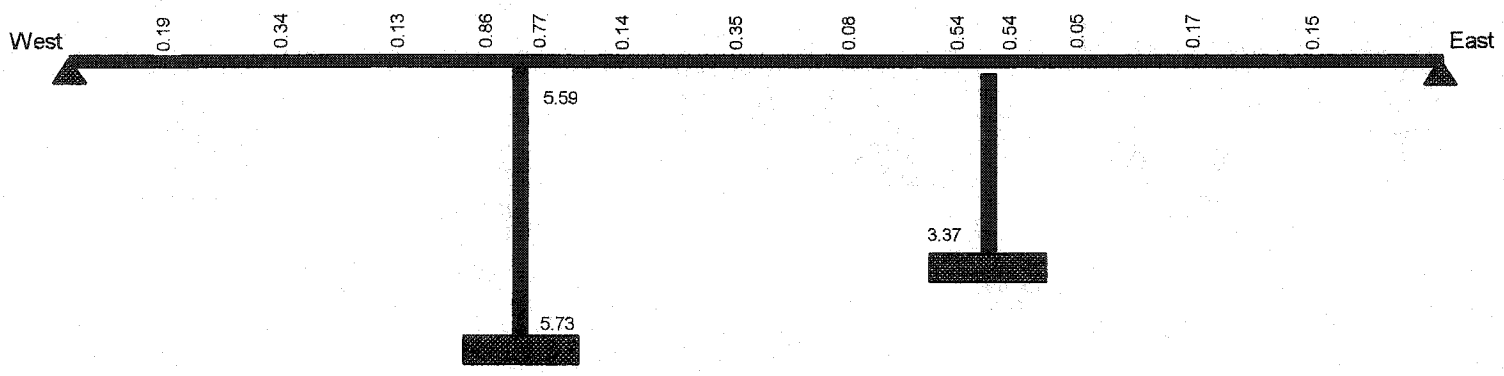

Bridge # 9
Longitudinal Direction

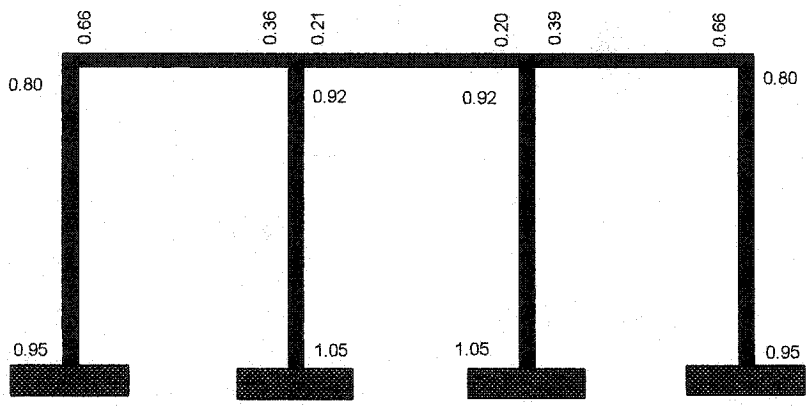

Bridge # 9
West Bent-Transverse Direction

Fig. 7.11 Maximum M+SD curvature ductility demands for Bridge #9.

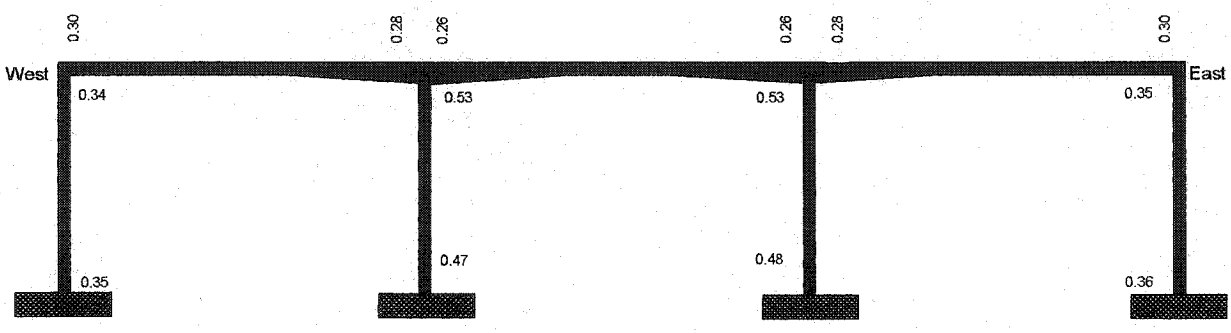

Bridge # 1
Longitudinal Direction

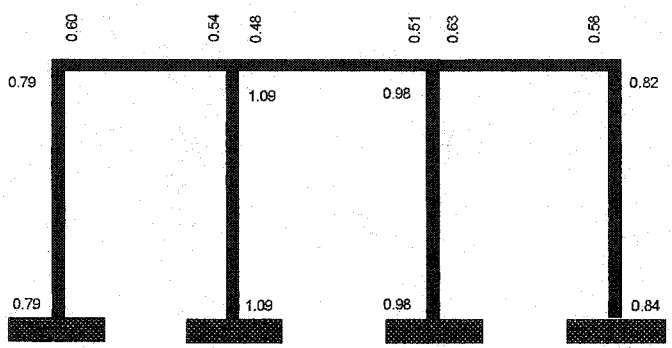

Bridge # 1
East Bent-Transverse Direction

Fig. 7.12 Maximum M+SD shear demand/capacity ratios for Bridge #1.

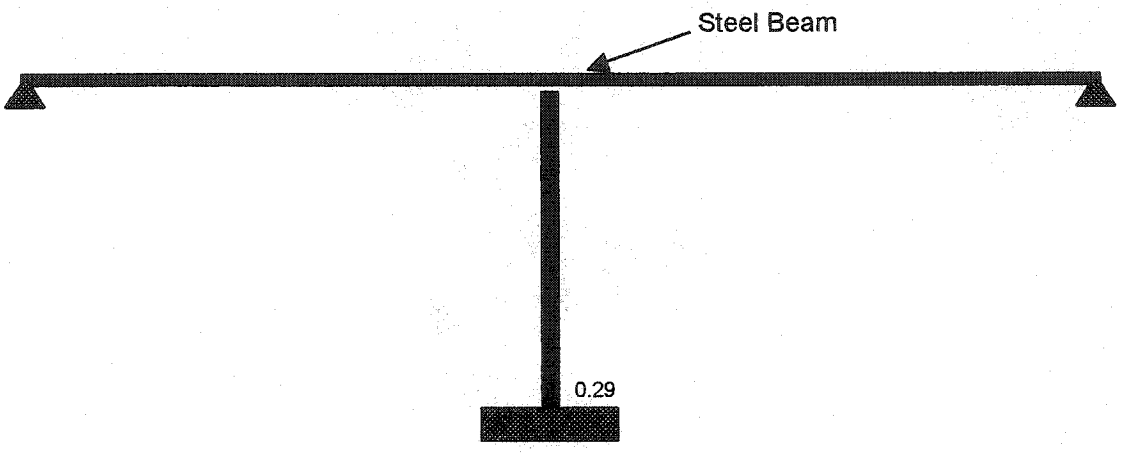

Bridge # 2
Longitudinal Direction

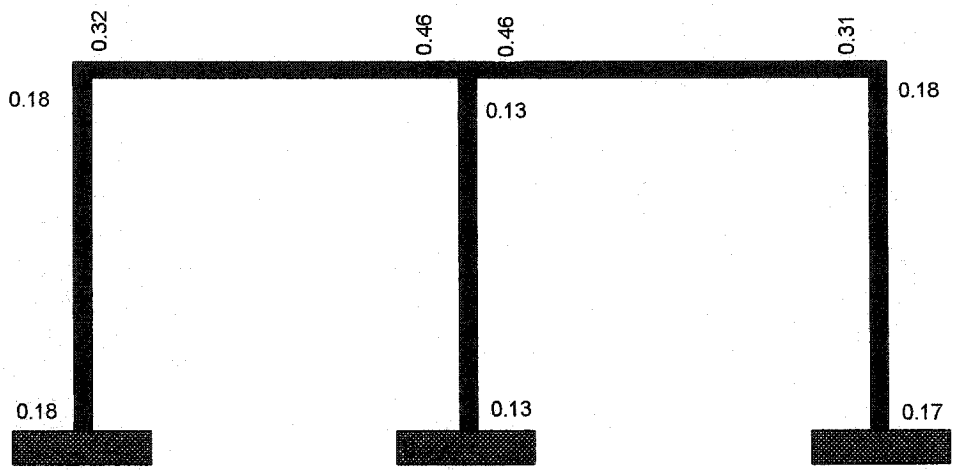

Bridge # 2
Transverse Direction

Fig. 7.13 Maximum M+SD shear demand/capacity ratios for Bridge #2.

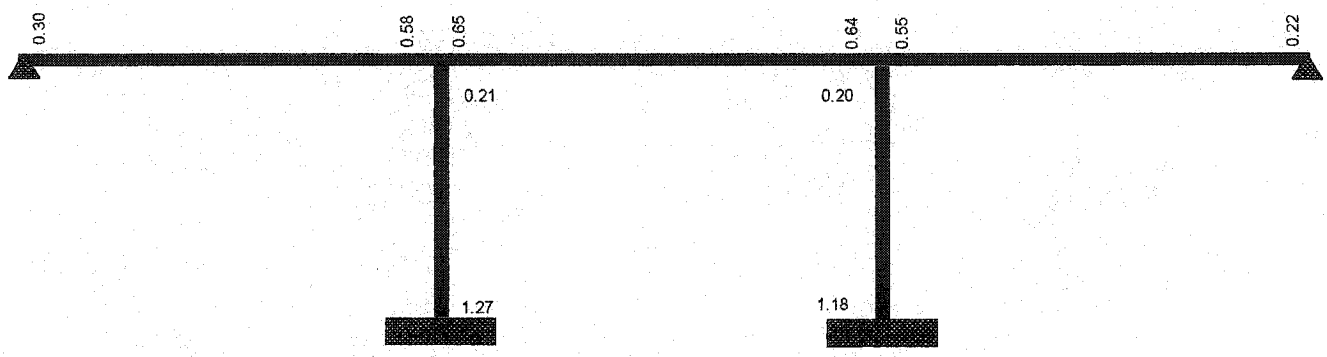

Bridge # 3
Longitudinal Direction

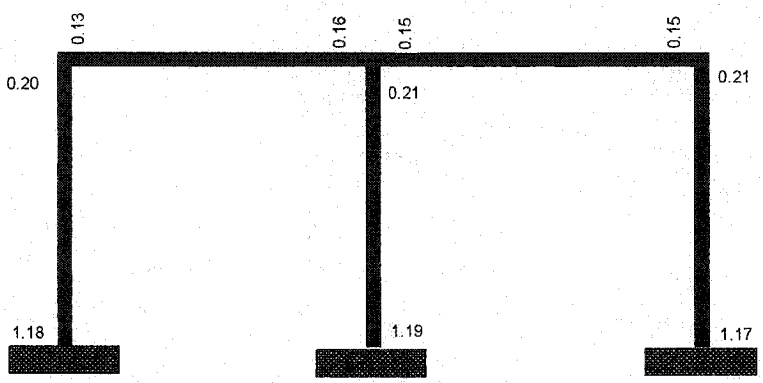

Bridge # 3
West bent-Transverse Direction

Fig. 7.14 Maximum M+SD shear demand/capacity ratios for Bridge #3.

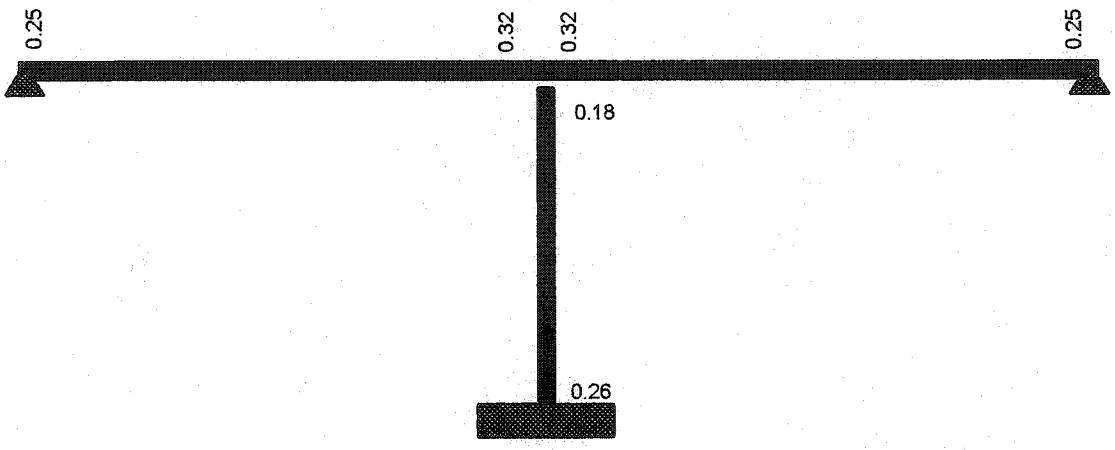

Bridge # 4
Longitudinal Direction

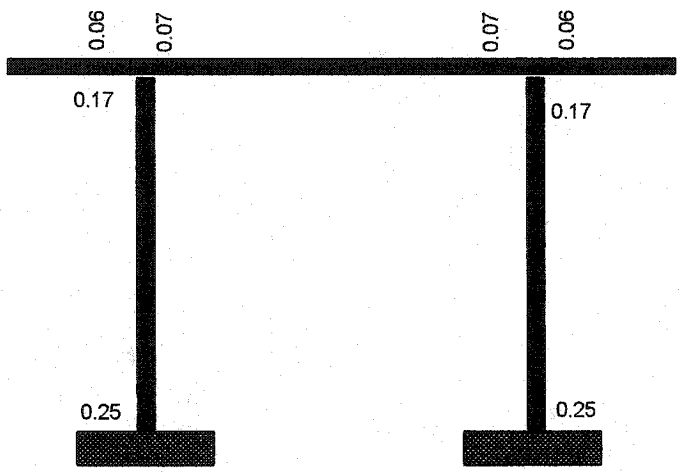

Bridge # 4
Transverse Direction

Fig. 7.15 Maximum M+SD shear demand/capacity ratios for Bridge #4.

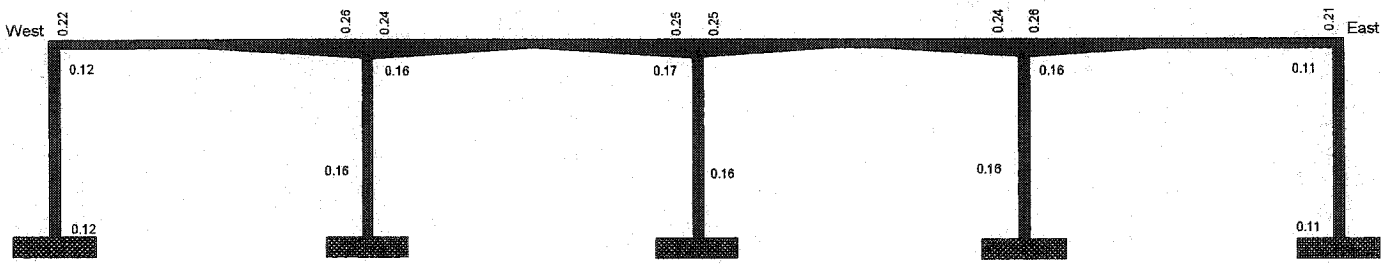

Bridge # 5
Longitudinal Direction

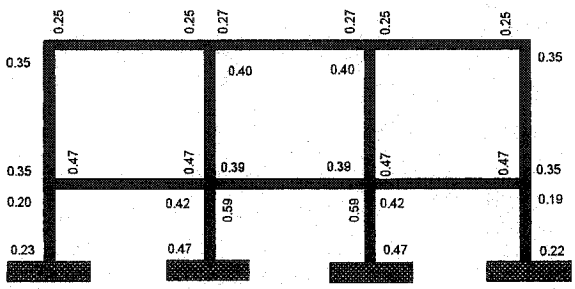

Bridge # 5
Middle Bent-Transverse Direction

Fig. 7.16 Maximum M+SD shear demand/capacity ratios for Bridge #5.

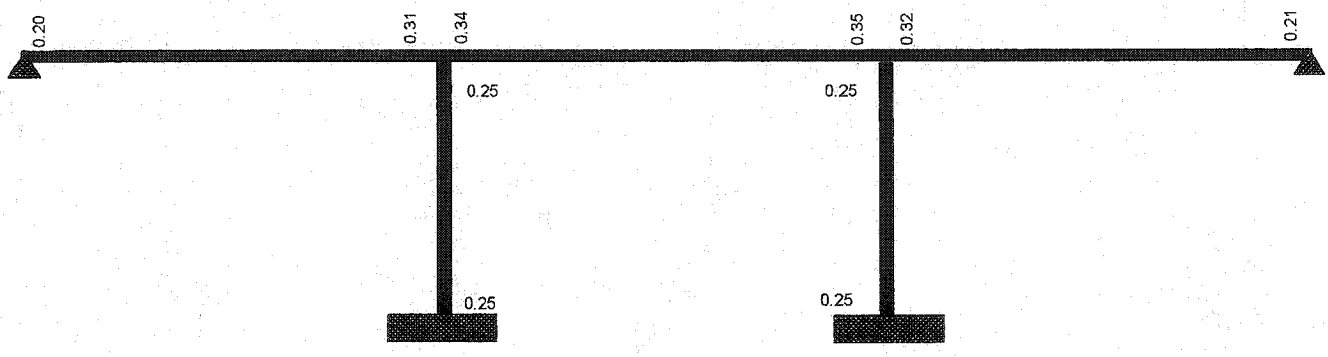

Bridge # 6
Longitudinal Direction

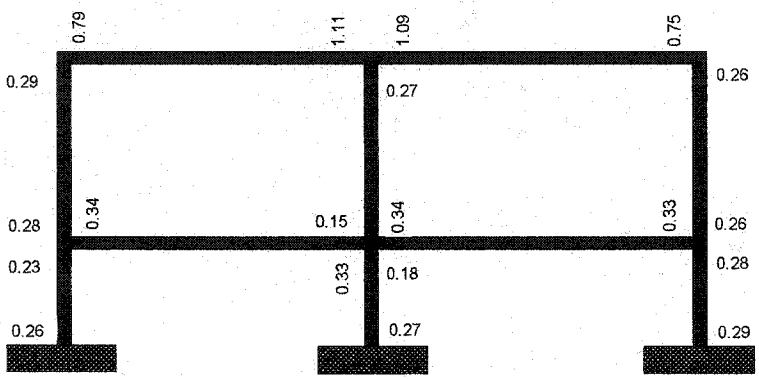

Bridge # 6
Transverse Direction

Fig. 7.17 Maximum M+SD shear demand/capacity ratios for Bridge #6.

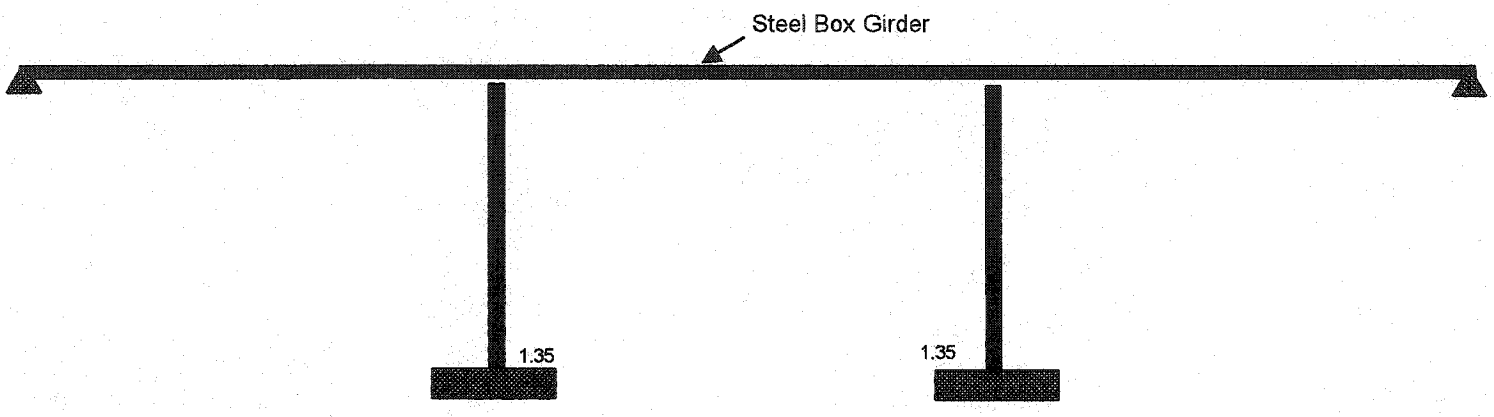

Bridge # 7
Longitudinal Direction

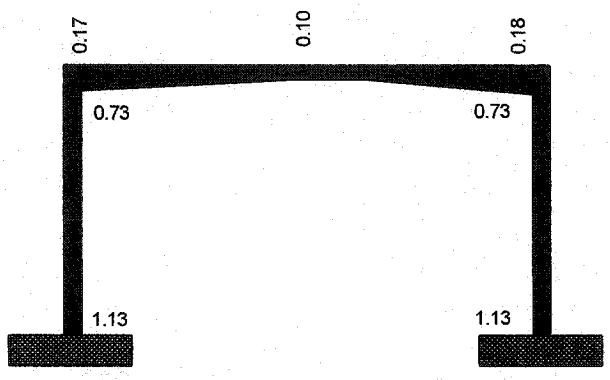

Bridge # 7
Transvers Direction

Fig. 7.18 Maximum M+SD shear demand/capacity ratios for Bridge #7.

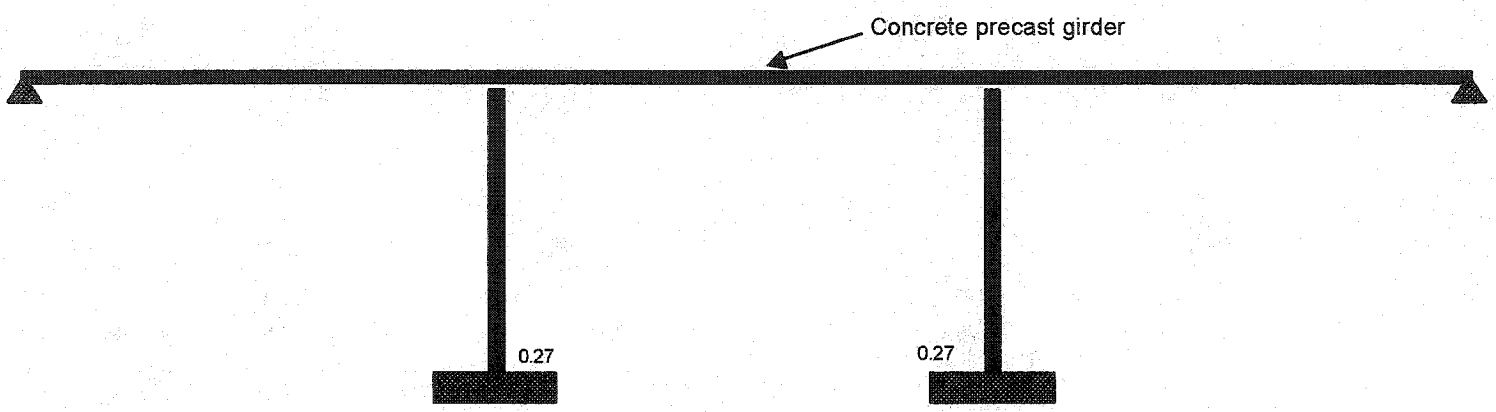

Bridge # 8
Longitudinal Direction

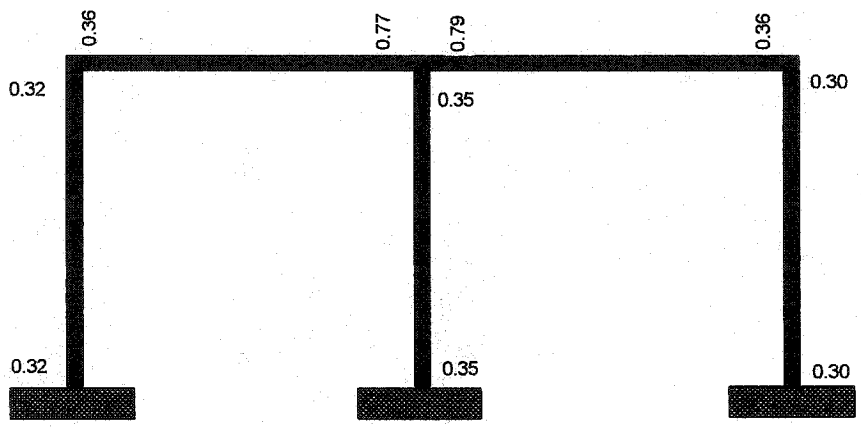

Bridge # 8
East Bent-Transverse Direction

Fig. 7.19 Maximum M+SD shear demand/capacity ratios for Bridge #8.

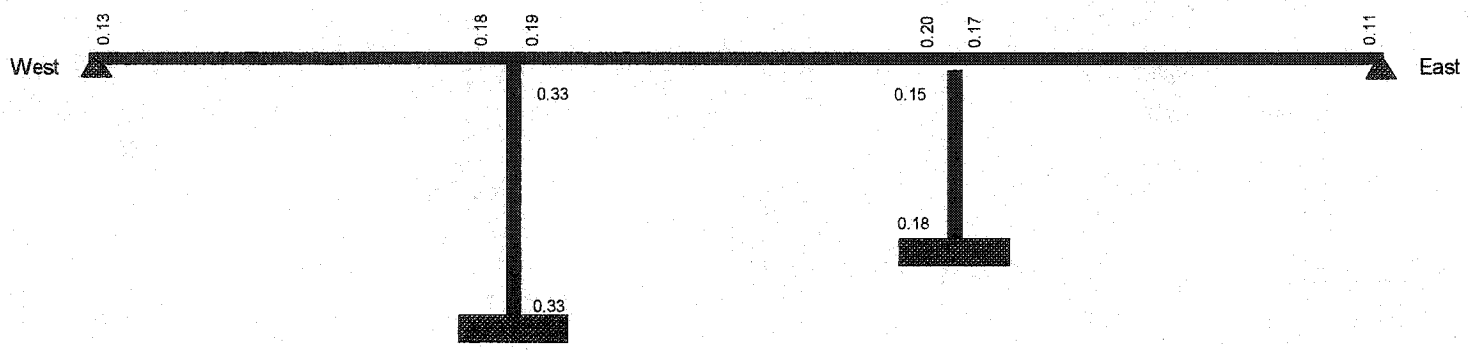

Bridge # 9
Longitudinal Direction

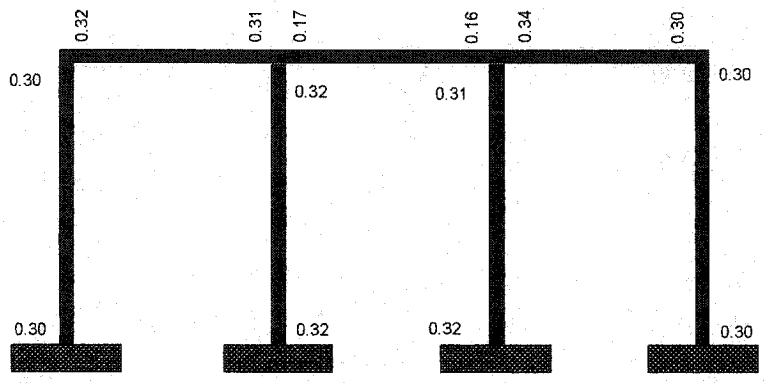

Bridge # 9
West Bent-Transverse Direction

Fig. 7.20 Maximum M+SD shear demand/capacity ratios for Bridge #9.

CHAPTER 8

CONCLUSIONS

8.1 Summary

Past earthquakes have shown that old bridges are very vulnerable when subjected to moderate and strong seismic motions. This was clearly illustrated during the 1989 Loma Prieta, the 1994 Northridge, and the 1995 Kobe earthquakes, when many old bridges collapsed or were extensively damaged. Given this, comprehensive seismic evaluations of the older bridges in an area are essential. The results from such studies can be used to prioritize the bridges for retrofitting plans, to select appropriate methods for retrofit, and to prepare post-earthquake preparedness plans.

In this study, nine reinforced concrete bridges in the City of Ottawa were selected as representative of the bridges in the region. Eight of these bridges were built between 1957 and 1973, and one was built in 1994. The bridge of 1994 was selected as representative of bridges designed according to the more recent bridge codes and was used as a reference for the assessment of the performance of the eight older bridges (i.e. those built between 1957 and 1973).

Analytical models were developed for the longitudinal and transverse directions of each bridge. Separate analyses were conducted for the longitudinal and transverse directions. For each direction, the bridge performance was investigated by using horizontal and vertical seismic excitations, consistent for the seismic conditions of the City of Ottawa. The evaluation of the seismic performance was based on the maximum ductility demand, shear demand/capacity ratios, and lateral drifts at mean plus one

standard deviation level. Based on results reported by a number of researchers, curvature ductilities of less than 5 for the pre-1973 bridges, and less than 20 for the new bridge were considered as acceptable values. In terms of the deformations due to shear forces, the bridges with shear demand/capacity ratios of less than 1.0 were considered to have sufficient shear resistance. Finally, the bridges having less than 2% drift ratio were considered as satisfactory. A detailed discussion on the acceptable level for each of these parameters is given in Chapter 7.

8.2 Main Observations and Conclusions

The following are the main observations and conclusions from this study:

- The maximum curvature ductility demands for the bridges built between 1957 and 1973 were all below 5, and those for the new bridge were below 5.7 (see Table 7.2). Given the acceptable curvature ductility levels of 5 for the pre-1973 bridges and 20 for the new bridge (as discussed above), the seismic performance of the bridges in terms of the curvature ductility, is considered satisfactory.
- The maximum values of the shear demand/capacity (D/C) ratios were found to be less than 1.0 for all the bridges, with the exception of bridges #3 and #7 for which the maximum D/C ratios for the columns were 1.27 and 1.35 respectively (see Table 7.3). This indicates that the shear resistance of these two bridges is not sufficient for seismic actions.
- The lateral drifts of the bridges were less than or very close to 2%, with the exception of bridge #4, which has a lateral drift of 2.79% (see Table 7.4). In terms of the drift, bridge #4 is considered unsatisfactory.
- In general, the seismic performance of the old bridges considered in this study was better than expected. Relatively light superstructures of the bridges, and reasonably good longitudinal and transverse reinforcement for the majority of the bridges, were the main reasons for such a performance.
- The new bridge (i.e. bridge #9) showed very good performance in terms of all three response criteria, i.e. curvature ductility demands, shear demand/capacity ratios, and lateral drift demands.

- The comparison of the evaluation response parameters of the old bridges with those of the new bridge, showed the following:
  (i) The maximum curvature ductilities of all old bridges were smaller than those of the new bridge,
  (ii) The drifts of six of the old bridges were smaller than the maximum drift of the new bridge, and the remaining two old bridges had somewhat larger drifts than that of the new bridge,
  (iii) The maximum shear D/C ratios of the old bridges were spread within a wide range, and no clear trend of these values in terms of those of the new bridge was observed. The maximum shear D/C values of the new bridge were of the order of 0.3 for both the substructure and the superstructure. The shear D/C values of the old bridges ranged between 0.18 and 1.37 for the substructures, and between 0.07 and 1.11 for the superstructures.

8.3 Further Studies

The evaluation presented in this study was based on the most common response parameters, i.e. curvature ductility, shear demand, and lateral drift. Further analyses should be conducted to consider the possibility of connection failures, foundation failures, loss of girder supports, and soil structure interaction effects. More sophisticated analytical models, such as finite element model and finite strip model should be used in the analyses, to take into account the torsional effects, and the effects of the slope and skewness of the bridges.

REFERENCES

Al-Haddad, M. 1995. "Curvature Ductility of Reinforced Concrete Beams under Low and High Strain Rates", *ACI Structural Journal*, V. 92, No. 5, pp. 526-534

Applied Technology Council, 1983. Seismic Retrofitting Guidelines for Highway Bridges, Report ATC-6-2

Aschheim, M., Moehle, J.P., and Mahin, S.A. 1997. "Design and Evaluation of Reinforced Concrete Bridges for Seismic Resistance", Report No. UCB/EERC-97/04, Earthquake Engineering Research Center, University of California, Berkeley

Associate Committee on the National Building Code. 1995. National Building Code of Canada 1995. National Research Council of Canada, Ottawa, Ont.

CSA. 2000. Canadian Highway Bridge Design Code. Canadian Standards Association, Rexdale, Ont.

Casas, J.R. 1999. "Evaluation of Existing Concrete Bridges in Spain", *Concrete International-Design and Construction*, V. 21, No. 8, pp. 48-53

Chai, Y.H., Priestley, M.J.N., and Seible, F. 1991. "Seismic Retrofit of Circular Bridge Columns for Enhanced Flexural Performance", *ACI Structural Journal*, V. 88, No. 5, pp. 572-584

Canadian Portland Cement Association, 1995. Concrete Design Handbook

Dodd, L.L., and Cooke, N. 1994. "Capacity of Circular Bridge Columns Subjected to Base Excitation" *ACI Structural Journal*, V. 97, No. 2, pp. 297-307

Filiatrault, A., Tremblay, S., and Tinawi, R. 1994. "A Rapid Seismic Screening Procedure for Existing Bridges in Canada", *Canadian Journal of Civil Engineering*, V. 21, pp.626-642

Gates, J., and Buckle. I.G. 1991. "Basic Design Concepts" Proceeding, International Workshop on Seismic Design and Retrofitting of Reinforced Concrete Bridges, Bormio, Italy, pp. 7-15

Ghobarah, A.A., and Tso, W.K. 1974. "Seismic Analysis of Skewed Highway Bridges with Intermediate Supports", *Journal of Earthquake Engineering and Structural Dynamics*, V. 2, pp. 235-248

Harik, I.E., Allen, D.L., Street, R.L., Guo, M., Graves, R.C., Harison, J., and Gawry, M.J. 1997. "Seismic Evaluation of Brent-Spence Bridge", *ASCE, Journal of Structural Engineering*, V. 123, No. 9, PP. 1269-1275

Harmon, T.G., Gould, N.C., Ramakrishnan, S., and Wang, E.H. 2002. "Confined Concrete Columns Subjected to Axial Load, Cyclic Shear, and Flexure-Part I: Analytical Models", *ACI Structural Journal*, V. 99, No. 1, pp. 32-41

Heidebrecht, A.C., and Naumoski, N. 2002. "The Influence of Design Ductility Capacity on the Seismic Performance of Medium Height Reinforced Concrete Frame Buildings", *American Concrete Institute,* SP-197, pp. 239-264

Kawashima, K., Ichimasu, H., and Ohuchi, H. 1991. "Retrofitting", Proceeding, International Workshop on Seismic Design and Retrofitting of Reinforced Concrete Bridges, Bormio, Italy, pp. 471-501

Kawashima, K., Unjoh, S., and Mukai, H. 1997. "Seismic Strengthening of Highway Bridges", Second U.S.-Japan workshop on seismic retrofit of bridges, Report No. UCB/EERC-97/09, Earthquake Engineering Research Center, University of California, Berkeley

Kunnath, S.K., and Reinhorn, A.M. 1992. "IDARC2D:Inelastic Damage Analysis of RC Building Structures", Technical Report NCEER-92-0022, National Center for Earthquake Engineering Research,

Lehman, D.E., and Moehle, J.P. 2000. "Seismic Performance of Well-Confined Concrete Bridge Columns", PEER 1998/01, Pacific Earthquake Engineering Research Center

Lowes, L.N., and Moehle, J.P. 1999. "Evaluation and Retrofit of Beam-Column T-joints in Older Reinforced Concrete", *ACI Structural Journal*, V. 96, No. 4, pp. 519-532

Lwin, M.M. 1997. "Bridge Seismic Design and Retrofit Practices in Washington State", Building to last: Proceedings of Structures congress XV, Portland. Oregon, pp. 1176-1180

Mander, J.B., Priestley, M.J.N., and Park, R. 1998. "Theoretical Stress-Strain Model for Confined Concrete", *Journal of structural Engineering*, V. 114, No. 8, pp. 1804-1826

Mander, J.B., Priestley, M.J.N., and Park, R. 1998. "Observed Stress-Strain Behavior of Confined Concrete", *Journal of structural Engineering*, V. 114, No. 8, pp. 1827-1849

Mes, D. 1999. "Seismic Retrofitting of Concrete Bridge Columns by External Prestressing", Master thesis, Department of civil engineering, University of Ottawa

Naumoski, N.N. 2001. " Program SYNTH, Generation of Artificial Accelerograms Compatible with a Target Spectrum"

Naumoski, N.N., Heidebrecht, A.C., and Rutenberg, A.V. 1993. "Representative Ensembles of Strong Motion Earthquake Records", EERG Report 93-1, Earthquake Engineering Research Group

Naumoski, N.N., and Heidebrecht, A.C. 1998. "Seismic Level of Protection of Medium Height Reinforced Concrete Frame Structures, Member Properties for Seismic Analysis", EERG Report 98-1, Earthquake Engineering Research Group

Naumoski, N.N., and Heidebrecht, A.C. 1998. "Seismic Level of Protection of Medium Height Reinforced Concrete Frame Structures, Modelling and Analysis", EERG Report 98-2, Earthquake Engineering Research Group

Paulay, T., Priestley, M.J.N. 1992. "Seismic Design of Reinforced Concrete and Masonry Buildings", John Wiley & Sons, Inc., New York, 744 p

Priestley, M.J.N., Seible, F., and Calvi, G.M. 1996. "Seismic Design and Retrofit of Bridges", John Wiley & Sons, Inc., New York, 686 p

Priestley, M.J.N., Seible, F., MacRae, G.A., and Chai, Y.H 1997. "Seismic Assessment of the Santa Monica Viaduct Bent Details", *ACI Structural Journal*, pp. 513-524

Saadatmanesh, H., Ehsani, M.R., and Jin, L. 1996. "Seismic Strengthening of Circular Bridge Pier Models with Fiber Composites", *ACI Structural Journal*, V. 93, pp. 639-647

Saiidi, M., Maragakis, E., and Sanders, D. 1998. "evaluation and seismic retrofit of highway bridge substructures with tapered columns", *Journal of Engineering Structures*, V. 12, Issue 2-3, pp. 161-173

Sexsmith, R., Anderson, D., and English, D. 1997. "Cyclic Behavior of Concrete Bridge Bent ", *ACI Structural Journal*, V. 94, No. 2, pp. 103-113

Xiao, Y., and Rui Ma, 1997. "Seismic Retrofit of RC Circular Columns Using Prefabricated Composite Jacketing", *Journal of sructural Engineering*, V. 123, No. 10, pp. 1375-1364

Yashinsky, M. 1998. "Performance of Bridge Seismic Retrofits During Northridge Earthquake", *Journal of Bridge Engineering*, V. 3, No. 1, pp. 1-14